# Confinement and driving effects on model interfaces

May 26, 2020

# Contents

# Introduction

Every statistical model is described by an order parameter, such as the mean magnetization in a magnetic system or the polymer's mean orientation. During a continuous phase transition, the correlation length diverges up to a macroscopical scale. When this length scale becomes as the same order of magnitude as the experimental or numerical cell, finite size effect arises, such as the critical Casimir effect.

We may study the statistical properties of interfaces between two phases through different though complementary methods. Historically, the first method was through lattice models, and more precisely the Ising model. Those models are well-suited for numerical analysis due to their discrete nature, while posing analytical challenges due to the big number of degrees of freedom. The Solid-On-Solid model is an approximation of the Ising model in $d-1$ dimensions allowing us to use the transfer matrix method, which holds analytical results directly comparable with numerical simulations. From the Ising model arises some mean-field approximations, with the Landau-Ginzburg Hamiltonian. This method allows for relatively easy analytical computations of the two-point space correlation function of the system, which gives us some insight about the properties of the interfaces. From the mean field theory we can derive the mean-field equations of a fluctuating interface, which then resembles to a brownian walker. This powerful analogy allows the use of quantum mechanics formalism, as we will see later on.

Systems may exist in many different contexts. Knowing how the thermodynamical ensemble in which we place the system affects its statistical properties is a key to understanding how to transpose the analytical results to actual experiments. A special attention will also be brought to the free energy. From the free energy between a bulk and an interface we can compute the its surface tension. The derivative of the free energy with respect to the length of the system also gives us a confinement force, called the Casimir force. This force is exerted on the boundary conditions because of the confinement of fluctuations.

The thesis' outline is as following :

- The first chapter derives the interface dynamics from mean field theory. In doing so, we will define all the main interface models that exist, and explain the main results from literature.

- In the second chapter we explain how do numerical simulations work, some methods to compute the free energy in lattice gas models, and some usefull tips.

- The third chapter is devoted to finite size effects, computed for all the models presented in chapter one, and compared to numerical results.

- The fourth chapter is about a paper we've published [1]. This paper is about the computation of the surface tension of a sheared interface, where we've coupled the field with a virtual one in order to proceed with the computation.

- In the last chapter we introduce a new lattice model which is a better approximation to the Ising model than the Solid-On-Solid model. This new model, the Particles-Over-Particles model, takes into account the entropy, in comparison to SOS.

# Chapter 1

# Equilibrium interface dynamics

In this chapter we will analyse the dynamics of statistical systems. The analysis will allow us to understand how phase transitions - in particular those who possess a phase separation - occur dynamically [3]. The most famous example is the Ising model without any external field, its order parameter being the total magnetization.

In the high temperature phase, the system is homogeneous and its total magnetization is zero. Below the critical temperature, when the order parameter is conserved (for example with a Kawasaki dynamic or Model B), the system will locally separate into two phases of opposite mean magnetization separated by and interface, this interface minimizing the surface energy between both phases. When the order parameter is not conserved (for example Glauber dynamics or Model A), a spontaneous symmetry breaking will make one of the two phases take over the whole system. In a continuous phase transition where the critical point is reached from the disordered state to the ordered stated, the domain size, which is equal to the system's correlation length, diverges close to the critical temperature $T_C$. In a thermodynamical system, it becomes infinite, implying that the system takes an infinite amount of time to reach equilibrium : it's the critical slowing down. The process of domain growth is known as coarsening and phase ordering kinetics is the theory that has been developed to understand the phenomenon of coarsening[4]. In Fig 1.1, we show an example of coarsening in the Ising model with respect to time.

Furthermore, for systems with a conserved order parameter which separate into two phases, the two phases will be separated by an interface. This interface will be characterised by a surface tension, its average position will be fixed but it will exhibit fluctuations. Later we will see how model of phase ordering kinetics and be used to determine the static and

1

t=0 MC                              t=100 MC

t=400 MC                            t=1000 MC
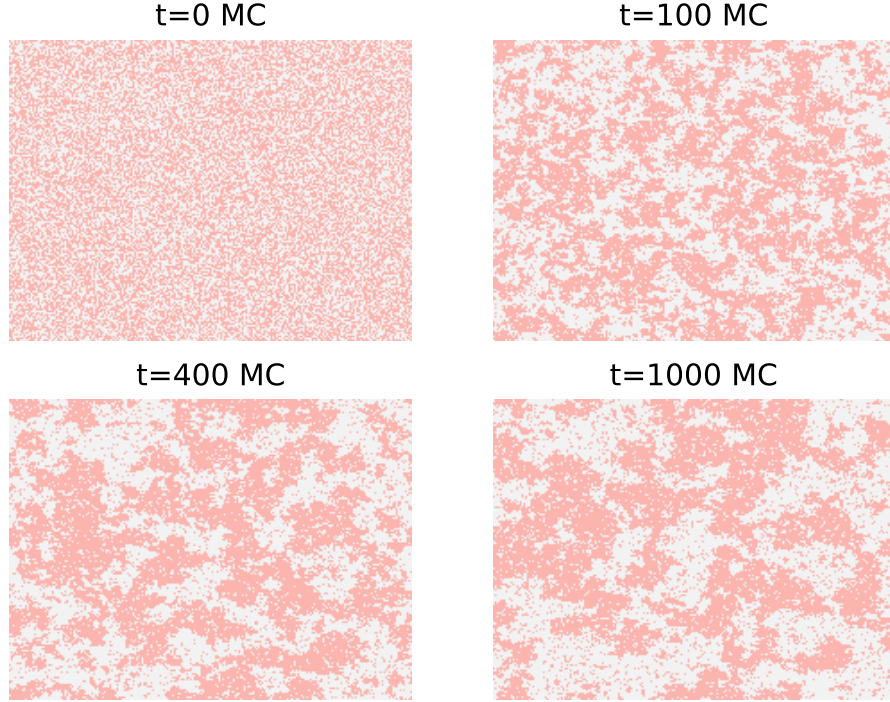
Figure 1.1: Numerical simulations of coarsening from a quench from a disordered state $T = \infty$ to an ordered state $T = T_{2D,C}$ [5] for different times, in Monte Carlo steps, for a $600 \times 600$ system with non-conserved Glauber dynamics.

dynamical properties of interfaces between two coexisting phases.

While the phase diagram of a system can be determined via its Hamiltonian and equilibrium statistical mechanics, the dynamics of coarsening depends on the details of the systems dynamics that do not show up in single time thermodynamic observables. Therefore, one needs to construct dynamical models that capture the underlying evolution of the state of the system. In particular, there is a big difference between systems where the order parameter is conserved and those where it is not conserved.

## 1.1 Models for equilibrium fields

### 1.1.1 Statics of systems with a finite number of degrees of freedom

Thermodynamic systems are naturally described in terms of fields, for example densities.

Measuring observables in experimental setups means to measure the derivative of the partition function $Z$ with respect to its conjugate variable. This measure is done with a certain degree of spatial and temporal resolution, which means in a statistical language that they measure the average of the observable over some space and time. If $\Phi(\mathbf{x}, t)$ is the physical field of our system, our device having a temporal resolution of $dt$ and a spatial resolutoin over a volume $V$ will measure

$$\phi(\mathbf{x}, t) = \frac{1}{V \, dt} \int_{t-dt}^{t} dt' \int_V \mathbf{x}' \Phi(\mathbf{x}', t') \tag{1.1}$$

This means that one is naturally lead to consider statistical field theories where the system is described in terms of a local field $\phi(\mathbf{x})$. Statistical field theories can be applied to both statics, to understand phase diagrams, and dynamics to understand phase ordering. However to start with we will examine the case of systems with a finite number of degrees of freedom.

Consider a system in the canonical ensemble with a Hamiltonian $H(\mathbf{q})$ where $q_i$ for $1 \leq i \leq N$ represent a finite number of continuous spatial degrees of freedom and where in a classical system we have already integrated over the corresponding momenta. The partition function for the system is given by

$$Z = \int d\mathbf{q} \exp\left(-\beta H(\mathbf{q})\right) \tag{1.2}$$

In general the integral which gives the partition function cannot be computed analytically. In equilibrium, the probability density function $P_{eq}(\mathbf{q})$ of the degrees of freedom is given by

$$P_{eq}(\mathbf{q}) = \frac{\exp\left(-\beta H(\mathbf{q})\right)}{Z} \tag{1.3}$$

The simplest approximation to compute $Z$ is the mean field approximation where the integral is approximated by the integrand at its largest value - in mathematics this is the Laplace method for approximating an integral and in this context it is just an expansion about the minimum energy configuration of the system. The mean field approximation is

thus

$$Z_{MF} = \exp\left(-\beta H(\mathbf{q}^*)\right) \tag{1.4}$$

where $\mathbf{q}^*$ is the value of $\mathbf{q}$ which minimises $H$ (note that the approximation becomes exact in the zero temperature limit - $\beta \to \infty$ - as the system will minimise its energy). The values $q_i^*$ are determined from

$$\frac{\partial H}{\partial q_i}\Big|_{\mathbf{q}=\mathbf{q}^*} = 0 \tag{1.5}$$

Within this approximation any thermodynamic observable is given by

$$\langle f(\mathbf{q}) \rangle = f(\mathbf{q}^*) \tag{1.6}$$

We now consider how one can model dynamics of such systems. We will look for a Langevin equation which is chosen to give the correct equilibrium Gibbs-Boltzmann distribution. We write

$$\frac{dq_i}{dt} = -L_{ij}\frac{\partial H(\mathbf{q})}{\partial q_j} + \eta_i(t) \tag{1.7}$$

where $L_{ij}$ is a matrix which discuss later and $\eta_i(t)$ is zero mean Gaussian white noise with correlation function

$$\langle \eta_i(t)\eta_j(t') \rangle = \Gamma_{ij}\delta(t - t') \tag{1.8}$$

The Gaussian white noise represents the effects of thermal fluctuations on the system we assume that the correlation time of these fluctuations is extremely short with respect to the dynamics of the degrees of freedom $q_i$ (in fact in critical systems the dynamics become very slow, critical slowing down, and this approximation becomes better and better as one approaches the critical point). There is no momentum term in this Langevin equation and for this reason it is often called the overdamped Langevin equation. Overdamped Langevin equations can also be derived staring from Newton's laws in the presence of friction, due to a solvent, and again white noise (again due to molecular collisions with the solvent) and by taking the limit where the frictional forces are greater than the acceleration term in Newton's equations (equivalent to setting the particle masses to zero).

As Eq. (1.8) is for a correlation function the matrix $\Gamma_{ij}$ must be symmetric and cannot have any negative eigenvalues.

In the absence of noise or thermal fluctuations, so at zero temperature, the system will

simply minimise its energy. Therefore if

$$\frac{\partial H(\mathbf{q})}{\partial q_j} = 0 \tag{1.9}$$

with no noise we have $\frac{dq_i}{dt} = 0$, that is to say it is the term $\frac{\partial H(\mathbf{q})}{\partial q_j}$ that drives the dynamics if there is no noise. As long as the matrix $L_{ij}^{-1}$ exists the zero temperature dynamics will take the system to the local minimum of $H$ and to the absolute minimum if there are no metastable configurations.

Under these assumptions, the Fokker-Planck equation for the probability density function of the degrees of freedom is

$$\frac{\partial p(\mathbf{q}, t)}{\partial t} = \frac{\partial}{\partial q_i} \left[ \frac{1}{2} \Gamma_{ij} \frac{\partial p(\mathbf{q}, t)}{\partial q_i} + p(\mathbf{q}, t) L_{ij} \frac{\partial H(\mathbf{q})}{\partial q_j} \right] \tag{1.10}$$

This can be written as

$$\frac{\partial p(\mathbf{q}, t)}{\partial t} + \frac{\partial}{\partial q_i} J_i(\mathbf{q}, t) = 0 \tag{1.11}$$

where the $\mathbf{J}(\mathbf{q}, t)$ is the probability current. We now insist that the system is in equilibrium with zero current when $p(\mathbf{q}, t) = P_{eq}(\mathbf{q})$ as given by Eq. (1.3), this gives

$$\left[ -\frac{\beta}{2} \Gamma_{ij} + L_{ij} \right] \frac{\partial H(\mathbf{q})}{\partial q_j} \tag{1.12}$$

and this holds for any choice of $H$ is we chose

$$\Gamma_{ij} = 2T L_{ij} \tag{1.13}$$

where we have taken units where Boltzmann's constant $k_B = 1$.

### 1.1.2 Statistical field theory

We now consider a system with Hamiltonian $H[\phi]$ which depends on a continuous field $\phi(\mathbf{x})$. The partition function is given by a functional integral

$$Z = \int d[\phi] \exp(-\beta H[\phi]), \tag{1.14}$$

the functional integral over all possible fields $\phi$ can be taken as a limit where $\phi$ is defined at a finite number of points on a lattice and then the lattice spacing is taken to zero. In many cases, the system has been coarse grained and $\phi$ represents a spatially varying order parameter, for instance the local density averaged over some small volume. In this case the Hamiltonian $H$ is strictly speaking a free energy and contains terms that depend on the temperature.

The mean field approximation to partition function is then given by

$$Z_{MF} = \exp(-\beta H[\phi_{MF}]) \tag{1.15}$$

where $\phi_{MF}$ is the mean field solution which minimises $H$. The definition of a functional derivative of a functional is

$$F[\phi + \delta\phi] - F[\phi] = \int d\mathbf{x}\frac{\delta F}{\delta\phi(\mathbf{x})}\delta\phi(\mathbf{x}) \tag{1.16}$$

Therefore if a field $\phi$ maximises $H$ we must have

$$\frac{\delta H}{\delta\phi(\mathbf{x})} = 0 \tag{1.17}$$

We now consider the standard Landau-Ginzburg Hamiltonian [6] describing Ising like systems where

$$H[\phi] = \int d\mathbf{x}\ \frac{\kappa}{2}[\nabla\phi]^2 + V(\phi) \tag{1.18}$$

The first term represents an energetic cost of varying the field $\phi$. The second potential term has two minima at $\phi = \pm\phi_c$, and, in the low temperature or phase separated phase, without loss of generality we can chose $V(\phi_c) = V(-\phi_c)$, while it has a single minimum at $\phi = 0$ in the high temperature phase.

The standard potential for phase separations, called the $\phi^4$ model, is given by the double-well

$$V(\phi) = \frac{1}{2}m^2\phi^2 + \frac{\lambda}{4!}\phi^4 \tag{1.19}$$

where $m^2 = T - T_C$. For $m^2 < 0$, the minima are at $\phi_C = \pm\sqrt{-\frac{6m^2}{\lambda}}\pm$, while at $m^2 \geq 0$, the single minimum is at $\phi_C = 0$. We can also couple our system with the magnetic field
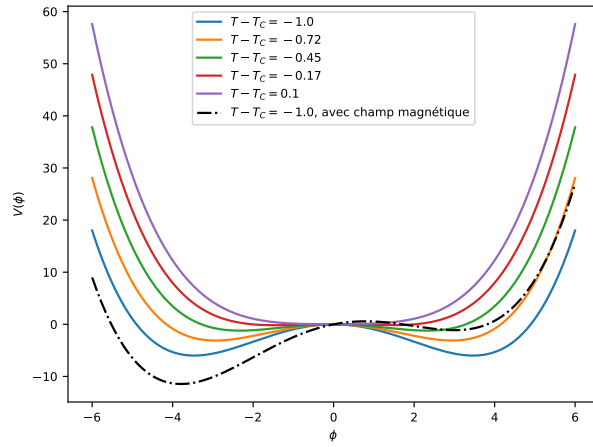
Figure 1.2: Double-well potential (1.19) for $\lambda = 1$ in function of the temperature difference with respect to the critical temperature with $m^2 = T - T_C$. In the ordered phase, the minima are at $\phi_C = \pm\sqrt{-\frac{6m^2}{\lambda}}$, while for the ordered phase it is at $\phi_C = 0$. In black, the addition of a uniform magnetic field $h(\mathbf{x}) = 1$ makes the positive phase metastable.

of Hamiltonian

$$H_1 = -\int d^d x h(\mathbf{x})\phi(\mathbf{x}) \tag{1.20}$$

As we in Fig 1.2, the addition of an uniform external field does favour one phase over the other one.

It is easy to see that

$$\frac{\delta H}{\delta\phi(\mathbf{x})} = -\kappa\nabla^2\phi(\mathbf{x}) + V'(\phi) \tag{1.21}$$

If we compare with systems with a discrete number of variables we should have a Langevin equation of the form

$$\frac{\partial\phi(\mathbf{x})}{\partial t} = -L\frac{\delta H}{\delta\phi(\mathbf{x})} + \eta(\mathbf{x}, t) \tag{1.22}$$

The white noise correlator should have the form

$$\langle\eta(\mathbf{x}, t)\eta(\mathbf{x}', t)\rangle = \delta(t - t')\Gamma(\mathbf{x}, \mathbf{x}'), \tag{1.23}$$

where here $\Gamma(\mathbf{x}, \mathbf{x}')$ is an operator (before it was a matrix) defined by its action on functions

$f$ as

$$\Gamma f(\mathbf{x}) = \int d\mathbf{x}' \Gamma(\mathbf{x}, \mathbf{x}') f(\mathbf{x}') \tag{1.24}$$

and $L$ is also an operator with

$$L f(\mathbf{x}) = \int d\mathbf{x}' L(\mathbf{x}, \mathbf{x}') f(\mathbf{x}') \tag{1.25}$$

Following the same arguments for systems with a finite number of degrees of freedom we thus have the relation (which is sometimes called the fluctuation dissipation theorem as it essentially is equivalent)

$$\Gamma(\mathbf{x}, \mathbf{x}') = 2TL(\mathbf{x}, \mathbf{x}') \tag{1.26}$$

The simplest form of dynamics is given by $L(\mathbf{x}, \mathbf{x}') = \alpha\delta(\mathbf{x} - \mathbf{x}')$ which gives the **model A dynamics**

$$\frac{\partial \phi(\mathbf{x})}{\partial t} = -\alpha \frac{\delta H}{\delta \phi(\mathbf{x})} + \eta(\mathbf{x}, t) \tag{1.27}$$

with the noise correlator

$$\langle \eta(\mathbf{x}, t)\eta(\mathbf{x}', t) \rangle = 2T\alpha\delta(t - t')\delta(\mathbf{x} - \mathbf{x}') \tag{1.28}$$

The average value of $\phi$

$$\overline{\phi}(t) = \frac{1}{V} \int d\mathbf{x} \ \phi(\mathbf{x}, t) \tag{1.29}$$

is clearly not generally conserved by this dynamics. Model A corresponds to a system in the grand-canonical ensemble, where $\alpha$ is the kinetic coefficient related to the relaxation time of the system [3].

**Model B dynamics** amounts to choosing

$$L(\mathbf{x} - \mathbf{x}') = -D\nabla^2\delta(\mathbf{x} - \mathbf{x}') \tag{1.30}$$

The fact that $L$ is a positive semi-definite operator can be seen by taking its Fourier transform. The evolution equation here is

$$\frac{\partial \phi(\mathbf{x})}{\partial t} = D\nabla^2 \frac{\delta H}{\delta \phi(\mathbf{x})} + \eta(\mathbf{x}, t) \tag{1.31}$$

where

$$\langle \eta(\mathbf{x}, t)\eta(\mathbf{x}', t) \rangle = -2TD\delta(t - t')\nabla^2\delta(\mathbf{x} - \mathbf{x}') \tag{1.32}$$

We notice that if we introduce the vectorial white noise with components $\eta_i(\mathbf{x}, t)$ such that

$$\langle \eta_i(\mathbf{x}, t)\eta_i(\mathbf{x}', t') \rangle = \delta_{ij}\delta(\mathbf{x} - \mathbf{x}')\delta(t - t) \tag{1.33}$$

where $\delta_{ij} = 1$ for $i = j$ and is zero otherwise, we can write

$$\eta(\mathbf{x}, t) = \nabla \cdot \boldsymbol{\eta}(\mathbf{x}, t) \tag{1.34}$$

as one can verify the two noises have the same correlation function. In this way Eq. (1.31) becomes

$$\frac{\partial \phi(\mathbf{x})}{\partial t} = \nabla \cdot [D\nabla \frac{\delta H}{\delta \phi(\mathbf{x})} + \boldsymbol{\eta}(\mathbf{x}, t)] \tag{1.35}$$

From this it is easy to see that the order parameter is conserved - thus model B describes conserved phase ordering dynamics. This model corresponds to the canonical ensemble, and is useful to describe diffusion or accretion systems.

Without the noise fluctuations, equations (1.27) and (1.31) are called the Time Dependant Ginzburg-Landau equation [7] and the Cahn-Hilliard equation[8] equations, which give the mean field's dynamics.

### 1.1.3 Surface tension

In order to minimize the free energy in a non-conserved system, we can simply choose $\phi(\mathbf{x}) = \phi_c$ or $\phi(\mathbf{x}) = -\phi_c$ everywhere, which corresponds to a free energy $F = H[\phi_c] = 0$. However in a system with a conserved order parameter

$$\int d\mathbf{x} \; \phi(\mathbf{x}) = 0 \tag{1.36}$$

the solutions $\phi = \pm\phi_c$ cannot hold. In this case the system will separate into two homogeneous phases where $\phi(\mathbf{x}) = \pm\phi_c$. We therefore choose an interface at $z = 0$ and take $\phi(\mathbf{x}) = \phi_K(z)$ ($K$ standing for kink as it is known as the kink solution in the literature) where $\lim_{z \to \infty} = -\phi_c$ and $\lim_{z \to \infty} = -\phi_c$. We therefore find from Eq. (1.21) that

$$-\kappa \frac{d^2}{dz^2}\phi_K(z) + V'(\phi_K) = 0 \tag{1.37}$$

We can write

$$H[\phi_K] = A \int dz \; \frac{\kappa}{2}\left(\frac{d\phi_K(z)}{dz}\right)^2 + V(\phi_K(z)) \tag{1.38}$$

where $A$ is the surface area of the system in the plane perpendicular to the direction $z$. However, if we multiply Eq. (1.37) by $d\phi/dz$ and integrate we find

$$-\frac{\kappa}{2}(\frac{d\phi_K}{dz})^2 + V(\phi_K) = C \tag{1.39}$$

where $C$ is a constant. However as $\phi_K(z) \to \pm\phi_c$ as $z \to \pm\infty$ and $V(\pm\phi_c) = 0$ we find that $C = 0$. Using this, we obtain

$$H[\phi_K] = A \int dz \; \kappa \left(\frac{d\phi_K(z)}{dz}\right)^2 \tag{1.40}$$

If the interface has a free energy per unit area of $\sigma$ then we have the Cahn-Hillard estimate of the surface tension [8]

$$\sigma = \int dz \; \kappa \left(\frac{d\phi_K(z)}{dz}\right)^2 \tag{1.41}$$

In the case of the $\phi^4$ model defined at Eq (1.19), the equation (1.37) becomes

$$\kappa\phi_K''(z) = m^2\phi_K(z)\left(1 + \phi_C\phi_K(z)^2\right) \tag{1.42}$$

This potential is only defined by the ratio between $m^2$ and $\lambda$, so without loss of generality we set $\phi_C = 1$. The solution becomes

$$\phi_K(z) = \tanh\left(\frac{z}{\xi}\right) \tag{1.43}$$

where $\xi = \sqrt{\frac{-2\kappa}{m^2}}$. This correlation length diverges when $T \to T_C$. From Fig 1.3 we see that the bigger the correlation length of the system, the smaller the surface tension is. The experimental study of quasi-critical systems, which have fluctuations at a macroscopic length scale, is a good way to probe the properties of ultra-low surface tension systems [9]. Such systems are very susceptible to hydrodynamic instabilities caused by thermal noise, as in microfluidics for example [10].
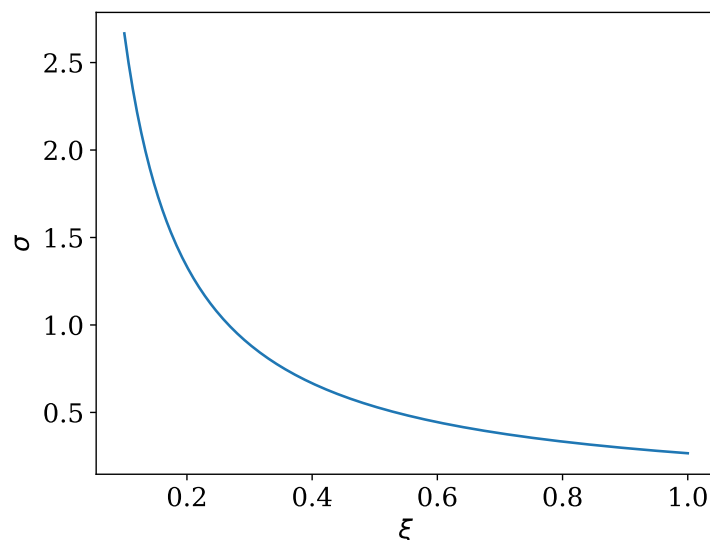
Figure 1.3: Superificial tension (1.41) with respect to $\xi$ for the $\phi^4$ solution (1.43).

## 1.2 Models for equilibrium interfaces

### 1.2.1 Basic continuous model

Here we discuss effective models of interfaces. The simplest model is to assume that the interface is parameterised by a height profile $h(\mathbf{r})$, where $\mathbf{x} = (\mathbf{r}, z)$ however one also has to assume that $h(\mathbf{r})$ is a single-valued function of $\mathbf{r}$. Given this one can write

$$H[h] = \sigma A[h] \tag{1.44}$$

where $A_h$ is the area of the interface. However, the interface area is given by

$$A[h] = \int_A d\mathbf{r} \sqrt{1 + [\nabla h]^2} \tag{1.45}$$

where the integral is over the plane perpendicular to the $z$ axis which is taken to be of area $A$. When the fluctuations of the interface are small, we can expand the above to quadratic order in $h$ to obtain

$$H[h] = A\sigma + \frac{\sigma}{2} \int_A d\mathbf{r} \, [\nabla h]^2 \tag{1.46}$$

The first term is independent of the height, so we can write the effective Hamiltonian for the surface as

$$H_{eff}[h] = \frac{\sigma}{2} \int_A d\mathbf{r} \ [\nabla h]^2 \tag{1.47}$$

The basic model describing the height of an interface at $z = h(\mathbf{r})$ above a plane with coordinates $\mathbf{r}$ has the Hamiltonian

$$H[h] = \int d\mathbf{x} \frac{\sigma}{2} [\nabla h(\mathbf{x})]^2 + V(h(\mathbf{x})) \tag{1.48}$$

The first term corresponds to the surface energy for a surface of size $A_s$

$$H_s[h] = \sigma A_s = \sigma \int d\mathbf{x} \sqrt{1 + [\nabla h(\mathbf{r})]^2} \approx \sigma A + \frac{\sigma}{2} \int d\mathbf{r} [\nabla h(\mathbf{r})]^2 \tag{1.49}$$

Here $A$ is the area of the projected plane below the surface which is taken to be constant and thus does not change the statistical mechanics of the system. In principle surfaces can also have bending energies, while surface energies correspond to stretching the surface to increase its size, bending energies correspond to curving the surface. The standard bending energy for small surface energies [11] is given by

$$H_b[h] = \int d\mathbf{r} \frac{\kappa_b}{2} [\nabla^2 h(\mathbf{r})]^2 \tag{1.50}$$

where $\kappa_b$ is called the bending rigidity.

The term $V(h)$ is taken to represent the potential energy of the surface. For instance if the surface interacts via an infinite hard-core potential with a solid surface at $z = 0$, this can be modelled by the potential $V(z) = 0$ for $z > 0$ and $V(z) = \infty$ for $z \leq 0$. Another example is where the surface describes the surface of a liquid such as water, again with a solid surface at $z = 0$, in the presence of gravity the potential energy of the water column above the area element $d\mathbf{x}$ is given by

$$\delta V = \int_0^{h(\mathbf{r})} dz \ \rho g z = \frac{1}{2} \rho g h^2(\mathbf{r}) \tag{1.51}$$

where $\rho$ is the (mass) density of the liquid. This then gives

$$H[h] = \int d\mathbf{r} \frac{\sigma}{2} [\nabla h(\mathbf{r})]^2 + \frac{1}{2} \rho g h^2(\mathbf{r}) \tag{1.52}$$

We see that the correlation length of the interface is given by

$$\xi = \left(\frac{\sigma}{\rho g}\right)^{\frac{1}{2}} \tag{1.53}$$

In the more general context, if $V(h)$ has a minimum at some point $h_m$ we can write $h = h_f(\mathbf{x}) + h_m$, where $h_f(\mathbf{x})$ represents the height fluctuations about the mechanically stable flat interface $h(\mathbf{x}) = h_m$. Now expand assuming that $h_f(\mathbf{x})$ is small we find the effective Hamiltonian for the fluctuations

$$H_{eff}[h_f] = \int d\mathbf{r} \frac{\sigma}{2} [\nabla h_f(\mathbf{r})]^2 + \frac{1}{2} V''(h_m) h_f^2(\mathbf{r}) \tag{1.54}$$

where we have dropped the constant term $AV(h_m)$. The above field theory is Gaussian and so, when the approximations made to derive it are valid, all of the statistical properties of the height fluctuations can be deduced. However for general potentials $V(h)$ the model cannot be solved exactly in two dimensions but can in principle be solved in one dimension as we will see below.

## 1.2.2 Effective dynamics of interface heights

We will now try and derive an approximation for the dynamics of the height of the interface from the original phase ordering kinetics. Here we use the method of Bray and Cavagnha [12, 13], which was used to study the dynamics of sheared interfaces, in the absence of shear to determine the dynamical properties of interfaces in phase separated systems for both model A and model B dynamics.

We imagine that the system is phase separated in the direction $z$, on average the interface is taken to be at $z = 0$, and we write

$$\phi(z, \mathbf{r}, t) = f(z - h(\mathbf{r}, t)) \tag{1.55}$$

where $f(z) = \phi_K(z)$ is the kink solution from mean field theory.

### 1.2.2.1   Model A dynamics

For model A dynamics, we substitute Eq. (1.55) into Eq. (1.27) and make use of the following results

$$\frac{\partial f(z - h(\mathbf{r}, t))}{\partial t} = - f'(z - h(\mathbf{r}, t))\frac{\partial h(\mathbf{r}, t)}{\partial t}$$

$$\nabla f(z - h(\mathbf{r}, t) = [\mathbf{e}_z - \nabla h(\mathbf{r}, t)]f'(z - h(\mathbf{r}, t))$$

$$\nabla^2 f(z - h(\mathbf{r}, t)) = f''(z - h(\mathbf{r}, t)) - \nabla^2 h(\mathbf{r}, t)f'(z - h(\mathbf{r}, t)) + [\nabla h(\mathbf{r}, t)]^2 f''(z - h(\mathbf{r}, t))$$

and thus find

$$
\begin{aligned}
-f'(z - h(\mathbf{r}, t))\frac{\partial h(\mathbf{r}, t)}{\partial t} =& \alpha\kappa\left[f''(z - h(\mathbf{r}, t)) - \nabla^2 h(\mathbf{r}, t)f'(z - h(\mathbf{r}, t)) + [\nabla h(\mathbf{r}, t)]^2 f''(z - h(\mathbf{r}, t))\right]\\
& - \alpha V'(f'(z - h(\mathbf{r}, t))) + \eta(\mathbf{r}, z, t)
\end{aligned}
$$

We now multiply both sides of this equation by $f'(z - h(\mathbf{r}, t))$ and defining $\zeta = z - h(\mathbf{r}, t)$, we integrate $\zeta$ over $[-\infty, \infty]$ while using the following identities

$$\int_{-\infty}^{\infty} d\zeta f'(\zeta)f''(\zeta) = [\frac{1}{2}f'^2(\zeta)]_{-\infty}^{\infty} = 0$$

$$\int_{-\infty}^{\infty} d\zeta f'(\zeta)V'(f) = \int_{-\infty}^{\infty} d\zeta \frac{dV(f)}{d\zeta} = [V(f(\zeta))]_{-\infty}^{\infty} = 0$$

Note that the first relation above holds as $f(\zeta) = \pm\phi_c$ as $\zeta \to \pm\infty$ and the second as $V(\phi_c) = V(-\phi_c) = 0$. The terms that are left then give

$$-\int_{-\infty}^{\infty} f'^2(\zeta)d\zeta \ \frac{\partial h(\mathbf{r}, t)}{\partial t} = -\alpha\int_{-\infty}^{\infty} f'^2(\zeta)d\zeta \ \kappa\nabla^2 h(\mathbf{r}, t) + \int_{-\infty}^{\infty} d\zeta\eta(\mathbf{r}, \zeta + h(\mathbf{r}, t))f'(\zeta) \tag{1.56}$$

Now using the Cahn-Hillard estimate of the surface tension, Eq. (1.41) thus becomes

$$\frac{\sigma}{\kappa}\frac{\partial h(\mathbf{r}, t)}{\partial t} = \alpha\sigma\nabla^2 h(\mathbf{r}, t) + \xi(\mathbf{r}, t) \tag{1.57}$$

where the noise term is given by

$$\xi(\mathbf{r}, t) = \int_{-\infty}^{\infty} d\zeta\eta(\mathbf{r}, \zeta + h(\mathbf{r}, t))f'(\zeta) \tag{1.58}$$

The noise term has zero mean and correlation function

$$\langle \xi(\mathbf{r}, t)\xi(\mathbf{r}', t')\rangle = 2\alpha T\delta(t - t')\delta(\mathbf{r} - \mathbf{r}') \int_{-\infty}^{\infty} d\zeta d\zeta'\delta(\zeta - \zeta')f'(\zeta)f'(\zeta')$$

$$= 2\alpha T\delta(t - t')\delta(\mathbf{r} - \mathbf{r}') \int_{-\infty}^{\infty} d\zeta f'^2(\zeta) = \frac{2\alpha T\sigma}{\kappa}\delta(t - t')\delta(\mathbf{r} - \mathbf{r}') \quad (1.59)$$

This now gives

$$\frac{\partial h(\mathbf{r}, t)}{\partial t} = \kappa\alpha\nabla^2 h(\mathbf{r}, t) + \eta(\mathbf{r}, t) \quad (1.60)$$

where

$$\langle \eta(\mathbf{r}, t)\eta(\mathbf{r}', t')\rangle = \frac{2\alpha T\kappa}{\sigma}\delta(t - t')\delta(\mathbf{r} - \mathbf{r}') \quad (1.61)$$

Now defining $\alpha' = \frac{\kappa\alpha}{\sigma}$ we can write

$$\frac{\partial h(\mathbf{r}, t)}{\partial t} = \alpha'\sigma\nabla^2 h(\mathbf{r}, t) + \eta(\mathbf{r}, t) \quad (1.62)$$

This has the form of model $A$ dynamics (as in Eq. (1.27)) for the height profile with Hamiltonian $H_{eff}$ as given in (1.47), that is to say we can write

$$\frac{\partial h(\mathbf{r}, t)}{\partial t} = -\alpha'\frac{\delta H_{eff}[h]}{\delta h(\mathbf{r})} + \eta(\mathbf{r}, t) \quad (1.63)$$

with

$$\langle \eta(\mathbf{r}, t)\eta(\mathbf{r}', t')\rangle = 2T\alpha'\delta(t - t') \quad (1.64)$$

This dynamical calculation is thus consistent with the idea of describing the surface in terms of a height variable with an energy given by the surface tension. The equation (1.63) is known as the Edwards-Wilkinson equation [14, 15]. We can use this equation to determine how the domains of a coarsening system grow at low temperatures. To do this we ignore the noise term and assume that at $t = 0$ the correlations of the height are short range. so

$$C(\mathbf{r} - \mathbf{r}', 0) = \langle h(\mathbf{r}, 0)h(\mathbf{r}', 0)\rangle = C_0\delta(\mathbf{r} - \mathbf{r}') \quad (1.65)$$

In Fourier space the noiseless Edwards-Wilkinson equation becomes

$$\frac{\partial \tilde{h}(\mathbf{k}, t)}{\partial t} = -\alpha'\sigma\tilde{h}(\mathbf{k}, t) \quad (1.66)$$

and so we find

$$\tilde{h}(\mathbf{k}, t) = h(\mathbf{k}, 0) \exp(-\alpha' \sigma \mathbf{k}^2 t) \tag{1.67}$$

The two point correlation function becomes

$$\langle \tilde{h}(\mathbf{k}, t) \tilde{h}(\mathbf{k}', t') \rangle = \langle h(\mathbf{k}, 0) h(\mathbf{k}', 0) \rangle \exp(-\alpha' \sigma [k^2 + k'^2] t) \tag{1.68}$$

Now recall that if

$$\langle h(\mathbf{r}, t) h(\mathbf{r}', t') \rangle = C(\mathbf{r} - \mathbf{r}', t) \tag{1.69}$$

then

$$\langle \tilde{h}(\mathbf{k}, t) \tilde{h}(\mathbf{k}', t') \rangle = (2\pi)^d \delta(\mathbf{k} + \mathbf{k}') \tilde{C}(\mathbf{k}, t) \tag{1.70}$$

where

$$\tilde{C}(\mathbf{k}, t) = \int d\mathbf{r} \exp(-i\mathbf{k} \cdot \mathbf{r}) C(\mathbf{r}, t) \tag{1.71}$$

is the Fourier transform of the correlation function, which is a function of a single position due to invariance by translation in space, and $d$ is the dimension of space (so here $d = 2$ for a surface in 3d space and $d = 1$ for a surface in a 2d space). Putting all this together gives

$$\tilde{C}(\mathbf{k}, t) = C_0 \exp(-2\alpha' \sigma k^2 t) \tag{1.72}$$

Inverting the Fourier transform, we have

$$C(\mathbf{r}, t) = \frac{C_0}{(8\pi \alpha' \sigma t)^{\frac{d}{2}}} \exp(-\frac{\mathbf{r}^2}{16\pi \alpha' \sigma t}) \tag{1.73}$$

From this we see that if $C(\mathbf{r}, t) \sim g(\frac{\mathbf{r}}{\ell(t)}) r(t)$ then the length scale $\ell(t) \sim t^{\frac{1}{2}}$, this agrees with what is found in the Ising model under Glauber dynamics, where the growth exponent is also given by $z = \frac{1}{2}$ [16].

### 1.2.2.2   Model B dynamics

For model B dynamics, we take the same ansatz as in Eq. (1.55) but we rewrite the model B dynamics as

$$-\nabla^{-2} \frac{\partial \phi(\mathbf{x}, t)}{\partial t} = -D \frac{\delta H}{\delta \phi(\mathbf{x})} + \theta(\mathbf{x}, t) \tag{1.74}$$

here $-\nabla^{-2}$ represents the Green's function $G$ which obeys

$$\nabla^2 G(\mathbf{x} - \mathbf{x}') = -\delta(\mathbf{x} - \mathbf{x}') \tag{1.75}$$

and

$$\theta(\mathbf{x}, t) = -\nabla^{-2}\eta(\mathbf{x}, t) = \int d\mathbf{x}' G(\mathbf{x} - \mathbf{x}')\eta(\mathbf{x}, t) \tag{1.76}$$

The correlation function of $\theta(\mathbf{x}, t)$ is given by

$$
\begin{aligned}
\langle\theta(\mathbf{x}, t)\theta(\mathbf{y}, t')\rangle = & -2DT\delta(t - t')\int d\mathbf{x}' G(\mathbf{x} - \mathbf{x}')d\mathbf{y}' G(\mathbf{y} - \mathbf{y}')\nabla^2\delta(\mathbf{x}' - \mathbf{y}') \\
= & -2DT\delta(t - t')\int d\mathbf{x}' G(\mathbf{x} - \mathbf{x}')d\mathbf{y}'\nabla^2 G(\mathbf{y} - \mathbf{y}')\delta(\mathbf{x}' - \mathbf{y}') \\
= & \, 2DT\delta(t - t')G(\mathbf{x} - \mathbf{y})
\end{aligned}
\tag{1.77}
$$

where we have integrated by parts in the second line and used

$$-\nabla^2 G(\mathbf{y} - \mathbf{y}') = \delta(\mathbf{y} - \mathbf{y}') \tag{1.78}$$

in the third.

Now multiplying by $f'(z - h(\mathbf{r}, t))$ and integrating $z$ over $[-\infty, \infty]$, we find

$$-\int dz f'(z - h(\mathbf{r}, t))\int dz' d\mathbf{r}' \; G(z - z', \mathbf{r} - \mathbf{r}')f'(z' - h(\mathbf{r}', t))\frac{\partial h(\mathbf{r}', t)}{\partial t} = -D\sigma\nabla^2 h(\mathbf{r}, t) + \chi(\mathbf{r}, t), \tag{1.79}$$

with the noise

$$\chi(\mathbf{r}, t) = \int dz f'(z - h(\mathbf{r}, t))\theta(\mathbf{r}, z, t). \tag{1.80}$$

As we assume that the height fluctuations are small, we keep only the lowest order terms in $h$ in the deterministic terms and the noise, we will see later that this is compatible thermodynamically. We thus have

$$-\int dz \; f'(z)\int dz' d\mathbf{r}' \; G(z - z', \mathbf{r} - \mathbf{r}')f'(z')\frac{\partial h(\mathbf{r}', t)}{\partial t} = -D\sigma\nabla^2 h(\mathbf{r}, t) + \chi(\mathbf{r}, t) \tag{1.81}$$

and now the noise is given by

$$\chi(\mathbf{r}, t) = \int dz \; f'(z)\theta(\mathbf{r}, z', t) \tag{1.82}$$

This equation which is linear in $h$ can now be Fourier transformed in the plane $\mathbf{r}$. In terms of the Fourier transform of $h$ we find

$$-\int dz \ f'(z) \int dz' d\mathbf{r}' \ \tilde{G}(z - z', \mathbf{k}) f'(z') \frac{\partial \tilde{h}(\mathbf{k}, t)}{\partial t} = Dk^2 \sigma \tilde{h}(\mathbf{k}, t) + \tilde{\chi}(\mathbf{k}, t) \qquad (1.83)$$

The Fourier transform of $G$ in the $\mathbf{r}$ plane obeys

$$\frac{d^2 \tilde{G}(z - z', \mathbf{k})}{dz^2} - k^2 \tilde{G}(z - z', \mathbf{k}) = -\delta(z - z') \qquad (1.84)$$

and the solution to this equation (with the boundary condition that $\tilde{G}(z - z', \mathbf{k}) \to 0$ as $|z - z'| \to \infty$) is

$$\tilde{G}(z - z', \mathbf{k}) = \frac{\exp(-k|z - z'|)}{2k} \qquad (1.85)$$

where we note $k = |\mathbf{k}|$. Next we make the sharp interface approximation where we write

$$f(z) = 2\phi_c \delta(z) \qquad (1.86)$$

that is to say we have replaced the smooth kink solution with a step like solution $f(z) = \phi_c \ \text{sgn}(z)$. This then gives

$$-4\phi_c^2 \tilde{G}(0, k) \frac{\partial h(\mathbf{k}, t)}{\partial t} = Dk^2 \sigma \tilde{h}(\mathbf{k}, t) + \tilde{\chi}(\mathbf{k}, t) \qquad (1.87)$$

which we rewrite as

$$\frac{\partial \tilde{h}(\mathbf{k}, t)}{\partial t} = -\frac{Dk^3 \sigma}{2\phi_c^2} \tilde{h}(\mathbf{k}, t) + \tilde{\xi}(\mathbf{k}, t) \qquad (1.88)$$

with

$$\tilde{\xi}(\mathbf{k}, t) = -\frac{k}{2\phi_c^2} \tilde{\chi}(\mathbf{k}, t) \qquad (1.89)$$

where

$$\tilde{\chi}(\mathbf{k}, t) = \int dz \ f'(z) \tilde{\theta}(\mathbf{k}, z, t) \qquad (1.90)$$

The correlation function of $\tilde{\theta}(\mathbf{k}, t)$ is

$$\langle \theta(\mathbf{k}, t) \theta(\mathbf{k}', t') \rangle = 2DT(2\pi)^d \delta(t - t') \delta(\mathbf{k} + \mathbf{k}') \tilde{G}(z - z', k) \qquad (1.91)$$

From this we find

$$\langle\chi(\mathbf{k},t)\chi(\mathbf{k}',t')\rangle = 2DT(2\pi)^d\delta(t-t')\delta(\mathbf{k}+\mathbf{k}')\int dz\,dz'\,f(z)f(z')\tilde{G}(z-z',k) \qquad (1.92)$$

Now, using the sharp interface approximation Eq. (1.86), we obtain

$$\langle\chi(\mathbf{k},t)\chi(\mathbf{k}',t')\rangle = 2DT(2\pi)^d\delta(t-t')\delta(\mathbf{k}+\mathbf{k}')\frac{2\phi_c^2}{k} \qquad (1.93)$$

and consequently

$$\langle\xi(\mathbf{k},t)\xi(\mathbf{k}',t')\rangle = 2DT(2\pi)^d\delta(t-t')\delta(\mathbf{k}+\mathbf{k}')\frac{k}{2\phi_c^2} \qquad (1.94)$$

Finally in we find the interface dynamics for model B in Fourier space is

$$\frac{\partial h(\mathbf{k},t)}{\partial t} = -\frac{Dk^3\sigma}{2\phi_c^2}\tilde{h}(\mathbf{k},t) + \tilde{\xi}(\mathbf{k},t) \qquad (1.95)$$

In real space this has the form

$$\frac{\partial h(\mathbf{r})}{\partial t} = -L\frac{\delta H_{eff}}{\delta h(\mathbf{r})} + \xi(\mathbf{r},t) \qquad (1.96)$$

where the operator $L$ is defined via its Fourier transform

$$\tilde{L}(\mathbf{k}) = \frac{Dk}{2\phi_c^2} \qquad (1.97)$$

Now if we look at Eq. (1.95) we see that solving the equation without noise will give a function of $k^3t$, which in real space corresponds to $x^3/t$. From this we see that the coarsening length scale grows as $\ell(t) \sim t^{\frac{1}{3}}$ and consequently the coarsening exponent is $z = \frac{1}{3}$. Coarsening for conserved model B or diffusive dynamics is slower than that of model A [17]. One of the reasons for this slowing down with respect to nonconserved dynamics is that material must be physically transported by diffusion (by exchanging spins in the language of lattice spin models), where as for model A dynamics the composition can change at any given point by *spin flipping*. As a cautionary note, if we had taken the Hamiltonian in Eq. (1.47) and applied model B conserved dynamics, as in Eq. (1.31), for the height field we would not have obtained this equation.

We can actually do better than the above sharp interface approximation as Eq. (1.83) can be written as

$$Q(k)\frac{\partial \tilde{h}(\mathbf{k},t)}{\partial t} = -Dk^2 \sigma \tilde{h}(\mathbf{k},t) - \tilde{\chi}(\mathbf{k},t) \tag{1.98}$$

where

$$Q(k) = \int dz dz' \ f'(z) \ \tilde{G}(z-z',\mathbf{k})f'(z') \tag{1.99}$$

Notice that from Eq. (1.98) that

$$\langle \chi(\mathbf{k},t)\chi(\mathbf{k}',t')\rangle = 2DT(2\pi)^d \delta(t-t')\delta(\mathbf{k}+\mathbf{k}')Q(k) \tag{1.100}$$

and so

$$\frac{\partial \tilde{h}(\mathbf{k},t)}{\partial t} = -\tilde{L}(k)\tilde{\mu}(\mathbf{k}) + \eta(\mathbf{k}) \tag{1.101}$$

where $\mu(\mathbf{x}) = \delta H_{eff}/\delta h(\mathbf{x})$, $\tilde{L}(k) = D/Q(k)$ and

$$\langle \eta(\mathbf{k},t)\eta(\mathbf{k}',t')\rangle = 2T(2\pi)^d \delta(t-t')\delta(\mathbf{k}+\mathbf{k}')\tilde{L}(k) \tag{1.102}$$

## 1.3   Lattice models

### 1.3.1   The Ising model

We take a system of size $L' \times L' \times L$, composed of $N$ sites $i$. At each site corresponds a value $\sigma_i = \pm 1$. The Hamiltonian of the Ising model is

$$H = -\sum_{\langle ij \rangle} J\sigma_i \sigma_j + \frac{V(\sigma_i) + V(\sigma_j)}{2} \tag{1.103}$$

where $\sum_{\langle ij \rangle}$ is a sum over all pairs of nearest neighbours, and the external field $V(\sigma_i)$ has been symmetrized. The Ising model[18, 19] is therefore a lattice model with short interactions between particles. Since all particles $\sigma_i$ in the system are equal to $\pm!$, this system is called a lattice based spin model. When $\sigma_i$ is continuous, it is called the XY model [20]. $J$ is called the coupling parameter of the system, and can be non-uniform, with the nearest neighbours interaction being $J = J_{ij}$. If $J_{ij} = 0$, the system favourises homogeneous phases and is called ferromagnetic. Otherwise, the system favourises configurations where each spin has an opposite sign with respect to all of their neighbours, which modelises antiferromagnetic materials. We will pose $J = 1$.
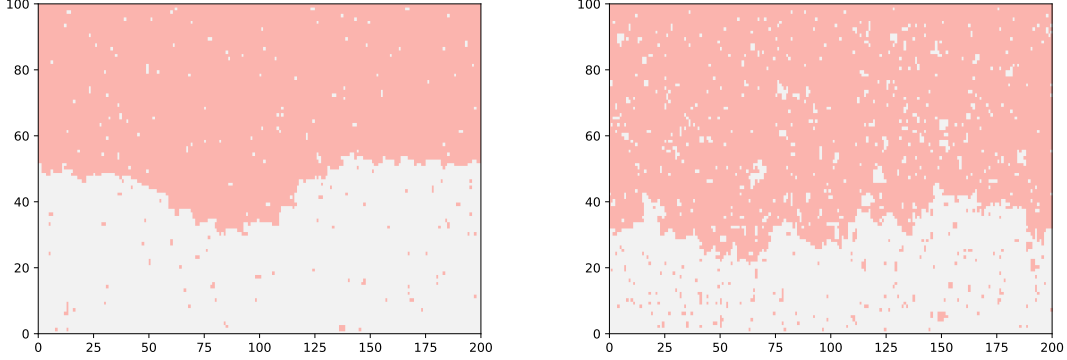
Figure 1.4: Snapshot of Monte Carlo simulations of the Ising model for two different temperatures in two dimensions($T = 0.7T_C$ (left) and $T = 0.95T_C$ (right)) with periodic boundary conditions in $x$ and fixed ones in $y$.

The mean-field theory with a $\phi^4$ potential has been developed from this model [21]. Exact relationship between both of them has been found in 4 dimensions and above [22]. A fast way to convince ourselves is to take the finite difference derivative at first order of Eq (1.18). If we suppose the sole role of the potential is to set the field to $\pm\phi_C$ on each site, then we have

$$
\begin{aligned}
[\boldsymbol{\nabla}\phi(i)]^2 &= \left(\frac{\partial\phi(i)}{\partial x}\right)^2 + \left(\frac{\partial\phi(i)}{\partial y}\right)^2 + \left(\frac{\partial\phi(\mathbf{i})}{\partial z}\right)^2 \\
&= (\phi(x,y,z) - \phi(x+1,y,z))^2 + (\phi(x,y,z) - \phi(x,y+1,z))^2 + (\phi(x,y,z) - \phi(x,y,z+1))^2 \\
&= 2(1 - \phi(x,y,z)\phi(x+1,y,z)) + 2(1 - \phi(x,y,z)\phi(x,y+1,z)) + 2(1 - \phi(x,y,z)\phi(x,y,z+1))
\end{aligned}
$$
(1.104)

where we've set the distance between two sites to 1. From this we easily see some bulk energy to which we add the sites' nearest neighbours interactions in an Ising-like fashion.

This model precisely describes phase transitions in uniaxial magnetic systems[23, 24, 25]. It is also the simplest model of its eponymous universality class, which also contains liquid/gas transitions and binary fluids.This model does not have a phase transition in 1D,

but a phase transition in 2D was foumd in 1944[5] at the critical temperature

$$T_{2D,C} = \frac{2J}{k_B \ln(1 + \sqrt{2})} \simeq 2.27 \frac{J}{k_B} \tag{1.105}$$

The renormalization group approaches have a deep connexion with the Ising model [26, 27]. Even though results have been found for $d = 4$ (which is the upper critical dimension), no analytical solution has been found in 3 dimensions. Numerous numerical simulations [28, 29] have shown that the 3-dimensional phase transition occurs at

$$T_{3D,C} \simeq 4.51 \frac{J}{k_B} \tag{1.106}$$

By doing the transformation[27]

$$n_i = \frac{\sigma_i + 1}{2} \tag{1.107}$$

so that $n_i(\sigma_i = 1) = 1$ and $n_i(\sigma_i = -1) = 0$, we obtain

$$H = -\sum_{\langle ij \rangle} J_{ij} \left(4n_i n_j - 2(n_i + n_j) + 1\right) + \sum_{\langle ij \rangle} J_{ij} \frac{V(\sigma_i) + V(\sigma_j)}{2} \tag{1.108}$$

where the constant term $\sum_{\langle ij \rangle} J_{ij}$ does not change the partition function behaviour. We have then

$$\begin{aligned} H_{LG} &= -4 \sum_{\langle ij \rangle} J_{ij} n_i n_j + 2 \sum_{\langle ij \rangle} J_{ij}(n_i + n_j) + \sum_{\langle ij \rangle} J_{ij} \frac{V(\sigma_i) + V(\sigma_j)}{2} \\ &= -4J \sum_{\langle ij \rangle} J n_i n_j + \mu \sum_i n_i + \sum_{\langle ij \rangle} J \frac{V(\sigma_i) + V(\sigma_j)}{2} \end{aligned} \tag{1.109}$$

where we have set $J_{ij} = J$ constant and defined the chemical potential for a liquid-gas system as $\mu = 4Jc$, with $c$ the number of nearest neighbours. A positive magnetic phase is thus analogous to a high density state such a liquid, while the negative magnetic phase is equal to a low density state such as a gas. The model also describes adsorption of a gas in a lattice or binary fluids between particles $A$ and $B$. The chemical potential $\mu$ is the conjugate variable to the total number of particles $\sum_i n_i$ in the grand-canonical ensemble, while the magnetic field $h$ is the conjugate variable to the total magnetisation $\sum_i \sigma_i$.

By imposing $+-$ boundary conditions in the $z$ direction, we force the existence of an

interface Those BC can be fixed, imposing $\sigma(z = 0) = -1$ and $\sigma(z = L) = +1$, or free but with a local external field $V(z) = h(\delta_{0,z} - \delta_{z,L})$. An interface is characterized by its mean and its width. The easiest way to do so is to fit the magnetization profile

$$m(z) = \frac{1}{L'^2}\langle\sum_{xy}\sigma(x, y, z)\rangle \tag{1.110}$$

to mean field results from Eq (1.43) . The mean position of the interface is

$$m = \langle h\rangle = \frac{1}{L'^2}\langle\sum_i\sigma_i\rangle \tag{1.111}$$

The width of the interface is then defined as

$$w^2 = \langle h^2\rangle - \langle h\rangle^2 \tag{1.112}$$

This can be rewrtiten [30] as

$$w^2 = 2\frac{\int_0^L dz z\frac{dm(z)}{dz}}{\int_0^L dz\frac{dm(z)}{dz}} \tag{1.113}$$

We now defined the surface tension of the interface as the free energy difference between the bulk and interface [31]. Is $Z^{++}$ si the partition function of a system with $(++)$ BC, and $Z^{+-}$ with $(+-)$ BC, then the surface tension [32] is given by

$$\sigma = \lim_{L',L\to\infty}\frac{1}{L'^2}\ln\left(\frac{Z^{+-}}{Z^{++}}\right) \tag{1.114}$$

By diagonalization of the transfer matrix (which we will define later), we find that the surface tension of a the interface between two pure phases $+$ and $-$ is given in a two-dimensional Ising model [33] by

$$\sigma = 2\beta J + \log(\tanh(\beta J)) \tag{1.115}$$

### 1.3.2   The Solid-On-Solid Model

In order to get the Edwards-Wilkinson equation of an interface from statistical field theory, we have used the approximation

$$\phi(\mathbf{x}, t) = f(z - h(\mathbf{r}, t)) \tag{1.116}$$

We translate the same approximation in order to study interfaces in lattice models by

$$\sigma_{i,j} = \text{sgn}(h_i - j) \tag{1.117}$$

where $\text{sgn}(x < 0) = -1$ and $\text{sgn}(x > 0) = 1$, and $h_i$ is the height of the interface at site $i$. This is the low temperature approximation of the Ising model, where there are no overhangs from the $+$ phase into the $-$ phase and vice versa. If we note $J_\perp$ the vertical bond energy between two Ising spins and $J_\parallel$ the horizontal bond energy, this approximation becomes equivalent to a highly anisotropic Ising model where $J_\perp \gg J_\parallel$ [34].

In a slab or semi-infinite geometry as seen in Fig 1.5, the height of the interface corresponds to the number of spins $-$ in the column $i$, while for an infinite geometry, we define $h_i$ as the number of excess spins $-$ with respect to the mean height, set in the figure at $= 0$ [35]. In this representation, height profiles represent an interface height and not a number of particles, since there is no entropy term associated with the number of ways that the $h_i$ particles on each site can be chosen from the $N$ particles available. In chapter 5, we will address a model with those characteristics. Using the identities

$$\min(a, b) = \frac{|a + b| - |a - b|}{2} \tag{1.118}$$

$$\max(a, b) = \frac{|a + b| + |a - b|}{2} \tag{1.119}$$

we have

$$\sum_{j=0}^{L} \text{sgn}(h - j)\,\text{sgn}(h' - j) = L - 2|h - h'| \tag{1.120}$$
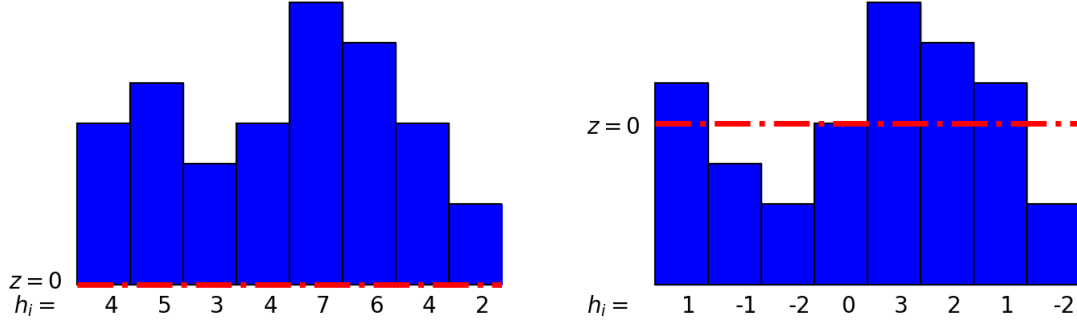
Figure 1.5: Possible configuration of the SOS model for a semi-infinite geometry (left) and infinite geometry (right). The red line shows the origin $z = 0$. In the $i$-th column the interface is at height $h_i$. Particles under the interface are from the Ising $-$ phase, while particles over it are from the $+$ phase.

For a 2-D Ising model of size $L' \times L$, the Ising Hamiltonian (1.103) is rewrtiten as

$$H = 2JL'(1 - L) + 2J \sum_{i=0}^{L'} |h_i - h_{i+1}| + \sum_{i=0}^{L'} V(h_i) \tag{1.121}$$

with external potential

$$V(h_i) = \sum_{j=0}^{L} V(\text{sgn}(h_i - j)) \tag{1.122}$$

For periodic boundary conditions, we set $h_{L'} = h_0$.

Another way to compute this energy for a SOS configuration is to directly count the number of energy bonds for a $L' \times L$ Ising model under the approximation (1.117). There are $L - 1$ vertical bonds per column, where all have an energy of $-J$, while the link that goes though the interface has an energy of $+J$. The total contribution to energy from vertical bonds is thus

$$E_\perp = -JL'(L - 2) \tag{1.123}$$

There are $L' \times L$ horizontal bonds. In a pure phase system, the horizontal energy would be $-JL'L$. Neverthelesss, there are $\sum_i |h_i - h_{i+1}|$ bonds which have an energy of $+J$, which

gives the horizontal energy contribution

$$E_{\parallel} = -JL'L + 2\sum_i |h_i - h_{i+1}|  \qquad (1.124)$$

By adding both, we find back Eq (1.121).

By setting $2J = J$ and getting rid of the bulk energy, we obtain the **Solid-On-Solid Hamiltonian**

$$H = J\sum_{i=0}^{L'} |h_i - h_{i+1}| + \frac{V(h_i) + V(h_{i+1})}{2} \qquad (1.125)$$

The first system where the SOS model has been applied was crystals' growth in 1972 [36]. Since then, the model has been used with some success in naphthalene cristals[37], experimental expitaxial growth[38], polymer membranes [39], or interfacial wetting [40].

In the SOS model, the sites $i$ of height $h_i$ can take any value in $[0, L]$. The Restrictied Solid-On-Solid model (RSOS) is a variation where sites can only take the value $h_{i+1} \in [h_i - 1, h_i, h_i + 1]$[41]. This approximation works for very low temperatures or very smooth interfaces [42, 43].

Another model, closer to the continuous model of Hamiltonian (1.47) is the Discrete Gaussian model which has the following gaussian interaction

$$H = J\sum_{i=0}^{L'} (h_i - h_{i+1})^2 + \frac{V(h_i) + V(h_{i+1})}{2} \qquad (1.126)$$

and also has a restricted version. The SOS model has an exact relation with the $XY$ model [44], no matter the power law used for the interaction. With a generalization of this model to continuous heights, it has been shown that extreme deviations statistics of the interface is described by a scaling function [45]. Since the energy costs of height differences $0, \pm 1$ are the same in every SOS model no matter the exponent in the energy costs of height differences, one expects the qualitative freatures of all those models to be the same at low temperature, since height differences are typically small [46].

Since the dimensionality of the system has been reduced in only taking into account the height interface $h_i$ at site $i$ instead of the position of all particles, we can think of an interface as a partially self-avoiding walk. This idea, which will be developed in section

**??**, has proven quiet powerfull in finding exact solutions of the generating function [47] or the extreme deviations statistics of the interface [48, 45].

In the canonical ensemble, the height interface is fixed to $N$, which is translated in the partition function as

$$Z(N) = \sum_{h_0 h_1 \dots h_{L'}} \exp(-\beta \sum_i H(h_i, h_{i+1})) \delta_{\sum_i h_i, N} \tag{1.127}$$

In the grand-canonical ensemble, the conjugate variable to the height interface is the chemical potential $\mu$, and the grand partition function $\Xi$ is related to the canonical partition function by

$$
\begin{aligned}
\Xi(\mu) &= \sum_N Z(N) \exp((\beta \mu N) \\
&= \sum_{h_0 h_1 \dots h_{L'}} \exp(-\beta H_{eff}(h_0, h_1, \dots, h_{L'}))
\end{aligned}
\tag{1.128}
$$

where

$$H_{eff} = J \sum_{i=0}^{L'} |h_i - h_{i+1}| + \sum_{i=0}^{L'} V(h_i) - \mu h_i \tag{1.129}$$

In Fig 1.6, we plot the mean number of particles per site with respect to the chemical potential, for different size of the system, in the thermodynamic limit $L' \to \infty$. When the chemical potential is too small, the Lagrange's multiplier of the mean height is negligible, allowing the interface to fluctuate freely. Since the height of the interface is then evenly spread over all possible configurations, the mean value for $\mu = 0$ becomes $\frac{L}{2}$.

### 1.3.3 Transfer matrix

In a more general fashion, we can rewrite the Hamiltonian as

$$H = \sum_{i=0}^{L'} f(h_i, h_{i+1}) + V(h_i, h_{i+1})$$
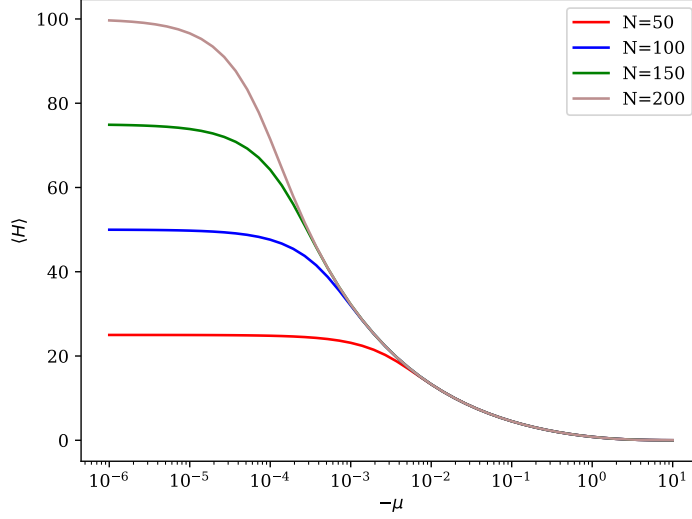
Figure 1.6: Mean height of the SOS interface (1.128) with respect to $-\mu$ through diagonalization of the transfer matrix for $\beta = 1$, in the limit $L' \to \infty$.

where $f(h_i, h_j)$ is the energy interaction between two nearest neighbours and $V(h_i, h_j) = \frac{V(h_i) + V(h_j)}{2}$ is the external potential. We can rewrite the partition function as

$$Z = \sum_{h_1=0}^{L} \sum_{h_2=0}^{L} ... \sum_{h_{L'}=0}^{L} \exp(-\beta \sum_{i=0}^{L'} H(h_i, h_{i+1})) = \sum_{h_1 h_2 ... h_{L'}} \prod_{i=0}^{L'} \exp(-\beta H(h_i, h_{i+1})) \quad (1.130)$$

We define the transfer matrix

$$T(h_i, h_j) = e^{-\beta H(h_i, h_j)} \quad (1.131)$$

In Fig 1.7, we have represented an infinite matrix corresponding the limit $L \to \infty$, where each site can take any value in $[-\infty, \infty]$. To diagonalize numerically such matrices, we translate the whole system with $h_i \to h_i - \frac{L}{2}$, where $L$ is the matrix's size, which me make tend to $\infty$. The constraint (1.127) cannot be expressed in the transfer matrix formalism, which induces a change in properties from this ensemble with respect to the transfer matric results [49].

Since the system has periodic boundary conditions $h_{L+1} = h_1$, we have $T(h_L, h_{L+1}) =$

$$
T = \begin{bmatrix}
\ddots & \vdots & \cdot^{\cdot^{\cdot}} \\
e^{-\beta H(-1,-1)} & e^{-\beta H(-1,0)} & e^{-\beta H(1,-1)} \\
\cdots & e^{-\beta H(0,0)} & \cdots \\
e^{-\beta H(1,-1)} & e^{-\beta H(1,0)} & e^{-\beta H(1,1)} \\
\cdot^{\cdot^{\cdot}} & \vdots & \ddots
\end{bmatrix}
\tag{1.135}
$$

Figure 1.7: Infinite and symmetrical transfer matrix 1.131.

$T(h_L, h_1)$ [50]. The matrix is thus symmetric, which means it can be diagonalized with eigenvectors and eigenvalues

$$
T|\lambda\rangle = \lambda|\lambda\rangle
\tag{1.132}
$$

Those eigenvectors are orthonormal

$$
\langle\lambda|\lambda'\rangle = \delta_{\lambda\lambda'}
\tag{1.133}
$$

We set $\lambda_0$ as the biggest eigenvalue of $T$, by $\lambda_1$ the second biggest eigenvalue, and so on. The partition function can then be rewritten, in terms of the transfer matrix [33] by

$$
Z = \sum_{h_1 h_2 \ldots h_{L'}} \prod_i T(h_i, h_{i+i}) = Tr(T^{L'}) = \sum_\lambda \langle\lambda|T^{L'}|\lambda\rangle = \sum_\lambda \lambda^{L'}
\tag{1.134}
$$

In the thermodynamic limit $L' \to \infty$, only the biggest eigenvector is relevant since the partition function becomes

$$
Z(L \to \infty) \simeq \lambda_0^{L'}
\tag{1.136}
$$

We find that the free energy per site is

$$
\Omega = -\frac{1}{L'\beta}\ln(Z) \simeq -\frac{1}{\beta}\ln(\lambda_0)
\tag{1.137}
$$

In Fig 1.8 we plot the evolution of the free energy per site $\Omega(L')$ without external field, compared to the thermodynamic limit. We determine that the thermodynamic limit becomes valid for $L' > 150$.
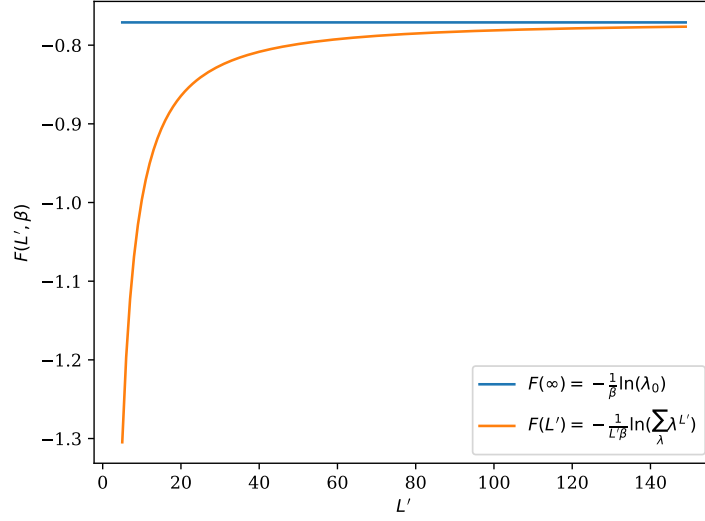
Figure 1.8: Free energy per site $\Omega(L')$ with respect to the number of sites $L'$ compared to the thermodynamic value $\Omega(\infty)$, for a system of maximum height $L = 100$, $\beta = 1$, $J = 1$ and $V(h_i) = 0$.

To compute the mean height value per site $M$, we introduce the height matrix $\hat{M}$ defined by its action over the vectors $|h\rangle$ in the matrix transfer's base by

$$= \delta_{h,h'} h \tag{1.138}$$

We thus find that the density is

$$M = \langle h \rangle = \frac{1}{L'} \sum_i h_i = \frac{1}{Z} \sum_\lambda \lambda^{L'} \langle \lambda | \hat{M} | \lambda \rangle \simeq \langle \lambda_0 | \hat{M} | \lambda_0 \rangle \tag{1.139}$$

We deduce the mean displacement per site

$$w^2 = \langle (h - M)^2 \rangle = \frac{1}{Z} \sum_\lambda \lambda^{L'} \langle \lambda | \hat{M}^2 | \lambda \rangle - \langle \lambda | \hat{M} | \lambda \rangle^2 \simeq \langle \lambda_0 | \hat{M}^2 | \lambda_0 \rangle - M^2 \tag{1.140}$$

We can find thos two obersables by computing the first and second moment of the proba-

bility distribution that a site $i$ is at height $h_i$

$$p(h) = \frac{1}{Z} \sum_\lambda \lambda^{L'} \langle \lambda | h \rangle^2 \simeq \langle \lambda_0 | h \rangle^2 \tag{1.141}$$

The two-point correlation function of the system is computed by

$$C(r) = \langle h_i h_{i+r} \rangle - M^2 = \frac{1}{Z} \sum_{\lambda \neq \lambda_0} \langle \lambda_0 | M | \lambda \rangle \langle \lambda | M | \lambda_0 \rangle \left( \frac{\lambda}{\lambda_0} \right)^r \tag{1.142}$$

which becomes, in the long distance $r$ limit,

$$C(r) \simeq \langle \lambda_0 | M | \lambda_1 \rangle \langle \lambda_1 | M | \lambda_0 \rangle \left( \frac{\lambda_1}{\lambda_0} \right)^r \tag{1.143}$$

The correlation function has an exponential decay at large distances, which allows us to define the correlation length at large distance $\xi$

$$\xi = -\frac{1}{\ln(\frac{\lambda_1}{\lambda_0})} \tag{1.144}$$

## 1.4 Systems driven by imposed hydrodynamic flows

Here we consider what happens when a system is driven out of equilibrium. By driven we mean that energy is injected into the system by a laser [52], by inducing a hydrodynamics flow, for instance a shear flow induced in a Couette cell in liquids [53, 51] or in glassy materials [54, 55]. In principle we should analyse this system with model H dynamics which couples diffusive model B dynamics to hydrodynamics in the low Reynolds number Stokes flow regime. In these dynamics the order parameter field will itself induce a hydrodynamics flow which will modify the imposed one. However this full situation is very difficult to analyse and to a first approximation we can assume that the back reaction of the order parameter field on the hydrodynamic flow is small with respect to the imposed hydrodynamic flow and so we can simply write

$$\frac{\partial \phi(\mathbf{x}, t)}{\partial t} + \nabla \cdot (\mathbf{v}(\mathbf{x}) \phi(\mathbf{x}, t)) = -L \frac{\delta H}{\delta \phi(\mathbf{x})} + \eta(\mathbf{x}, t), \tag{1.145}$$

where $L$ is given by the underlying model A or B dynamical operator and the noise has the correlation function as given by Eq. (1.26), and $\mathbf{v}(\mathbf{x})$ is the imposed (time indepen-
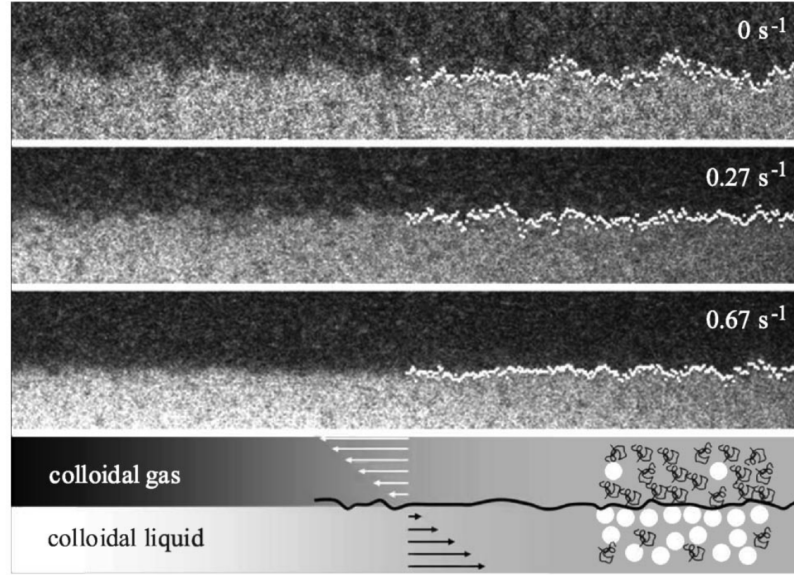
Figure 1.9: Snapshot of the interface a sample of fluorescently labeled poly(methyl methacry-late) (PMMA) colloidal spheres in polystyrene close to the critical point, for different shear rates. The bottom panel schematically shows the flow geometry with the plane of zero velocity located at the interface. From [51].
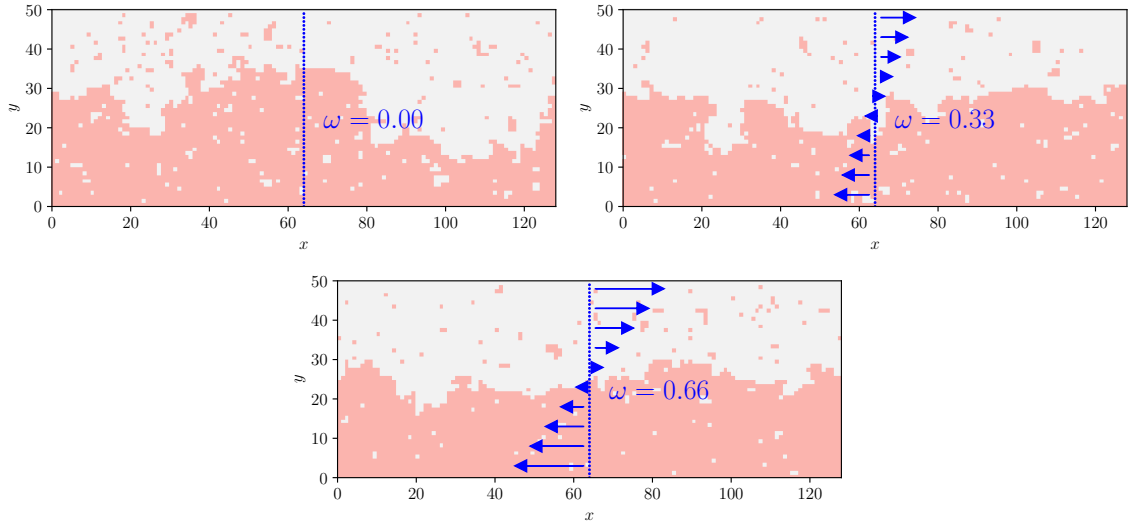


Figure 1.10: Snapshot of a 2D Ising model with respect to the shear (1.147) with Kawasaki dynamics at $T = 0.9T_{2D,C}$.

dent) hydrodynamic flow or can equally well be an external drive imposed on the colloidal particles, due to the gravitational or electric field for example.

The simplest case one can consider is where the driving field $\mathbf{v}(\mathbf{x}) = \mathbf{v}_0$ is uniform [**?** ]. Unfortunately this simple driving does not lead to a new steady state. Basically all of the colloidal particles acquire an average velocity $\mathbf{v_0}$ and so move along at the same speed relative to each other. Mathematically this can be seen by making the Galilean transformation

$$\phi(\mathbf{x}, t) = \phi(\mathbf{x} - \mathbf{v}_0 t, t) = \phi(\mathbf{y}, t) \tag{1.146}$$

This transformation eliminates the driving from the evolution equation (1.145) and so we find an equilibrium system.

The most studied example is where the driving is a shear flow [51, 56]. The effective dynamics of the surface term in the presence of a shear flow, parallel to the interface [12, 13**?** ], is written as

$$\mathbf{v}(\mathbf{x}) = \gamma z \mathbf{e}_x \tag{1.147}$$

and was studied using the method explained in section (**??**). The addition of a shear flow leads to the appearance of a nonlinear term in $h$ and the interface statistics thus become non-Gaussian. In Fig 1.10 we show the influence of such a shear flow in numerical simulations, which is exactly the behaviour to be seen in capillary waves in polymer melts [53, 51], see Fig 1.9 . The shear has a confining effect on the interface [57, 58, 59], thus increasing the effective surface tension of the system.

## 1.5 Conclusion

Statistical field theory [4] gives us a method to study the dynamics of equilibrium fields [21]. The surface tension of such a system is then defined as the difference of free energy between the bulk and the interface [8, 33]. The two main models are model A and model B [3], which decribe the dynamics of a field respectively in grand-canonical and the canonical ensemble. From those equations, we have defined what is an interface and have derived the Edwards-Wilkinson equation [14] for both ensembles. The Ising model [18**?** ] provides a good way to study the bahviour of the field by discretization, which is easier to compute in numerical simulations [60]. The same kind of dimensional reduction can be done in order to get an interface lattice model which is called the Solid-On-Solid model [36]. This model allows the use of the transfer method in an easier way than the Ising model[61]. Also, the

presence of out-of-equilibrum hydrodynamic flows tend to present interesting features. One such example is thee Couette shear [51], which has been found to smoothen the interface [58].

# Chapter 2

# Numerical methods

In 1949, Metropolis [62] discovers a method to compute, through Monte Carlo simulations, the expectation value of statistical quantities. If $Q$ is an observable quantity of a statistical system, such as the total energy or density of particles per site, then the expectation value is computed by weighting its value over all configurations $C$ with respect to their statistical weight. If we consider the system to be at thermodynamic equilibrium, then every configuration $C$ follows the Gibbs-Boltzmann distribution, and the mean value $\langle Q \rangle$ is

$$\langle Q \rangle = \frac{\sum_C Q(C) \exp(-\beta E(C))}{\sum_C \exp(-\beta E(C))} \tag{2.1}$$

For example, in a SOS system of size $100 \times 100$ - which is small compared to the thermodynamic limit as discussed in figure 1.8 - there exist $100^{100}$ different possible configurations. In comparison, numerical simulations can explore up to $10^9$ configurations in a reasonable amount of CPU time.

Nevertheless, lattice models are well fitted for Monte Carlo simulations, where the goal is to compute is to compute such quantities. In the SOS model, all observables (and even quantities not observable such as the free energy) can be directly computed thanks to the matrix transfer in the grand-canonical ensemble. Nevertheless, as stated prior, the canonical ensemble stays out of reach of that method.

In this chapter, we start by explaining how Monte Carlo Metropolis algorithm works based upon the statistical ensemble we're interested in, at or out of equilibrium. At last, I will give some technical considerations about optimizing numerical simulations.

This work has been made possible thanks to the Mésocentre de Calcul Intensif Aquitain (MCIA)[2], where I've made the vast majority of the numerical simulations. All the code I've produced can be found on Github [63] under Creative Commons BY 3.0 licence[1]. Numerical simulations where made with C++, parallelization with MPI, data treatment with Python, and some minor scripts in Bash.

## 2.1   Estimator

Monte Carlo simulations explore the configurations' space in a random fashion [60] with a probability $p(C)$ which we will define later one. By choosing $M$ states $C_0, ..., C_M$, the estimator $Q_M$ of $Q$ is given by

$$Q_M = \frac{\sum_{i=0}^{M} Q(C_i)p(C_i)^{-1}\exp(-\beta E(C_i))}{\sum_{i=0}^{M} p(C_i)^{-1}\exp(-\beta E(C_i))} \tag{2.2}$$

The bigger the $M$, the better estimate the estimator provides for $\langle Q \rangle$, up to the limit $Q_{M\to\infty} = \langle Q \rangle$. If we select the configurations over which we sample the system according to the Gibbs-Boltzmann distribution $p(\nu) = Z^{-1}e^{-\beta E(C)}$, the estimator of $\langle Q \rangle$ is

$$Q_M = \frac{1}{M}\sum_{i=0}^{M} Q(C_i) \tag{2.3}$$

The error over this estimate is

$$E(Q) = \sqrt{\frac{2\tau}{M}(\langle Q^2 \rangle - \langle Q \rangle^2)} \tag{2.4}$$

This error does depend from the correlation time $\tau$ since if two states are really close in time, they would be strongly correlated, adding little information to the estimator. In practice, we just need $\frac{\tau}{M} < 10^{-4}$ to obtain an error under 1%. This correlation time $\tau$ is computed through the autocorrelation function

$$\mathcal{C}(t) = \langle Q(t')Q(t+t') \rangle - \langle Q \rangle^2 = \frac{1}{t}\int_0^t Q(t')Q(t+t') - \langle Q \rangle^2 dt' \tag{2.5}$$

---

[1]`https://creativecommons.org/licenses/by/3.0/fr/deed.en`

which behaves as an exponential at long time[64]. A first order estimate of $\tau$ is thus given
for

$$\tau = \int_0^\infty \mathcal{C}(t)/\mathcal{C}(0)dt \tag{2.6}$$

Similarly, the measurement of the correlation length $\xi$ is given at first order by integration
the two-point correlation function

$$\mathcal{C}(j) = \frac{1}{L'} \sum_{i=0}^{L'} \langle h_i h_{i+j} \rangle - \langle h \rangle^2 \tag{2.7}$$

## 2.2 Monte Carlo Metropolis algorithm

We know want to know how to choose configurations, so all of them has the good equilibrium probability.

A dynamic for systems with a discrete configuration state can be built using Markov chains. Let the dynamic evolve in a discrete time $n$, and $p_n(C)$ the probability that the system is in configuration $C$ at time $n$. On the time step, if the system is in state $C$, it can jump to another state $C'$ with a transition probability $\rho(C \rightarrow C')$. The system at time $n+1$ thus only depends of the state at time $n$ : that's a Markovian process. The probability $p_{n+1}(C)$ to be in state $C$ at time $n+1$ is equal to the probability that the system was already in state $C$ at time $n$ and stays put with a transition probability $\rho(C \rightarrow C)$ , plus the probability that it was in state $C'$ and jumps towards $C$ with a transition probability $\rho(C' \rightarrow C)$. The master equation of such a dynamic is

$$p_{n+1}(C) = \rho(C \rightarrow C)p_n(C) + \sum_{C' \neq C} \rho(C' \rightarrow C)p_n(C') \tag{2.8}$$

Since $\rho(C' \rightarrow C)$ is a probability, it meets the requirements

$$\sum_{C'} \rho(C' \rightarrow C) = 1 \tag{2.9}$$

Now, if the dynamics describes a system in interaction with a heat bath, the equilibrium

distribution is given by

$$p_{eq}(C) = \frac{\exp(-\beta E(C))}{Z} \qquad (2.10)$$

with $Z$ the partition function. Since the equilibrium distribution is also stationary, we have

$$p_{eq}(C) = \rho(C \to C)p_{eq}(C) + \sum_{C' \neq C} \rho(C' \to C)p_{eq}(C') \qquad (2.11)$$

Another condition that we need in order to generate Gibbs-Boltmanzz states, is that it complies with detailed balance. To comply with detailed balance, the transition rate from a state to another one is equal to the rate from the reciprocal transition, which gives

$$\sum_{C'} p(C)\rho(C \to C') = \sum_{C'} p(C')\rho(C' \to C) \qquad (2.12)$$

We can show that this relation is equivalent to [60]

$$\frac{\rho(C' \to C)}{\rho(C \to C')} = \frac{p(C)}{p(C')} = \frac{\exp(-\beta E(C))}{\exp(-\beta E(C'))} \qquad (2.13)$$

By adopting the detailed balance, we easily see that the equilibrium distribution computed by Eq (2.11) gives back the Gibbs-Boltzmann distribution. During a Metropolis step, the transition probability of $C \to C'$ depends of the probability $g(C \to C')$ that this transition would be chosen amongst all the other possible transitions, and the acceptance rate $A(C \to C')$, which gives

$$\rho(C \to C') = g(C \to C')A(C \to C') \qquad (2.14)$$

For a lattice model site $L'$ sites, we say that a Monte Carlo time step is done when we have proceeded to $L'$ transition tries.

### 2.2.1  Glauber dynamics

In the SOS model with $L'$ sites of height comprised in $[0, L]$, the Glauber algorithm [65] makes us chose a site $i$ at random with a uniform probability $\frac{1}{L'}$ and an integer $\alpha = \pm 1$ with probability $\frac{1}{2}$. If the configuration $C$ has the Hamiltonian $H(h_0, h_1..., h_i, ...h_{L'})$, then the new generated configuration will have the Hamiltonian $H(h_0, h_1..., h_i + \alpha, ...h_{L'})$. If

$\alpha = +1$, then we add a particle at site $i$, otherwise we remove one. In the case that $h_i + \alpha \notin [0, L]$, the generated configuration is not valid and discarded. If the generated configuration is valid, the probability of selecting this transition is

$$g(C \to C') = \frac{1}{2L'} \tag{2.15}$$

We thus have

$$\frac{\rho(C \to C')}{\rho(C' \to C)} = \frac{A(C \to C')}{A(C' \to C)} = \exp(-\beta(E(C') - E(C'))) \tag{2.16}$$

Is it possible to choose any acceptance rate $A(C \to C')$ which satisfies detailed balance. A Metropolis algorithm is an algorithm which has the following acceptance rate

$$A(C \to C') = \begin{cases} \exp(-\beta(E(C') - E(C))) & \text{if } E(C') - E(C) > 0 \\ 1 & \text{otherwise} \end{cases} \tag{2.17}$$

In practice, if $\Delta E > 0$, we randomly choose an integer uniformly in $r \in [0, 1]$. If $r < A(C \to C')$ then the transition is accepted. Otherwise, the transition is rejected and the system stays in the configuration $C$.

Since $\sum_i h_i$ is not conserved over time, Glauber dynamics corresponds to model A.

The energy difference between two configurations is

$$\Delta E = |h_{i-1} - (h_i + \alpha)| + |h_{i+1} - (h_i + \alpha)| - |h_{i-1} - h_i| - |h_{i+1} - h_i| \tag{2.18}$$

It is not needed to compute the total height at each time step. We can stock $\sum_i h_i$ in a variable that is updated each time a transition is accepted by

$$\langle h \rangle_{M+1} = \langle h \rangle_M + \alpha \tag{2.19}$$

We can do the same for $\sum_i h_i^2$, which gives us the interface's width, or the total energy of the system with $\sum_i |h_i - h_{i+1}|$.

In order to accelerate the equilibration process, we can directly start from the total height computed by the transfer matrix. We then get the equilibrium time by looking at $E(t)$. It is better practice to choose study the equilibration time by taking the total energy instead of the magnetization, since without external potential, the interface is delocalised

Figure 2.1: Plot of the energy per site (top) and the autocorrelation function (bottom) with Glauber dynamics from an initial state where $h_i = 0$, for different temperatures.
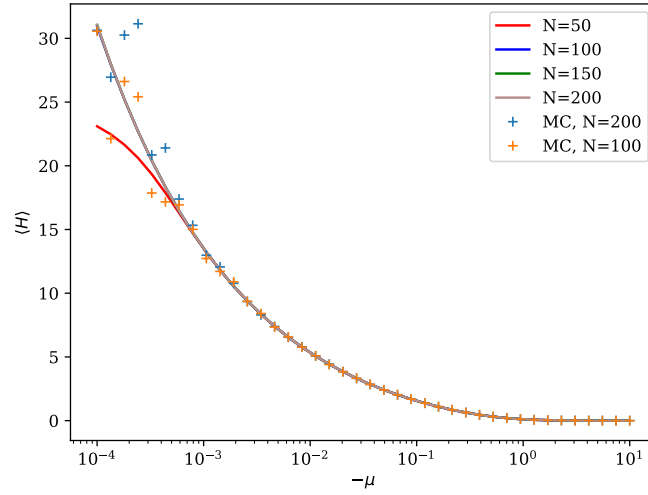


Figure 2.2: Mean height value per site with respect to $\mu$ different system size $L$ both by Glauber dynamics and diagonalization of the transfer matrix (which has already been shown in Fig 1.6) for $\beta = 1$ and $L' = 256$.

and magnetization is only bounded by the boundary conditions. In Fig 2.1, we show the energy with respect to time and the autocorrelation function of the system in absence of chemical potential from a ground state $h_i = 0$ for all $i$. The very small correlation and equilibration times means that numerical simulations reach the equilibrium distribution after $10^3$ MC steps, and that only $10^7$ MC steps will give accurate results.

In the SOS model, we expect to have the results from the Glauber dynamics to be exactly the same as the transfer matrix method, as shown in Fig 2.2. Since the interface is not localised for small $\mu$, even though we reach thermal equilibrium fast, the mean height fluctuates a lot, making its measurement irrelevant in the delocalised limit. Since we can get exact results from the transfer matrix, the Glauber dynamics presents little interest for SOS models in the grand-canonical ensemble. Nevertheless, because there does not exist a transfer matrix formulation of the canonical ensemble, Monte Carlo simulations become interesting.

### 2.2.2 Kawasaki dynamics

Now we would like to have an algorithm for the canonical ensemble, where the total height stays constant. In the Kawasaki's algorithm [66], we randomly choose a site $i$ with probability $\frac{1}{L'}$, and one of its two neares neighboors $i-1$ or $i+1$ with probability $\frac{1}{2}$. For example, if we take the neighboor site $i-1$ (it holds the same for the site $i+1$), we generate a new configuration with Hamiltonian $H(h_0, ..., h_{i-1} + 1, h_i - 1, ...h_{L'})$, where we have taken a particle from site $i$ to diffuse it to the other site. The selection probability is

$$g(C \to C') = \frac{1}{2L'} \tag{2.20}$$

We also chose the same acceptance rate as in Glauber's dynamics (2.17).

Here, the total height is obviously conserved. In the case that we transfer a particle to site $i$ to site $i+1$, the energy difference is

$$\Delta E = |h_{i-1} - (h_i - 1)| + |h_{i+1} + 1 - (h_i - 1)| + |h_{i+1} + 1 - (h_{i+2})|$$
$$- (|h_{i-1} - h_i| + |h_{i+1} - h_i| + |h_{i+1} - h_{i+2}|) \tag{2.21}$$

In Fig 2.3, we remark that both the equilibration and the correlation time are larger than for non-conserved dynamics, which is normal since the correlation length during coarsening goas as $t^{\frac{1}{2}}$ in model A and as $t^{\frac{1}{3}}$ in model B. Nevertheless they are of the same
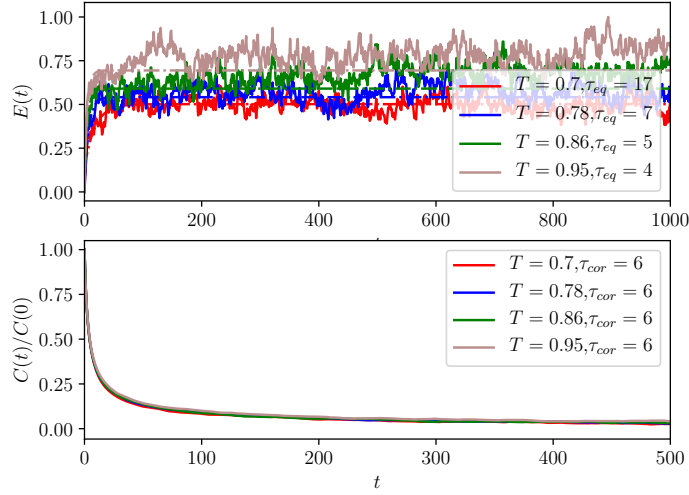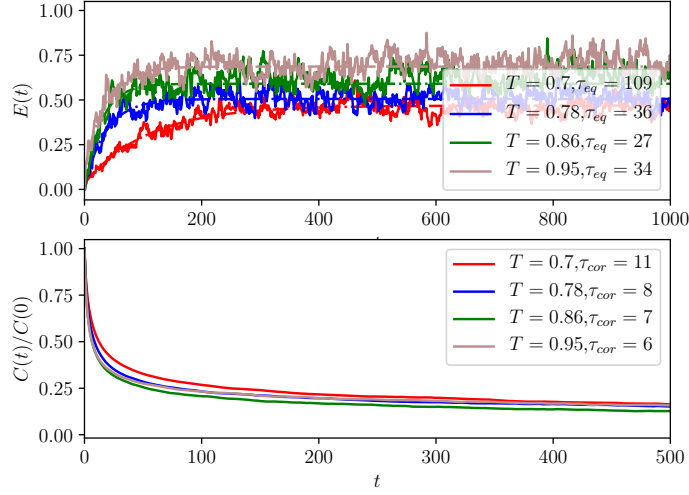
Figure 2.3: Plot of the energy per site (top) and the autocorrelation function (bottom) with Kawasaki dynamics from an initial state where $h_i = 0$, for different temperatures.

order of magnitude, which means that numerical simulations will take the same CPU time.

This dynamic describes the diffusion of particles at the interface. It is thus possible to add some hydrodynamic flow which breaks equilibrium. Since we have supposed that our configurations obeys the Gibbs-Boltzmann distribution, the Metropolis method stays pertinent if we assume that the dynamic is slow compared to the heat exchange with the reservoir.

## 2.3   Computing size dependent free energy

### 2.3.1   The Layer method

It is not possible to compute from Monte Carlo simulations the free energy of a system, since it is not a derivative of the partition function. However, we can compute its derivative with respect to the system. This is useful to compute the Casimir force

$$F(t, h, L) = -\frac{\partial \Omega}{\partial L} \tag{2.22}$$

$$H_0 \qquad\qquad H(\lambda) \qquad\qquad H_1$$
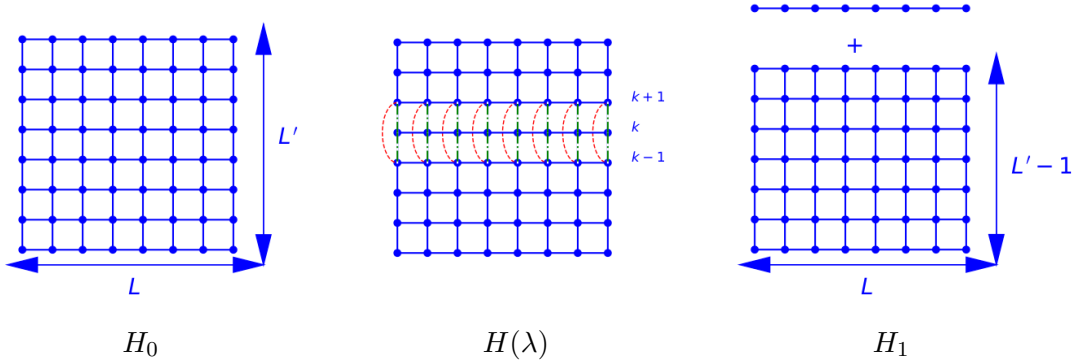
Figure 2.4: Progessive decoupling of the $k$-th layer of the system in order to compute the freen energy through the Crossover Hamiltonian. Blue bonds have an energy of $\beta J$, red ones an energy of $\lambda\beta J$ and the green ones an energy of $(1-\lambda)\beta J$. Reproduction 2D of [67].

To achieve that, Vasilyec [67] developed a method to compute this derivative thanks to a dummy coupling parameter. Even though the system's size is discrete, it is possible to obtain a continuous-like size of the system thanks to the progressive decoupling the $k$-th layer of the system. If $H_0$ is the Hamiltonian of size $L$ and $H_1$ the Hamiltonian of size $L-1$ (see Fig 2.4), then we define the crossover Hamiltonian as

$$H_{cr}(\lambda) = (1-\lambda)H_0 + \lambda H_1 \tag{2.23}$$

with $\lambda \in [0,1]$, which interpolates from $H_0$ to $H_1$ when $\lambda$ goes from 0 to 1. As $\lambda$ goes on, we gradually decouple the $k$-th layer of the system, which means that the interaction energy of all vertical bonds between layer $k$ and layers $k-1$ and $k+1$ are now equal to $(1-\lambda)\beta J$, while we gradually couple the layers $k+1$ and $k-1$ with an energy $\lambda\beta J$. The crossover Hamitlonian $H_{tr}(\lambda)$ also depends from the position of the decoupled layer $k \in 1, 2, ..., L$. The free energy associated to this system is

$$\Omega_{cr}(\lambda) = -k_B T \ln\left(\sum_{h_1...h_L} \exp(-\beta H_{tr}(\lambda))\right) \tag{2.24}$$

From the derivative of the free energy with respect to $\lambda$, we find

$$\frac{\Omega_{cr}(\lambda)}{d\lambda} = \langle H_1 - H_0 \rangle_{H_{cr}(\lambda)} \tag{2.25}$$

where $\langle \cdot \rangle_{H_{cr}(\lambda)}$ represents the statistical mean value in the crossover system, easily computable in numerical simulations. By integrating over the coupling constant, we have

$$\Omega_1 - \Omega_0 = \int_0^1 d\lambda \langle H_1 - H_0 \rangle_{H_{cr}(\lambda)} \tag{2.26}$$

Finally, in the thick limit where $L \gg 1$, we find

$$-\frac{\partial \Omega(t, h, L)}{\partial L} \simeq \int_0^1 d\lambda \langle H_1 - H_0 \rangle_{H_{cr}(\lambda)} \tag{2.27}$$

Even though $H_{cr}(\lambda)$ depends of which layer we decided to decouple, and by transition $H_1 - H_0$ and $\langle H_1 - H_0 \rangle_{H_{cr}(\lambda)}$, the integrand $\int_0^1 d\lambda \langle H_1 - H_0 \rangle_{H_{tr}(\lambda)}$ should be independent of this choice, as long as boundary conditions are not affect by the $k$-th layer.

For the SOS model, it is possible to exactly compute the energy variation produced by the decoupling. We find that

$$H_{cr,SOS}(\lambda) = H_{0,SOS} -$$
$$\frac{\lambda J}{2} \sum_x \left[ \mathrm{sgn}(k-1-h(x))\,\mathrm{sgn}(k+1-h(x)) - \mathrm{sgn}(k-h(x))\left(\mathrm{sgn}(k-1-h(x)) + \mathrm{sgn}(k+1-h(x))\right) \right]$$
$$\tag{2.28}$$

where the prefactor $\frac{1}{2}$ take into account the prefactor between Ising and SOS models in Hamiltonian (1.121). By doing the ?? <span style="color:red">how do you translate "tableau de valeurs" ?</span> , we notice that every term in the sum is equal to $-1$ independently of $k$, since contrary to Ising models, SOS models do not possess any bulk energy. We

### 2.3.2 The Lopes method

Since the Layer method does not work for our models, we have to look to other ways. In the case of a chemical potential conjugated with the total height, we see that [68]

$$\langle \sum_i h_i \rangle(\mu, L) = -\frac{\delta \Omega(\mu, L)}{\delta \mu} \tag{2.29}$$

If we integrate over the chemical potential, we have

$$\Delta\Omega(\mu_1, \mu_2) = \Omega(\mu_1, L) - \Omega(\mu_2, L) = -\int_{\mu_1}^{\mu_2} \langle h \rangle d\mu \tag{2.30}$$

In the case where we know the analytical forme of the free energy in the limits $\mu_2 \to \infty$ or $\mu_1 \to 0$, this method provides a way to directly measure the free energy of the system for any temperature or size by integrating over the chemical potential.

In the limit $\mu_2 \to \infty$, the correlation length at the reference state will be small so that the reference free energy will be essentially that of the bulk. As a consequence, it should contain all the information of the Casimir force (2.22). That derivative force can then be computed by

$$\delta L \frac{\partial \Omega(\mu_1, L)}{\partial L} = \Delta\Omega(\mu_1, \mu_2, L) - \Delta\Omega(\mu_1, \mu_2, L - \delta L) \tag{2.31}$$

where $\delta L$ is the difference thickness between two systems, and which is then independent of $\mu_2$ in the large chemical potential limit as the free energy $\Omega(\mu_2, L)$ converges to the bulk energy.

Since in Kawasaki dynamics the total height is constant, this method does work only for model A.

## 2.4   Tips and tricks

The simulation's speed of SOS models is so great compared to Ising ones that it is possible to study systems over a wider range of parameters. A SOS simulation of $10^7$ MC steps takes roughly 20 minutes to complete once fully optimized. We see that if we want to launch hundreds of those simulations, it can easily take days, which forces us to optimize the code. In C++, if compiling with g++, the first thing to do is to compile the programme with the $-O3$ flag, which makes you gain an order of magnitude in CPU time.

The most important part of Monte Carlo simulations are the pseudo Random Number Generator (pRNG), which are called at least twice for each transition attempt. The C++ standard library proposes the function *default_random_engine* as the default pRNG. A lot of CPU time can be saved by switching to *sfc64* or *xoroshiro* pRNGs. Furthemore, the generation of $\pm 1$ numbers only require one bit, while the pRNG always generates a 64-bits number, thus wasting 63-bits at each boolean generation. A wasteless method which speeds considerably the simulation's speed can be found in [69].

Lastly, the easiest way to gain real time is to make the code parallel. We can do that either by domain decomposition - which would allow us to simulate larger systems - or parallelise directly over the simulation's parameters (as the temperature or the chemical

potential). While the first one is useless in SOS model because of the short correlation length of such systems, the latter can be done via two libraries : OpenMP and MPI. It took me some time to understand that the memory-shared OpenMP protocol has a lot of problems with pRNGs, making this library not suited for Monte Carlo simulations. On the contrary, the MPI library provides impermeability between threads, which makes it the better choice.

## 2.5   Conclusion

In this chapter, we have explained how to compute expectation values of observables in our system [60], thanks to the Monte Carlo Metropolis algorithm [62]. For that, we need to suppose that the system is in thermal equilibrium with a heat bath, and that it respects detailed balance. We have two different possible algorithms : the Glauber dynamics [65] allows to study the systems in the grand-canonical ensemble, while the Kawasaki dynamics [66] is for canonical ones. Nevertheless, since the transfer matrix method gives exact results for the grand-canonical ensemble, only the Kawasaki dynamics is relevant for SOS models.

In addition to that, measuring the free energy of the system is not an easy task, as we can only compute its derivative. The first method we have presented is about progressively decoupling a layer of the system [67], even though for SOS models, which do not possess a bulk energy, the method does not work. Another method is to integrate over the conjugate variable coupled to the total height [68], which is the chemical potential. This method does not work for Kawasaki algorithms. Since as we have discussed Glauber simulations are not relevant for our models, we find that we have no way to compute the free energy in Monte Carlo methods for the only relevant ensemble which is the canonical one. In a latter chapter, we will see how to fix this issue.c

# Chapter 3

# Equilibrium Interface models and their finite size effects

Models for interfaces arise naturally in phase separated systems, as explained in 1. Finite size corrections are manifested when the correlation length becomes of the order of magnitude of the system's size. When undergoing a continuous phase separation, the system exhibits finite size corrections which are manifested by a long range critical Casimir interaction, which we describe in the first section. In the second section we examine finite size effects in continuous interface models in one dimension, and show that while they have similar long range interactions, the forces induced by interface confinement are quite different, and wille be compared to the GSOS model. In the last section, we compute the size-dependent eigenvalues of the transfer matrix for the free SOS model, and compare the results with previous works.

## 3.1 The Casimir effect

Here we explain the critical Casimir effect. For completeness we start by explaining the quantum Casimir effect as it was in the quantum context that the effect was first observed [70]. We also describe the basis of the Lifshitz theory that generalises Casimir's contribution to general dielectric materials beyond the perfectly conducting plate paradigm.

### 3.1.1 Quantum Casimir effect

In an ideal conductor, the free charges can move artibrarily quickly to cancel out any electric in the plane [71]. Thus, a perfectly conducting plate in the $(x, y)$ plane imposes boundary conditions on the electromagnetic field

$$\mathbf{E} \times \mathbf{n} = \mathbf{0}; \ \mathbf{B} \cdot \mathbf{n} = 0 \tag{3.1}$$

The quantum Hamiltonian for the electromagnetic field is given by

$$H = \sum_{\mathbf{k}, \lambda} \hbar\omega(\mathbf{k}, \lambda) \left[ a^\dagger(\mathbf{k}, \lambda) a(\mathbf{k}, \lambda) + \frac{1}{2} \right] \tag{3.2}$$

Here $\lambda$ denotes the polarisation (there are two polarisation states) and $\mathbf{k}$ the wave vector. The dispersion relation for photons is

$$\omega(\mathbf{k}, \lambda) = |\mathbf{k}|c. \tag{3.3}$$

The ground state energy of the electromagnetic field [70] is given by

$$E_0 = \langle 0|H|0 \rangle = H = \sum_{\mathbf{k}, \lambda} \frac{1}{2} \hbar\omega(\mathbf{k}, \lambda) = \sum_{\mathbf{k}} \hbar|\mathbf{k}|c \tag{3.4}$$

The presence of conduction plates at $z = 0$ and $z = L$ means that the wave vectors $k_z$ must be quantised according to $k_z = n\pi/L$ where $n \in \{0, \ 1, \ 2, \ \cdots\}$ while if the $(x, y)$ plane has a large area $A$ we can write

$$\sum_{k_x, k_y} \cdot = \frac{A}{(2\pi)^2} \int d^2\mathbf{k} \cdot \tag{3.5}$$

This then gives

$$\begin{aligned} E_0(L) &= \frac{\hbar c A}{(2\pi)^2} \sum_{n=0}^{\infty} \int d^2\mathbf{k} \left( \mathbf{k}^2 + \frac{n^2\pi^2}{L^2} \right)^{\frac{1}{2}} \tag{3.6} \\ &= \frac{\hbar c A}{(2\pi)} \sum_{n=0}^{\infty} \int_0^\infty k dk \left( \mathbf{k}^2 + \frac{n^2\pi^2}{L^2} \right)^{\frac{1}{2}} \tag{3.7} \end{aligned}$$

The problem with the above expression is that it is clearly divergent. However it can be

rendered finite by cutting off the high momentum degrees of freedom by writing

$$E_0(L) = \frac{\hbar c A}{(2\pi)} \sum_{n=0}^{\infty} \int_0^{\infty} k dk \left( \mathbf{k}^2 + \frac{n^2 \pi^2}{L^2} \right)^{\frac{1}{2}} f\left( (\mathbf{k}^2 + \frac{n^2 \pi^2}{L^2})^{\frac{1}{2}} \right) \tag{3.8}$$

where $f$ is a smooth function such that $f(p) = 1$ for $p \ll \Lambda$ and $f(p) = 0$ for $p \gg \Lambda$. Here, $\Lambda$ is an ultraviolet cut-off and $f$ thus only counts the contribution of photons with a momentum less than $\hbar\Lambda$. For this sort of calculation to make physical sense the physical result we get at the end should be independent of both the choice of $f$ and $\Lambda$.

In the limit $L \to \infty$ we can replace the sum over discrete modes by an integral, as usual in statistical physics,

$$E_0(L) = \frac{\hbar c A}{(2\pi)} \int_0^{\infty} \frac{L}{\pi} d\nu \int_0^{\infty} k dk \left( \mathbf{k}^2 + \nu^2 \right)^{\frac{1}{2}} f\left( (\mathbf{k}^2 + \nu^2)^{\frac{1}{2}} \right) \tag{3.9}$$

where we have used $d\nu = \pi/L$. We thus see that for large $L$ we have

$$E_0(L) = AL\epsilon_{bulk} \tag{3.10}$$

where $\epsilon_{bulk}$ is a bulk energy density per unit of volume. Clearly the bulk free energy is intensive, since it counts both the volume interior and exterior to the plates. This is basically the idea of a disjoining pressure in colloidal science [72] where to compute the effective interaction the bulk pressure has to be removed. The computation above only calculates the energy of the EM field between the plates. If the physical system extends up to $L' \gg L$, then the total energy of both the interior and the exterior of the plates is given by

$$E_{total}(L) = E_0(L) + A(L' - L)\epsilon_{bulk} \tag{3.11}$$

We see that the part of the energy that depends on $L$ is given by

$$U(L) = E_0(L) - AL\epsilon_{bulk} \tag{3.12}$$

Now we simply write

$$AL\epsilon_{bulk} = \frac{\hbar c A}{(2\pi)} \int_0^{\infty} dn \int_0^{\infty} k dk \left( \mathbf{k}^2 + \frac{n^2 \pi^2}{L^2} \right)^{\frac{1}{2}} f\left( (\mathbf{k}^2 + \frac{n^2 \pi^2}{L^2})^{\frac{1}{2}} \right) \tag{3.13}$$

where we have put the $L$ dependence in the integral. This then gives

$$U(L) = \frac{\hbar cA}{(2\pi)} \left[ \sum_{n=0}^{\infty} g(n) - \int_0^{\infty} dn \; g(n) \right] \tag{3.14}$$

where

$$g(n) = \int_0^{\infty} kdk \left( \mathbf{k}^2 + \frac{n^2\pi^2}{L^2} \right)^{\frac{1}{2}} f\left( (\mathbf{k}^2 + \frac{n^2\pi^2}{L^2})^{\frac{1}{2}} \right) = \frac{1}{2} \int_{\frac{n^2\pi^2}{L^2}}^{\infty} duu^{\frac{1}{2}} f(u^{\frac{1}{2}}) \tag{3.15}$$

We now use the Euler-Mauclarin formula

$$\sum_{n=0}^{\infty} g(n) - \int_0^{\infty} dn \; g(n) = -B_1 g(0) - \frac{1}{2}B_2 g'(0) - \frac{1}{24}B_4 g'''(0) - \cdots \tag{3.16}$$

where $B_n$ are the Bernoulli numbers[1]. We find that

$$g'(n) = -\frac{\pi^3}{L^3} n^2 f\left(\frac{n\pi}{L}\right) \tag{3.17}$$

and noticing than in the region around $n = 0$, $f = 1$ is a constant, we show that

$$g'(0) = 0 \tag{3.18}$$

$$g''(0) = 0 \tag{3.19}$$

$$g'''(0) = -\frac{2\pi^3}{L^3} \tag{3.20}$$

Higher order derivatives are zero so the full result is given by the first three terms of the Euler-Maclaurin formula. We thus find

$$U(L) = \frac{\hbar cA}{(2\pi)} \left[ -g(0) - \frac{\pi^3}{360L^3} \right] \tag{3.21}$$

The first term independent of $L$ can be interpreted as a surface energy. The effective $L$ dependent interaction is given by

$$U_{int}(L) = -\frac{\hbar\pi^2 cA}{720L^3} \tag{3.22}$$

---

[1]The first Bernoulli numbers are explicitly given by $B_1 = 1$ , $B_2 = \frac{1}{2}$, $B_4 = -\frac{1}{30}$

We see that the effective interaction is attractive. Interestingly Casimir thought that his calculation could explain the stability of the electron [70, 73] The model of the electron is one of a perfectly conducting shell carrying an electric charge $e$. If the radius of the shell is $a$ then the electrostatic energy of due to the charge is given by

$$E_{Charge} = \frac{e^2}{8\pi a \epsilon_0} \tag{3.23}$$

There is thus a repulsive force on the shell which should make it expand. Casimir thought that the Casimir force on a spherical geometry, if is an attractive force as is the case for the parallel plate geometry, could stabilise the electron. Clearly by dimensional analysis

$$E_{Cas} = -\frac{Z\hbar c}{a} \tag{3.24}$$

The balance of the Casimir and electric forces would then require

$$Z = \frac{e^2}{8\pi\hbar c}. \tag{3.25}$$

However, in the case of conducting spherical shell, the constant $Z \simeq -0.046175$ is negative [74, 75, 76], while the same calculation for a cylindrical geometry predicts an attractive force [77].

### 3.1.2 Lifshitz Theory

<span style="color:red">I've retouched some phrases and removed the names, instead just citing the papers, since I feel you've said the names so I could find the papers.</span> The Casimir calculation is based on the boundary conditions imposed on the EM field due to a conductor. However this is an ideal mathematical limit, conductors being conductors because free charges can move to cancel out the electric field in the conducting surface. The Casimir force can also be seen as due to correlations induced in the charge fluctuations in each plate, which allows for an alternative method based on sources which recovers the Casimir force [78, 79]. In a sense therefore the effect can be interpreted without reference to the zero point energy of the vacuum and the Casimir calculation works due to the fact that the mathematical limit in going to a perfect conductor works. Using a stochastic formulation of electrodynamics by Rytov [80], the Casimir calculation was generalized by Lifshitz for interactions between arbitrary electrical bodies, characterized by their local electric and

magnetic response[81]. Even though this theory is very general, the microscopic justification is not completely rigorous, source terms (random currents and dipole fluctuations) are introduced to Maxwell's equations to give a Langevin formulation of Maxwell's equations in the presence of dielectric bodies. The correlation functions of the white noise terms depend on the temperature of the system and are determined via the quantum fluctuation dissipation theorem. The Lifshitz theory is computationally difficult to work with and it was reformulated in a way more useful for practical calculations and that can be applied to experimental setups [82, 83]. Rytov's formulation has the advantage that it can be used to treat out of equilibrium situations where different bodies at held at different temperatures interact. This allows both the computation of out of equilibrium forces and radiative heat transfer.

The theory in the presence of electromagnetic media is written in terms of the electric and magnetic fields $\mathbf{E}$ and $\mathbf{B}$ and the displacement and magnetizing fields $\mathbf{D}$ and $\mathbf{H}$ which are assumed to obey local relations in real space and Fourier space

$$\tilde{\mathbf{D}}(\omega) = \epsilon(\omega)\tilde{\mathbf{E}}(\omega); \ \tilde{\mathbf{B}}(\omega) = \mu(\omega)\tilde{\mathbf{H}}(\omega) \tag{3.26}$$

where $\tilde{\epsilon}(\omega)$ and $\tilde{\mu}(\omega)$ are the frequency dependent permittivity and permeability. The boundary conditions at the interface between two materials 1 and 2 are given by

$$B_{1n} = B_{2n} \qquad D_{1n} = D_{2n} \tag{3.27}$$

$$E_{1t} = E_{2t} \qquad H_{1t} = H_{2t} \tag{3.28}$$

where $n$ denotes the normal component and $t$ the tangential component to the interface.

Forces can be computed using the vacuum (assuming that the surface where the force is computed is next to the vacuum) Maxwell stress tensor.

$$T_{ij} = \epsilon \left( E_i E_j - \frac{1}{2}\delta_{ij}E^2 \right) + \frac{1}{\mu} \left( B_i B_j - \frac{1}{2}\delta_{ij}B^2 \right) \tag{3.29}$$

Notice that the stress tensor is quadratic in the fields $\mathbf{E}$ and $\mathbf{B}$, this means that even if the fields are on average zero, both thermal and quantum fluctuations give rise to forces.

In media Maxwells equations are

$$\nabla \times \mathbf{E} = -\frac{\partial \mathbf{B}}{\partial t} \tag{3.30}$$

$$\nabla \times \mathbf{H} = \mathbf{J} - \frac{\partial \mathbf{D}}{\partial t} \tag{3.31}$$

$$\nabla \cdot \mathbf{D} = \rho \tag{3.32}$$

$$\nabla \cdot \mathbf{B} = 0 \tag{3.33}$$

In a dielectric medium or conductor where there are no applied external fields there is no free charge or current . As such, the average values of $\mathbf{E}$ and $\mathbf{B}$ are zero. Rytov's idea was to add a random current to induce both thermal and quantum fluctuations into the problem. If we assume that the only contribution to the current comes from a fluctuating polarization density $\mathbf{P}$ we can write

$$\frac{\partial \rho}{\partial t} + \nabla \cdot \mathbf{J} = 0 \implies \nabla \cdot \left[ -\frac{\partial \mathbf{P}}{\partial t} + \mathbf{J} \right] = 0 \tag{3.34}$$

where we have used

$$\rho = -\nabla \cdot \mathbf{P} \tag{3.35}$$

This means that the current is given by

$$\mathbf{J} = \frac{\partial \mathbf{P}}{\partial t} \tag{3.36}$$

or in Fourier space

$$\tilde{\mathbf{J}}(\omega) = i\omega \tilde{P}(\omega) \tag{3.37}$$

Now if we assume that the fluctuations in the polarization density are uncorrelated in space, the fluctuation dissipation theorem tells us that the correlation function of the polarization density in Fourier space is given by

$$\langle P_\alpha(\omega; \mathbf{x}) P_\beta^\dagger(\omega; \mathbf{x}') \rangle_{sym} = \frac{\hbar \epsilon''(\omega)}{2} \coth\left( \frac{\hbar \omega}{2 k_B T} \right) \delta(\omega - \omega') \delta(\mathbf{x} - \mathbf{x}') \delta_{\alpha\beta} \tag{3.38}$$

$$\epsilon(\omega) = \epsilon'(\omega) + i\epsilon''(\omega) \tag{3.39}$$

The Lifshitz calculation for slab geometries gives a force per unit area between two slabs

of media separated by a distance $L$

$$
\begin{aligned}
\frac{F}{A} &= -\frac{k_B T}{\pi c^3} \sum_{n=0}^{\infty} \omega_n^3 \int_1^{\infty} dp p^2 \left[ 1 - \frac{(s_1 + p)(s_2 + p)}{(s_1 - p)(s_2 - p)} \exp(-\frac{2p\omega_n L}{c}) \right] \\
&+ \left[ 1 - \frac{(s_1 + p\varepsilon_1)(s_2 + p\varepsilon_2)}{(s_1 - p\varepsilon_1)(s_2 - p\varepsilon_2)} \exp(-\frac{2p\omega_n L}{c}) \right]
\end{aligned}
\tag{3.40}
$$

where $\epsilon = \epsilon_0 \varepsilon$, $s_i = \sqrt{\epsilon_i - 1 + p^2}$, $\omega = \frac{2\pi n k_B T}{\hbar}$ are the Mastubara frequencies [84] and $\varepsilon_i = \varepsilon_i(i\omega_n)$. Note that the integral over real frequencies has become a sum over discrete Matsubara frequencies, they come from the poles in the hyperbolic cotangent.

One needs to know the dielectric response at imaginary frequency, this is done using the Kramers-Kronig relation

$$
\varepsilon(i\omega) = 1 + \frac{2}{\pi} \int_0^{\infty} d\zeta \frac{\zeta \varepsilon''(\zeta)}{\omega^2 + \zeta^2}
\tag{3.41}
$$

### 3.1.3 Critical Casimir effect

Critical systems have a macropscopic correlation length, which leads to finite-size effects in the free energy. Following De Gennes and Fisher steps [85], we transpose the Casimir effect into critical systems. We consider a system of $N$ spins.

#### 3.1.3.1 Bulk scaling for near critical systems

The free energy for a system consisting of $N$ spins has a singular part at a critical temperature $T_c$ which can be written as

$$
F(t, h) = N f(t, h)
\tag{3.42}
$$

where $t = (T - T_c)/T_c$ measures the distance from the critical point and $h$ is the external applied magnetic field. We assume that we are in a system where the only relevant parameters are $T$ and $h$ (equivalently the concentration or chemical potential of a binary mixture), which is true for $d < 4$ [86]. Now if we carry out a renormalisation group transformation blocking spins in blocks of linear size $b$ into new effective spins, the RG transformation gives

$$
N f(t, h) = N' f(t', h')
\tag{3.43}
$$

Clearly the number of spins in the blocked system is given by $b^d N' = N$ and the RG transformation for $t$ and $h$ are given by $t' = b^{y_1} t$ and $h' = b^{y_2} h$, where $y_1$ and $y_2$ are positive and are the RG exponents for the fields $t$ and $h$ (from which all critical exponents can be deduced). This then means that

$$f(t, h) = \frac{1}{b^d} f(b^{y_1} t, b^{y_2} h) \tag{3.44}$$

We begin by working with $t > 0$ but the arguments here are trivially generalisable to the case $t < 0$. In Eq. (3.44) is we choose $b$ such that $b^{y_1} t = 1$, then, at the critical field $h = 0$, we find

$$f(t, 0) = t^{\frac{d}{y_1}} f(1, 0) \tag{3.45}$$

The singularity in the specific heat is defined via

$$c \sim \frac{\partial^2}{\partial t^2} f(t, 0) \tag{3.46}$$

and so we find

$$c \sim t^{\frac{d}{y_1} - 2} \sim t^{-\alpha} \tag{3.47}$$

where $\alpha$ is the exponent associated with the divergence of the specific heat. This means that

$$\alpha = 2 - \frac{d}{y_1} \tag{3.48}$$

The RG transformation for the correlation function has the form

$$C(r, t, h) = \lambda^2(b) C(r/b, b^{y_1} t, b^{y_2} h) \tag{3.49}$$

Clearly length scales transform as $r' = r/b$. Again setting $h = 0$ and choosing $b^{y_1} t = 1$ gives

$$C(r, t, h) = \lambda^2(t^{-\frac{1}{y_1}}) C(r/t^{-\frac{1}{y_1}}, 1, 0). \tag{3.50}$$

The correlation function, by definition is given by

$$C(r, t) \sim f(r/\xi), \tag{3.51}$$

where $\xi$ is the correlation length. This immediately tells us that $\xi = t^{-\frac{1}{y_1}}$ and from the usual definition

$$\xi \sim t^{-\nu} \tag{3.52}$$

we have $\nu = 1/y_1$. These two formula for $y_1$ then give the hyper scaling relation

$$\alpha = 2 - d\nu. \tag{3.53}$$

The exponents $\alpha$ and $\nu$ are the ones that are important in the critical Casimir effect.

### 3.1.3.2    Finite size scaling

Consider a system which is finite in one direction with either periodic boundary systems or two surfaces. While the critical system has $h = 0$ there can be local surface fields at each surface $a$ and $b$. This represents a preference of the surfaces for one phase or the other. The finite scaling hypothesis for a slab system of large area $A$ but with finite width $L$ can be stated as

$$f(t, h_a, h_b, L^{-1}) = \frac{1}{b^d} f(b^{y_1} t, b^{y_a} h_a, b^{y_b} h_b, bL^{-1}) \tag{3.54}$$

We thus see that the field $L^{-1}$ is a relevant field with RG exponent $y_L = 1$. The surface fields are not necessarily relevant so we can have $y_a$ and $y_b$ positive or negative. The important point about finite size scaling is that when $L$ is finite the singularity due to the thermodynamic phase transition is smoothed out by the system's finite size (note that we assume that the system has no two dimensional phase transition in the region we are looking at). First we see that when $L$ is large there should be a bulk contribution to the free energy plus a surface term (so we are considering the limit $L \to \infty$ before $\xi \to \infty$)

$$
\begin{aligned}
f(t, h_a, h_b, L^{-1}) =& f(t, h_a, h_b, 0) + L^{-1} \frac{\partial f(t, h_a, h_b, 0)}{\partial x_4} \\
=& \frac{1}{b^d} f(b^{y_1} t, b^{y_a} h_a, b^{y_b} h_b, 0) + \frac{1}{b^{d-1}} L^{-1} \frac{\partial f(b^{y_1} t, b^{y_a} h_a, b^{y_b} h_b, 0)}{\partial x_4}
\end{aligned} \tag{3.55}
$$

where we have carried out the Taylor expansion for $L^{-1}$ small using both versions of Eq. (3.58) and $\frac{\partial}{\partial x_n}$ indicates the partial derivative with respect to the $n^{th}$ argument. The second term gives a total contribution to the singular part of the free energy of the order

$AL \times L^{-1}$ and is thus a surface tension $\gamma$ and so we have

$$\gamma = \frac{1}{b^{d-1}} \frac{\partial f(b^{y_1} t, b^{y_a} h_a, b^{y_b} h_b, 0)}{\partial x_4} \tag{3.56}$$

Setting $bt^{y_1} = 1$ then gives close to the critical point

$$\gamma \sim t^{\frac{d-1}{y_1}} \frac{\partial f(1, \lim_{t \to 0} t^{-\frac{y_a}{y_1}} h_a, \lim_{t \to 0} t^{-\frac{y_a}{y_1}} h_b, 0)}{\partial x_4} = t^{(d-1)\nu} C' = \xi^{-(d-1)} C' \tag{3.57}$$

The formula relating the surface tension and the correlation length, in the above $C'$ is a constant depending on the universality class.

Now if we keep $L$ finite and set $b^{y_1} t = 1$ in Eq. (3.58) we find

$$f(t, h_a, h_b, L^{-1}) = t^{\frac{d}{y_1}} f(1, t^{-\frac{y_a}{y_1}} h_a, t^{-\frac{y_b}{y_1}} h_b, t^{-\frac{1}{y_1}} L^{-1}) \tag{3.58}$$

which can be written as

$$f(t, h_a, h_b, L^{-1}) = \frac{1}{\xi^d} f(1, \xi^{y_a} h_a, \xi^{y_b} h_b, \xi/L) \tag{3.59}$$

This can then be written as

$$f(t, h_a, h_b, L^{-1}) = \frac{1}{L^d} \theta(\frac{L}{\xi}, \xi^{y_a} h_a, \xi^{y_b} h_b) \tag{3.60}$$

Now crucially as $\xi \to \infty$ the function $\theta$ is analytic so we can take the limit $\xi \to \infty$ without any problems to find

$$f(0, h_a, h_b, L^{-1}) = \frac{1}{L^d} \theta(0, \lim_{\xi \to \infty} \xi^{y_a} h_a, \lim_{\xi \to \infty} \xi^{y_b} h_b) \tag{3.61}$$

Clearly for each surface we have 3 possibilities: $\lim_{\xi \to \infty} \xi^{y_a} h_a = \pm\infty$, if the surface fields are relevant, as well as $\lim_{\xi \to \infty} \xi^{y_a} h_a = 0$ if the surface fields are irrelevant. There is clearly also a similar argument when the system has periodic boundary conditions and there are no surface fields. Near the critical point depending on the boundary conditions there should be scaling functions when the surface fields attract the same phase $\theta_{++}(x)$, where they attract different phases and $\theta_{+-}(x)$, and $\theta_{pbc}(x)$ when the boundary conditions are periodic. There should also be a zero surface field case $\theta_{00}$ when the surfaces fields are irrelevant or zero (this is however unlikely). Fisher and de Gennes argued, without proof,

that the force for $(++)$ boundary conditions should be attractive where as the $(+-)$ case should produce repulsive forces [85, 87] .

The total singular part of the free energy is thus given by

$$F = ALf(t, h_a, h_b, L^{-1}) = \frac{A}{L^{d-1}}\theta(\frac{L}{\xi}, \xi^{y_a}h_a, \xi^{y_b}h_b). \tag{3.62}$$

The scale of the energy is set by the energy of thermal fluctuations $k_B T$ we thus find that

$$F(t=0) = \frac{k_B T A C}{L^{d-1}} \tag{3.63}$$

where $C$ is a constant depending on the surface universality class.

## 3.2 Finite size scaling in one dimensional interface models

Confinement forces appear wherever the correlation length of the fluctuations is close to the minimum size of the system, be it for perfect conductor plates in vacuum or in confined critical systems. The free energy of interfaces behaves in a similar way. Using the interface model defined in Sec (1.2), we derive a general method to study the disjoining pressure for any potential, and present the solutions for the two specific cases.

### 3.2.1 Continuous models in one dimension

In one dimension the partition function for a surface model of the type discussed in Sec 1.2 can be written as a functional integral

$$Z(L) = \int d[h] \exp\left(-\frac{\beta\sigma}{2}\int_0^L h'^2(x)dx - \beta\int_0^L V(h(x))dx\right) \tag{3.64}$$

It is convenient to fix both the starting point $h(0) = x$ and the end point $h(L) = x$ and define what is known as the propagator

$$K(h, h', L) = \int_{h(0)=h} d[h]\delta(h' - h(L)) \exp\left(-\frac{\beta}{2}\int_0^L \sigma h'^2(x)dx - \beta\int_0^L V(h(x))dx\right) \tag{3.65}$$

The propagator is an example of a path integral and is the sum over all paths going between $h$ and $h'$ in what can be taken to be the time $L$. It can be shown [84, 88] that the path

integral obeys an imaginary time Schrödinger equation

$$\frac{\partial K(h, h', L)}{\partial L} = -\hat{H} K(h, h', L) \tag{3.66}$$

where $\hat{H}$ is the Hamiltonian operator

$$\hat{H} = -\frac{1}{2\sigma\beta} \frac{\partial^2}{\partial h^2} + \beta V(h) \tag{3.67}$$

and, with a suitable normalisation, the initial condition

$$K(h, h', L) = \delta(h - h') \tag{3.68}$$

If the Hamiltonian operator $\hat{H}$ has eigenfunctions $\psi_n$, normalised so that

$$\int dh \; \psi_n^2(h) = 1 \tag{3.69}$$

and with eigenvalues $\epsilon_n$. It is easy to see that the propagator can be written as

$$K(h, h', L) = \sum_n \exp(-L\epsilon_n) \psi_n(h) \psi_n(h') \tag{3.70}$$

If we take a system with periodic boundary conditions but otherwise leave the initial value $h(0)$ of the height to be free, then using the normalisation of the eigenfunctions, we find

$$Z(L) = \int dh K(h, h', L) = \sum_n \exp(-L\epsilon_n) \tag{3.71}$$

Now in the thermodynamic limit $L \to \infty$ if there is a gap between the ground state energy $\epsilon_0$ and the first excited state, $g = \epsilon_1 - \epsilon_0$, which is non-zero, we can apply ground state dominance

$$Z(L) = \exp(-L\epsilon_0) \tag{3.72}$$

which gives the free energy per unit length as

$$f = \frac{1}{\beta} \epsilon_0 \tag{3.73}$$

We remark that the energy of the ground and excited states are related to the transfer matrix by

$$\epsilon_n = -\ln(\lambda_n) \tag{3.74}$$

As well as the free energy we are interested in the probability distribution of the height at a single point (which is independent of the point chosen due to invariance by translation of the system). For instance the probability distribution of $h$ is given by

$$
\begin{aligned}
p_1(h) &= \frac{\int d[h]\delta(h(0) - h)\exp\left(-\frac{\beta}{2}\int_0^L h'^2(x)dx - \beta\int_0^L V(h(x))dx\right)}{Z(L)} \\
&= \frac{K(h, h, L)}{Z(L)} \\
&= \frac{\sum_n \exp(-L\epsilon_n)\psi_n^2(h)}{\sum_n \exp(-L\epsilon_n)}
\end{aligned}
\tag{3.75}
$$

and so as $L \to \infty$, ground state dominance gives

$$p_1(h) = \psi_0^2(h) \tag{3.76}$$

We see that the normalisation of the probability density function for $h$ follows from the normalisation of the wave functions.

The joint probability density function for two heights separated by a time or distance $x$ is given by

$$
\begin{aligned}
p_2(h, h', x) &= \frac{\int d[h]\delta(h(0) - h)\delta(h(x) - h')\exp\left(-\frac{\beta}{2}\int_0^L h'^2(x)dx - \beta\int_0^L V(h(x))dx\right)}{Z(L)} \\
&= \frac{K(h, h', x)K(h', h, L - x)}{Z(L)} \\
&= \frac{\sum_{nm}\exp(-x\epsilon_n)\psi_n(h)\psi_n(h')\exp(-[L - x]\epsilon_m)\psi_m(h')\psi_m(h)}{\sum_n \exp(-L\epsilon_n)}.
\end{aligned}
\tag{3.77}
$$

Due to ground state dominance only the term with $m = 0$ survives in the sum above ( as

$x$ is taken such that $x \ll L$) and we find

$$p_2(h, h', x) = \sum_n \psi_0(h')\psi_0(h)\psi_n(h')\psi_n(h)\exp(-x[\epsilon_n - \epsilon_0]))$$

$$= p_1(h)p_1(h') + \sum_{n>0} \psi_0(h')\psi_0(h)\psi_n(h')\psi_n(h)\exp(-x[\epsilon_n - \epsilon_0])) \tag{3.78}$$

From this we see that when $x[\epsilon_n - \epsilon_0] \gg 1$ for all $n$, and in particular when $x[\epsilon_1 - \epsilon_0] \gg 1$, we have

$$p_2(h, h', x) \sim p_1(h)p_2(h') \tag{3.79}$$

so that the height at large distances are uncorrelated or equivalently are independent random variables. This gives a correlation length

$$\xi = \frac{1}{\epsilon_1 - \epsilon_0}. \tag{3.80}$$

### 3.2.2 The confined elastic line

for coherence, changed notations from $\ell$ to $L$. I didn't find any reference to compare this results, do you have any ?

Here we consider the case where $V(h) = 0$ for $0 < h < L$ and $V(h) = +\infty$ otherwise. This corresponds to a one dimensional elastic line confined between two impenetrable walls separated by a distance $L$. The Hamiltonian $\hat{H}$ is that for a quantum well of width $L$, whose solutions are [89]

$$\psi_n(h) = \sqrt{\frac{2}{L}} \sin\left(\frac{\pi(n+1)h}{L}\right) \tag{3.81}$$

where $n \geq 0$ are integers. From this we see that the ground state energy is

$$\epsilon_0 = \frac{1}{2\sigma\beta}\frac{\pi^2}{L^2} \tag{3.82}$$

and so in the thermodynamic limit

$$f = \frac{1}{2\sigma\beta^2}\frac{\pi^2}{L^2} = \frac{T^2\pi^2}{2\sigma L^2} \tag{3.83}$$

Here the pressure (in this case pressure in a force per unit length) is given by

$$P = -\frac{\partial f}{\partial L} = \frac{\pi^2 T^2}{\sigma L^3} \tag{3.84}$$

and we see that it is repulsive. Physically, the fluctuations of the surface repel the walls. The pressure has the Casimir like characteristic that it behaves as a long range power law type interaction. However a two dimensional critical Casimir system (see Eq (3.63)) would have a free energy per unit length $f = CT/L$. We also see that the free energy scales a $T^2$ rather than $T$ (as is the case for the Casimir interaction).Having said this, a critical system has zero surface tension and so using a model with a finite surface tension for the interface is clearly not appropriate.

Here, using Eq. (3.80) we find that the correlation length is given by

$$\xi = \frac{2}{3} \frac{\sigma L^2}{T \pi^2} \tag{3.85}$$

thus it increases as the surface tension is increased or the temperature is lower, which makes physical sense as the surface should become *flatter* under these conditions. Also as the system becomes more confined the correlation length increases, again as confinement kills fluctuations. The correlation length tells us that if we wanted to simulate this system then we need to take

$$L \gg \xi, \tag{3.86}$$

in order to be in the thermodynamics limit and so $L \gg \frac{\sigma L^2}{T \pi^2}$, thus for $L$ large, in general we would need to simulate rather large systems. The probability distribution function of the height at a single point is given by

$$p_1(h) = \frac{2}{L} \sin^2(\frac{\pi h}{L}) \tag{3.87}$$

and from this we find

$$\langle h \rangle = \frac{L}{2}, \tag{3.88}$$

which is rather obvious. The width of the interface is given by

$$w = \sqrt{\langle h^2 \rangle - \langle h \rangle^2}, \tag{3.89}$$

and here it is given by

$$w = L\sqrt{\frac{1}{12} - \frac{1}{2\pi^2}} = 0.0326727 \ L \tag{3.90}$$

### 3.2.3 The Airy line

In the above well known example we confine the surface and then compute the pressure. This is an example of the constant volume ensemble. Physically we could also consider the case of a system which is confined softly by an externally imposed pressure $P_0$ the constant pressure ensemble. In this case the potential is given by

$$V(h) = P_0 h \text{ for } h \rangle 0 \ ; = \infty \text{ for } h \leq 0. \tag{3.91}$$

The time independent Schrödinger equation for the eigenfunctions here is

$$-\frac{1}{2\sigma\beta}\frac{d^2\psi_n(h)}{dh^2} + P_0\beta h\psi_n(h) = \epsilon_n\psi_n(h). \tag{3.92}$$

The corresponding eigenfunctions have boundary conditions $\psi_n(0) = 0$ due to the hard wall potential at $h = 0$ and they must also decay to zero as $h \to \infty$ so as to be normalisable.

The key to finding the eigenfunctions is to transform the Schrödinger into the Airy equation which is

$$\frac{d^2y(x)}{dx^2} - xy(x) = 0. \tag{3.93}$$

This equation has solutions $\text{Ai}(x)$ which decay as

$$\text{Ai}(x) \sim \frac{\exp(-\frac{2}{3}x^{\frac{3}{2}})\Gamma(\frac{5}{6})\Gamma(\frac{1}{6})}{4\pi^{\frac{3}{2}}x^{\frac{1}{4}}}, \tag{3.94}$$

as $x \to \infty$ and so are normalizable as eigenfunctions. For $x\langle 0$ the Airy function oscillates and has an infinite number of negative zeros $-\alpha_n$ such that $\text{Ai}(-\alpha_n) = 0$.

We make the change of variable $h = \mu z'$ to find

$$\frac{1}{2\sigma\beta\mu^2}\frac{d^2\psi_n(z')}{dz'^2} - P_0\beta\mu(z' - \varepsilon_n)\psi_n(z') = 0, \tag{3.95}$$

where $\varepsilon_n = \epsilon_n/(P_0\beta\mu)$. Now we chose $\mu$ so that

$$2\sigma\beta^2 P_0\mu^3 = 1, \tag{3.96}$$

and we see that

$$\mu = \left(\frac{1}{2\beta^2\sigma P_0}\right)^{\frac{1}{3}}, \tag{3.97}$$

is an intrinsic length scale.

$$\frac{d^2\psi_n(z')}{dz'^2} - (z' - \varepsilon_n)\psi_n(z') = 0. \tag{3.98}$$

Finally if we use $z = z' - \varepsilon_n$ we obtain Airy's equation

$$\frac{d^2\psi_n(z)}{dz^2} - z\psi_n(z) = 0 \tag{3.99}$$

and so

$$\psi_n(z) = c_n\text{Ai}(z), \tag{3.100}$$

where $c_n$ is a normalisation constant. This means that in terms of the original height variable $h$,

$$\psi_n(h) = c_n\text{Ai}(\frac{h}{\mu} - \varepsilon_n). \tag{3.101}$$

The boundary condition $\psi_n(h)$ then show that we must choose $\varepsilon_n = \alpha_{n+1}$. This means that the ground state energy is

$$\epsilon_0 = \alpha_1 P_0\beta\mu = \frac{\alpha_1 P_0\beta}{(2\sigma\beta^2 P_0)^{\frac{1}{3}}} = \frac{\alpha_1 P_0^{\frac{2}{3}}\beta^{\frac{1}{3}}}{2^{\frac{1}{3}}\sigma^{\frac{1}{3}}}, \tag{3.102}$$

and where we note that $\alpha_1 = 2.33811$.

$$f = \frac{\alpha_1 P_0^{\frac{2}{3}}}{2^{\frac{1}{3}}\sigma^{\frac{1}{3}}\beta^{\frac{2}{3}}}. \tag{3.103}$$

From the original partition function we see that $h$ is conjugate to $P_0$ and so we find the average height is given by

$$\bar{h} = \langle h \rangle = \frac{\partial f}{\partial P_0} = \frac{2}{3}\frac{\alpha_1}{2^{\frac{1}{3}}\sigma^{\frac{1}{3}}\beta^{\frac{2}{3}}P_0^{\frac{1}{3}}} = \frac{2}{3}\alpha_1\mu, \tag{3.104}$$

and solving for $P_0$ in terms of $\overline{h}$ gives

$$P_0 = \frac{4}{27} \frac{\alpha_1^3 T^2}{\sigma \overline{h}^3}, \tag{3.105}$$

we see that $P_0$ behaves exactly in the same way as the pressure of a confined elastic line in term of the temperature and surface tension. Only the overall numerical prefactor is different.

The correlation length is given by

$$\xi = \frac{2^{\frac{1}{3}} (\sigma T)^{\frac{1}{3}}}{(\alpha_2 - \alpha_1) P_0^{\frac{2}{3}}}. \tag{3.106}$$

When written in terms of $\overline{h}$ the above correlation length behaves in the same way as for the free elastic line, however when $P_0$ is fixed we see that the behavior as a function of $T$ and $\sigma$ is quite different. The correlation length still increases with $\sigma$ but now decreases as the temperature is decreases.

The probability density function for the height of the interface at a single point is given by

$$p_1(h) = \frac{\text{Ai}^2(\frac{h}{\mu} - \alpha_0)}{\int_0^\infty dh' \text{Ai}^2(\frac{h'}{\mu} - \alpha_0)} \tag{3.107}$$

However if we write the height variable in terms of the length scale $\mu$, $h(x) = \mu z(x)$ we find that $z$ has the single point probability density function

$$p(z) = \frac{\text{Ai}^2(z - \alpha_0)}{\int_0^\infty dz' \text{Ai}^2(z' - \alpha_0)}. \tag{3.108}$$

**Make a nice plot of p(z) with a properly referenced legend** Using this we find the average height is given by

$$\langle h \rangle = \overline{h} = \mu z_0, \tag{3.109}$$

where

$$z_0 = \frac{\int_0^\infty dz z \text{Ai}^2(z - \alpha_0)}{\int_0^\infty dz \text{Ai}^2(z - \alpha_0)}. \tag{3.110}$$

Interestingly comparison with the thermodynamic calculation giving Eq. (3.104) shows

that the identity

$$z_0 = \frac{2}{3}\alpha_0, \tag{3.111}$$

must hold- this surprising identity can be verified numerically. Here we find that the width is given by

$$w = 0.697089 \ \mu \tag{3.112}$$

## 3.3 The generalized Lopes Method

In Sec 2.3.2, we have shown a way to numerically compute the free energy of a ssytem at a chemical potential $\mu$ in absence of another potential. Here we generalise the method for any kind of external potential. We will explain the method for the Ising model, but the derivation for the SOS model is straigthforward.

The Hamiltonian of the SOS model is

$$H = -J\sum_{\langle ij\rangle}\sigma_i\sigma_j - \mu\sum_i V(\sigma_i) \tag{3.113}$$

where $V(\sigma)$ is an external potential taking any form. The mean value of the external potential is

$$\begin{aligned}
\langle\sum_i V(\sigma_i)\rangle &= \sum_{\mathbf{h}}\sum_i V(\sigma_i)\exp(-\beta H)\\
&= \frac{1}{\beta}\frac{\partial\Omega(\mu)}{\partial\mu}
\end{aligned} \tag{3.114}$$

where $\Omega$ is the free energy of the system. We see that for any potential of the form (3.115), we can integrate the previous equation to find

$$\Omega(\mu_1) - \Omega(\mu_2) = \beta\int_{\mu_1}^{\mu_2}d\mu'\langle\sum_i V(\sigma_i)\rangle_{\mu'} \tag{3.115}$$

In the case where we know the analytical form of the free energy in the limits $\mu_2 \to \infty$ or $\mu_1 \to 0$, this method provides a way to directly measure it for any temperature or size by integrating over the chemical potential.

In the case of the classical chemical potential, $V(h) = h$, all spins tend to align to $+1$ in the limit $\mu \to +\infty$, which means there is only one possible configuration. The free energy

is thus $\Omega(\beta, \mu = \infty) = 0$. Thanks to Eq (3.115), by integration over the chemical potential $\mu$, we can directly measure in Glauber simulations the free energy for any finite $\mu$.

In the SOS model, Eq (3.115) writes as

$$\Omega(\mu_1) - \Omega(\mu_2) = \beta \int_{\mu_1}^{\mu_2} d\mu' \langle \sum_i V(h_i) \rangle_{\mu'} \tag{3.116}$$

Nevertheless, the integrand is constant in the Kawasaki dynamics, so we have to find another way.

In the limit $\mu_2 \to \infty$, the correlation length at the reference state will be small so that the reference free energy will be essentially that of the bulk. As a consequence, it should contain all the information of the Casimir force (2.22). That derivative force can then be computed by

$$\delta L \frac{\partial \Omega(\mu_1, L)}{\partial L} = \Delta\Omega(\mu_1, \mu_2, L) - \Delta\Omega(\mu_1, \mu_2, L - \delta L) \tag{3.117}$$

where $\delta L$ is the difference thickness between two systems, and which is then independent of $\mu_2$ in the large chemical potential limit as the free energy $\Omega(\mu_2, L)$ converges to the bulk energy.

Since in Kawasaki dynamics the total height is constant, this method does work only for model A.

on saute de potentiel à champ à chaque fois généralisation de la méthode de David pour n'importe quel observable Contexte de David, appliqué au modèle d'Ising, dans son contexte. PUIS traduire dans le contexte -¿ particule -¿ molécuilaire. Si l'aimantation doit être conservée ça doit être adapté. Utilisation de plusieurs types de champ magnétique, nouveauté. Pour un système d'Hamiltonien

$$H = J \sum_i |h_i - h_{i+1}| + \mu \frac{V(h_i) + V(h_{i+1})}{2} \tag{3.118}$$

on a la différence d'énergie le long d'une isotherme entre un état de référence $(T, \mu_0)$ et $(T, \mu)$ [68]

expliquer un petit peu plus en détail d'où vient l'équation Dans les modèles d'interface SOS, il est assez simple de calculer analytiquement $\Omega(\beta, L, \infty)$ par dénombrement de tous les états possibles. Cela nous permet d'obtenir via les simulations numériques l'énergie libre d'un système soumis à un potentiel quelconque de la forme 3.118 lorsque l'on intègre

le système dans la limite $\mu \to \infty$.

Dans le cas où on a un potentiel chimique normal, c'est-à-dire $V(h_i) = h_i$, alors l'intégration se fait directement sur le paramètre d'ordre $\langle \sum_i h_i \rangle$. Dans ce cas, dans la limite $\mu \to \infty$, la seule configuration possible est celle où $h_i = 0$ pour tout $i$, ce qui mène à l'énergie libre $\Omega(\beta, L, \infty) = 0$.

Si l'on désire mesurer l'énergie libre d'un tel système dans le cas d'une dynamique de Kawasaki, cette méthode ne donnera rien puisque par définition, $\langle \sum_i h_i \rangle$ est une constante. L'étude d'un Hamiltonien au chapitre **??** nous a conduit à un champ $V(h_i)$ possédant la même limite à $\mu \to \infty$. Considérons le champ suivant

$$V(h_i) = -|h_i - \frac{L}{2}| \tag{3.119}$$

Ce champ a tendance à plaquer l'interface loin de $\frac{L}{2}$, c'est-à-dire en $h = 0$ et $h = L$ pour un système de taille $L \times L'$, contrairement à un potentiel chimique classique où l'interface est plaquée en $h = 0$. Proche des limites du système, on observe que les deux champs sont équivalents à une constante près de l'énergie. Il existe donc deux positions d'équilibre stables de l'interface d'énergie équivalente au potentiel classique. Il y a ici une compétition entre l'énergie qui essaie de conserver l'interface lisse, et l'entropie, qui rend l'interface extrêmement rugueuse, comme dans la figure **??**.

Dnas la limite $\mu \to \infty$, on a donc un système éparpillé à $h = 0$ et $h = L$. On a la matrice de transfert

$$T = e^{\beta\mu\frac{L}{2}} \begin{pmatrix} 1 & e^{-\beta JL} \\ e^{-\beta JL} & 1 \end{pmatrix} \tag{3.120}$$

Les valeurs propres sont $\lambda_\pm = e^{\beta\mu\frac{L}{2}}(1 \pm e^{-\beta JL})$, ce qui nous donne dans la limite thermodynamique l'énergie libre

$$\Omega(\mu \to \infty) = -\mu\frac{L}{2} \tag{3.121}$$

Il est donc aisé de calculer l'énergie libre pour un champ donné grâce à l'intégration

$$\Omega(\beta, L, \mu) = \Omega(\beta, L, \infty) + \int_\mu^\infty d\mu' \langle \sum_i V(h_i) \rangle_{\beta, L, \mu'} \tag{3.122}$$

Cette méthode d'intégration est particulièrement adaptée aux modèles sur réseau où l'on

connait la limite du système soumis à un potentiel extrême. Dans le cas du modèle SOS, on pourrait avoir envie de diagonaliser directement la matrice de transfert pour $\mu = 0$, et ainsi obtenir

$$\Omega(\beta, L, \mu) = \Omega(\beta, L, 0) + \int_0^\mu d\mu' \langle \sum_i V(h_i) \rangle_{\beta, L, \mu'} \tag{3.123}$$

<span style="color:red">les longueurs de corrélation sont zéro, dans une limite est donnée uniquement par omega bulk+omefa surface. fluctuations divergentes. Le système critique est $\mu \to 0$ Pour petits champs, cette intégration est certes plus rapide, mais possède une limite divergente à $\mu = 0$, qui correspond à une interface libre dont la magnétisation moyenne est une valeur sans intérêt, ce qui nous oblige à garder la limite $\mu \to \infty$.</span>

<span style="color:red">mettre en valeur figure 4.4, ÇA MARCHE avec le numérique, PLUS DE CONTEXTE !!</span>

<span style="color:red">Besoin MCIA pour faire Casimir Kawasaki, ajouter cisaillement</span>

## 3.4 The confined solid on solid model

Here we consider the effect of confining the solid on solid model. The finite size effects in the SOS for both the restricted and unrestricted model were studied by Svravick et al. The formula for the eigenvalues of the even eigenvectors was given without derivation and the eigenvectors and odd eigenvalues were not discussed. In addition the limiting behavior of the free energy at high and low temperatures was not analysed and the correlation length was not discussed either.

Here we give the derivation for a system with sites between 0 and $H$ and with $V = 0$. The SOS transfer matrix is thus given by

$$T_{ij} = \exp(-\beta\sigma|j - i|). \tag{3.124}$$

We no proceed to find the eigenvectors of $T$. Consider the vector denoted by $[a]$ which has components

$$[a]_i = a^i, \tag{3.125}$$

where $i$ is an index ranging from 0 to $H$. The action of the SOS transfer matrix on this

vector is given by

$$[T[a]]_i = \sum_{j=0}^{H} \exp(-\beta\sigma|i-j|)a^j \tag{3.126}$$

and we find

$$
\begin{aligned}
[T[a]]_i &= \exp(-\beta\sigma i)\sum_{j=0}^{i}\exp(\beta\sigma j)a^j + \exp(\beta\sigma i)\sum_{j=i+1}^{H}\exp(-\beta\sigma j)a^j \\
&= \exp(-\beta\sigma i)\sum_{j=0}^{i}\exp(\beta\sigma j)a^j + \exp(\beta\sigma i)\sum_{k=0}^{H-i-1}\exp(-\beta\sigma[i+1+k])a^{i+1+k} \\
&= \exp(-\beta\sigma i)\frac{1-\exp(\beta\sigma(i+1))a^{i+1}}{1-\exp(\beta\sigma)a} + \exp(-\beta\sigma)a^{i+1}\frac{1-\exp(-\beta\sigma(H-i))a^{H-i}}{1-\exp(-\beta\sigma)a} \\
&= \left[\frac{\exp(-\beta\sigma)a}{1-\exp(-\beta\sigma)a} - \frac{\exp(\beta\sigma)a}{1-\exp(\beta\sigma)a}\right]a^i + \frac{\exp(-\beta\sigma i)}{1-\exp(\beta\sigma)a} - \frac{\exp(-\beta\sigma(H+1))a^{H+1}\exp(\beta\sigma i)}{1-\exp(-\beta\sigma)a} \\
&= \left[\frac{ra}{1-ra} - \frac{\frac{a}{r}}{1-\frac{a}{r}}\right]a^i + \frac{r^i}{1-\frac{a}{r}} - \frac{r^{H+1}a^{H+1}\frac{1}{r^i}}{1-ra}
\end{aligned}
$$

where we have introduced

$$r = \exp(-\beta\sigma). \tag{3.127}$$

We now define

$$\lambda(a) = \frac{ra}{1-ra} - \frac{\frac{a}{r}}{1-\frac{a}{r}} = \frac{\frac{1}{r}-r}{\frac{1}{r}+r-a-\frac{1}{a}} \tag{3.128}$$

and notice that

$$\lambda(a) = \lambda(a^{-1}). \tag{3.129}$$

We can thus write

$$[T[a]]_i = \lambda(a)a^i + \frac{r^i}{1-\frac{a}{r}} - \frac{r^{H+1}a^{H+1}\frac{1}{r^i}}{1-ra}. \tag{3.130}$$

Now consider the action of the transfer matrix on the vector $[a^{-1}]$, we find

$$\left[T[a^{-1}]\right]_i = \lambda(a)a^{-i} + \frac{r^i}{1-\frac{1}{ra}} - \frac{r^{H+1}a^{-(H+1)}\frac{1}{r^i}}{1-\frac{r}{a}}. \tag{3.131}$$

We now look for an eigenvector of the form

$$\mathbf{v} = [a] + c[a^{-1}].$$ (3.132)

The action of $T$ on $\mathbf{v}$ is this

$$\left[T\left([a] + c[a^{-1}]\right)\right]_i = \lambda(a)[a^i + ca^{-i}] + r^i \left(\frac{1}{1 - \frac{a}{r}} + \frac{c}{1 - \frac{1}{ra}}\right) - \frac{r^{H+1}}{r^i}\left(\frac{a^{H+1}}{1 - ra} + c\frac{a^{-(H+1)}}{1 - \frac{r}{a}}\right).$$ (3.133)

and we see that $\mathbf{v}$ is an eigenvector, with eigenvalue $\lambda(a)$, if

$$\frac{1}{1 - \frac{a}{r}} + \frac{c}{1 - \frac{1}{ra}} = 0$$ (3.134)

$$\frac{a^{H+1}}{1 - ra} + c\frac{a^{-(H+1)}}{1 - \frac{r}{a}} = 0.$$ (3.135)

The above equations imply that

$$c = -\frac{ra - 1}{a(r - a)}$$ (3.136)

and

$$c^2 = a^{2H}.$$ (3.137)

Therefore we find

$$v_i = a^i \pm a^{H-i},$$ (3.138)

however we expect the ground state eigenvector (corresponding to the largest eigenvalue) to be symmetric about the middle of the system and so

$$v_i = v_{H-i},$$ (3.139)

which implies that we should have $c = a^H$.


This then gives the equation determining the values of $a$ for the largest eigenvalue, and in general for the eigenvalues which are symmetric $c = 1$,

$$a^{H+1} = \frac{1 - ra}{r - a}.$$ (3.140)

As a check on the above derivation we can consider the case $H = 1$ so we have two sites.

Here we see that the transfer matrix is given explicitly by

$$T = \begin{pmatrix} 1 & r \\ r & 1 \end{pmatrix} \tag{3.141}$$

and the largest eigenvector is easily seen to be given by

$$\lambda_0 = 1 + r \tag{3.142}$$

Now for $H = 1$ we that Eq. (3.140) gives

$$a^2 = \frac{1 - ra}{r - a} \tag{3.143}$$

has three solutions

$$
\begin{align}
a_1 &= -1 \tag{3.144} \\
a_2 &= \frac{1}{2}\left(-\sqrt{r^2 + 2r - 3} + r + 1\right) \tag{3.145} \\
a_3 &= \frac{1}{2}\left(\sqrt{r^2 + 2r - 3} + r + 1\right) \tag{3.146}
\end{align}
$$

We see that $a_2 = 1/a_3$, and $|a_2| = |a_3| = 1$, also

$$\lambda(-1) = \frac{1 - r}{1 + r} \tag{3.147}$$

while

$$\lambda(a_2) = \lambda(a_3) = 1 + r \tag{3.148}$$

corresponds to the maximal eigenvalue. Note that $\lambda(-1)$ is not the other eigenvector of the transfer matrix, this has to be found by considering solutions with $c = -1$, as we will see later.

The equation (3.140) determining $a$ can also be written as

$$a^H = -\frac{r - \frac{1}{a}}{r - a}, \tag{3.149}$$

from this we see that if $a$ is a solution then $1/a$. Also we see that $a = -1$ is always a solution.

If we write $a = \exp(i\theta)$ then

$$\exp(iH\theta) = -\frac{r - \exp(-i\theta)}{r - \exp(i\theta)},$$ (3.150)

while

$$\lambda(\theta) = \frac{\sinh(\beta\sigma)}{\cosh(\beta\sigma) - \cos(\theta)}.$$ (3.151)

Notice that in order to construct a real eigenvector corresponding to $\lambda_0$ we can use the fact that both $v_i(a) = a^i + a^{H-i}$ and $v_i(a^{-1}) = a^{-i} + a^{-H+i}$ are both eigenvectors with the same eigenvalue. This means that $u_i(a) = v_i(a) + v_i(-a)$ is also and eigenvector and all its components are real.

Clearly the largest eigenvalue corresponds to the value of $\theta$ closest to 0. For $H$ large we look for an eigenvalue such that $H\theta \sim 1$ and so we write

$$\theta = \frac{\phi}{H}$$ (3.152)

for $H$ large this gives

$$\exp(i\phi) \approx -\frac{r - 1 + i\frac{\phi}{H}}{r - 1 - i\frac{\phi}{H}} \approx -1 + 2i\frac{\phi}{H(1-r)}$$ (3.153)

and so we find to leading order in $1/H$,

$$\theta = \frac{(2n+1)\pi}{H}.$$ (3.154)

However we notice that this approximation is only valid if $H(1-r) \gg 1$. For large $\beta$ this approximation is simply equivalent to $H \gg 1$, however when $\beta$ is small it requires that $H\beta \gg 1$.

The closest to the real axis has $n = 0$ and so we have

$$\lambda_0 \approx \frac{\sinh(\beta\sigma)}{\cosh(\beta\sigma) - \cos(\frac{\pi}{H})} \approx \frac{\sinh(\beta\sigma)}{\cosh(\beta\sigma) - 1 + \frac{\pi^2}{2H^2}} \approx \coth(\frac{\beta\sigma}{2})(1 - \frac{\pi^2}{4\sinh^2(\frac{\beta\sigma}{2})H^2}) \quad (3.155)$$

In order to compute the second eigenvalue $\lambda_1$ we look for and odd an antisymmetric

solution with $c = -1$. We thus find

$$\exp(iH\theta) = \frac{r - \exp(-i\theta)}{r - \exp(i\theta)}. \tag{3.156}$$

For large $H$ we look for a solution of the form $\theta = \phi/H$ and this gives

$$\exp(i\phi) \approx 1, \tag{3.157}$$

and so we chose solutions $\phi = 2n\pi$ for integer $n$, however the solution $n = 0$ which corresponds to $a = 1$ has $v(i) = a^i - a^{H-i} = 0$ and so does not correspond to an eigenvector. We thus take the next solution $\phi = 2\pi$ which gives

$$\lambda_1 \approx \frac{\sinh(\beta\sigma)}{\cosh(\beta\sigma) - \cos(\frac{2\pi}{H})} \approx \frac{\sinh(\beta\sigma)}{\cosh(\beta\sigma) - 1 + \frac{2\pi^2}{H^2}} \approx \coth(\frac{\beta\sigma}{2})(1 - \frac{\pi^2}{\sinh^2(\frac{\beta\sigma}{2})H^2}) \tag{3.158}$$

The correlation length is then given by

$$\xi = \frac{1}{\ln(\frac{\lambda_0}{\lambda_1})} = \frac{1}{\ln(\frac{\cosh(\beta\sigma) - \cos(\frac{\pi}{H})}{\cosh(\beta\sigma) - \cos(\frac{2\pi}{H})})} \approx \frac{4}{3} \frac{\sinh^2(\frac{\beta\sigma}{2})H^2}{\pi^2}, \tag{3.159}$$

and we see that this has the same form as that for the free elastic line in Eq. (3.85). Furthermore, the free energy per site is given in the thermodynamic limit and for large $H$ by

$$f = -\frac{1}{\beta} \ln(\lambda_0) \approx -\frac{1}{\beta} \left[ \ln(\coth(\frac{\beta\sigma}{2})) - \frac{\pi^2}{4\sinh^2(\frac{\beta\sigma}{2})H^2} \right] \tag{3.160}$$

and this gives a pressure

$$P = -\frac{\partial f}{\partial H} = \frac{T\pi^2}{2\sigma \sinh^2(\frac{\beta}{2})H^2}. \tag{3.161}$$

This has the same form as the pressure for the elastic line in Eq. (3.84) if we make the identification of the effective surface tension to be used in the elastic line model

$$\sigma_{eff} = \frac{2}{\beta} \sinh^2(\frac{\beta\sigma}{2}). \tag{3.162}$$

We should note that this is also consistent with the equality deduced by comparing the correlation length of the two models.

We see that in the limit of large $H$ and for appropriately low temperatures, the finite size

SOS model reproduced the phenomenology of the elastic line (confined Edwards-Wilkinson surface). This is not surprising as a low temperatures jumps of more that two lattice spacings in the height are suppressed by a factor or $\exp(-\beta\sigma)$ with respect to staying at the same height moving up or down by one site. The low temperature SOS model thus becomes effectively equivalent to the RSOS model and thus is equivalent to a local random walk model.

To explore the high temperature limit we can note that if we write

$$z = r - \exp(-i\theta), \tag{3.163}$$

we can write Eq. (3.150) as

$$\exp(iH\theta) = -\frac{z}{\bar{z}} = \exp(2i\psi + i\pi), \tag{3.164}$$

where

$$\tan(\psi) = \frac{\sin(\theta)}{r - \cos(\theta)}. \tag{3.165}$$

This then gives

$$H\theta = 2\psi + \pi, \tag{3.166}$$

and so

$$\tan(\psi) = \frac{\sin(\theta)}{r - \cos(\theta)} = \tan(\frac{H\theta}{2} + \frac{\pi}{2}) = -\cot(\frac{H\theta}{2}) \tag{3.167}$$

which finally gives

$$\tan(\frac{H\theta}{2}) = \frac{\cos(\theta) - r}{\sin(\theta)}. \tag{3.168}$$

In this form we see that our calculations agree with those of Svravick et al. Futhermore when $\beta \to 0$ we know that the elements of the transfer matrix all tend to one and that the largest eigenvalue has all components equal. This means that in the infinite temperature limit $\theta = 0$. Therefore in Eq. (3.168) we look for solutions where $\theta$ is small. Taylor expanding gives to leading order

$$\frac{H\theta^2}{2} \approx 1 - r - \frac{\theta^2}{2}, \tag{3.169}$$

which gives

$$\theta \approx \sqrt{\frac{2(1-r)}{H+1}}. \tag{3.170}$$

However the above expansion assumes that $\theta H \ll 1$ and so

$$\sqrt{2H(1-r)} \ll 1. \tag{3.171}$$

Therefore at high temperature this means that $H\beta\sigma \ll 1$. This means that the height can fluctuate by of order $H$ from site to site. The high temperature approximation is thus equivalent to

$$\theta \approx \sqrt{\frac{2\beta\sigma}{H+1}}. \tag{3.172}$$

This gives a maximal eigenvalue

$$\lambda_0 = H + 1, \tag{3.173}$$

and the free energy

$$f = -\frac{1}{\beta}\ln(H+1), \tag{3.174}$$

which is the obvious result coming from the infinite temperature entropy.

This result suggests that the solution for $\theta$ at small $\beta$ can be written as a perturbation series of the form

$$\theta = \sqrt{\beta\sigma}\sum_{n=0}^{\infty} b_n(\beta\sigma)^n. \tag{3.175}$$

The first two terms give

$$\theta = \sqrt{\beta\sigma}\left[\sqrt{\frac{2\beta\sigma}{H+1}} - \beta\sigma\frac{2+2H+H^2}{6\sqrt{2}(1+H)^{\frac{3}{2}}}\right], \tag{3.176}$$

and from this we find

$$f = -\frac{1}{\beta}\ln(H+1-\beta\sigma\frac{H^2+2H}{3}). \tag{3.177}$$

As pointed out above this result gives the high temperature entropy but it also exhibits the correct average energy $\epsilon$ per unit length at high temperature. To see this we note that

all values of $h$ are equiprobable at infinite temperature and so

$$\epsilon = \frac{1}{(H+1)^2}\sigma \sum_{i,j=0}^{H} |i-j| = \sigma\frac{H^2 + 2H}{3}. \tag{3.178}$$

### 3.4.1 Numerical tests of finite size dependence

# Chapter 4

# Driven model C interfaces

We consider the effect of uniform driving on the interface between two phases which are described by model C dynamics. The non-driven system has a classical Gaussian interface described by capillary wave theory. The model under driving retains Gaussian statistics but the interface statistics are modified by driving, notably the height fluctuations are suppressed and the correlation length of the fluctuations is increased.

## 4.1 Introduction

The model we introduce can also be used as a model for the effect of activity on interface dynamics. One of the most natural ways of creating a non-equilibrium steady state is by applying external driving forces. Driving arises naturally in sedimenting systems due to gravity, in systems with free charges under the action of an electric field and also due to the radiation pressure exerted by a laser. Experiments where a phase separated colloidal system is sheared parallel to the interface show that driving due to shear tends to suppress surface fluctuations [**?** ], and similar results are found where Ising models are numerically sheared [**?  ?** ]. These results are somewhat surprising, for instance they are contrary to the observation that wind generates waves on the ocean. One may think that the precise nature of the driving plays a role, for instance uniformly driving a system may be intrinsically different to applying a shear field which is manifestly nonuniform. In this paper we investigate analytically the effect of uniform driving on a simple interface model. We find that the effect of this type of driving is also to reduce surface fluctuations.

Constructing a continuum model which is analytically tractable and is also affected by

uniform driving is straightforward but contains some subtleties. In a continuum system it is clear that uniform driving can only move a system away from equilibrium when the driving acts differently on different particle types. For instance, consider a system of identical interacting Brownian particles driven by a uniform force. The force will induce the same average velocity on all the particles, consequently, in the frame moving with this average velocity, we will recover the unmodified equilibrium state. However, when multiple particle types are present, the mean velocity induced on different species are different and no Galilean transformation is possible. Perhaps the first such study of this phenomenon was due to Onsager [**?**], who studied the conductivity of electrolytes and in doing so showed how the correlation functions in the steady state were modified by the electric field. Recently there have been many studies of driven multi-particle Brownian systems [**? ? ? ? ? ? ?**], including the electrolyte problem, and rich new physics has been found, even in the case of purely Gaussian theories [**? ?**] based on stochastic density functional theory [**?**].

The dynamics of discrete particle systems is however affected by uniform driving of identical particles. The study of driven lattice gases has revealed a wide range of intriguing physical phenomena and indeed shown how driving can even lead to phase separation [**? ? ? ? ?**]. The discrete nature of the dynamics of these systems, both in space and time, means that no Galilean transformation to an equilibrium state exists. Analytical studies of these systems require a phase ordering kinetics description in terms of a continuum order parameter. In order to break Galilean invariance the local mobility of the particles can be taken to be dependent on the local order parameter, this is then sufficient to induce non-trivial steady states under driving [**? ? ? ?**]. Interfaces between the separated phases in uniformly driven systems have non capillary behaviors which are, even today, not fully understood [**?**]. Taking random driving in a given direction also leads to non-equilibrium steady states, if the noise is Gaussian and white, the fluctuation dissipation theorem is violated and novel interface fluctuations are induced which, again, are not of the capillary type [**?**].

Driving can also be deterministic but space dependent, for instance if one considers applied shear flows, the spatial dependence of the flow means no Galilean transformation to an equilibrium steady state is possible and this therefore leads to non-equilibrium steady states. The effect of shear on interfaces in these type of systems yields interface equations of the stochastic Burgers type and the statistics are no thus longer Gaussian due to the presence of nonlinearities [**? ? ? ? ? ?**].

In this paper we analyse what is known, in the classification of Hohenberg and Halperin [**?** ], as model C type dynamics for two fields, one with conserved model B type dynamics, which is in addition convected at a uniform velocity to mimic driving. We refer to this first field as the colloid field. This colloid field is coupled to an additional field which undergoes model A non-conserved dynamics and which is not subjected to the driving. The model A field can be thought of a passive solvent and its coupling to the model B field is chosen in such a way that it has no influence on the non-driven equilibrium steady state. We then derive the effective dynamics between two separated low temperature phases by using a method introduced in [**? ?** ] for the study of interfaces under shear flow. This method yields a Gaussian theory for the interface statistics and driving introduces interesting new physics, notably we find that the effective surface tension of the system is increased but also the correlation length of interface fluctuations (due to an effective gravitational term) are increased. These observations are in qualitative agreement with experimental results on sheared low tension interfaces in phase separated colloidal systems [**?** ]. In this experimental system the interface fluctuations were also found to be well described by Gaussian statistics and this is our principal motivation for studying theories which remain Gaussian but are modified by driving. While the long wavelength theory we find is of a capillary type, we also find new, higher derivative terms, which are generated in the spectrum of the height fluctuations.

As an aside, we also show how the model introduced here can be used to analyse the effect of activity on the dynamics of the surface between two phases of active colloids. The activity is implemented by taking a different temperature for the colloid and solvent fields, this difference in temperatures leads to significantly modified surface statistics which again develop dependencies on static and dynamical variables of the model which otherwise remain hidden for the equilibrium version of the problem.

## 4.2   The underling two field model

We consider a coarse grained model for two scalar fields $\psi$ and $\phi$ with Hamiltonian

$$H[\psi, \phi] = H_1[\psi] + H_2[\psi, \phi] \tag{4.1}$$

The Hamiltonian $H_1$ is of the classic Landau-Ginzburg form

$$H_1[\psi] = \int d\mathbf{x} \left[ \frac{\kappa}{2} [\nabla \psi(\mathbf{x})]^2 + V(\psi(\mathbf{x})) - gz\psi(\mathbf{x}) \right]. \tag{4.2}$$

The last term represents the energy due to a gravitational field and will introduce a finite correlation length in the fluctuations between the two phases. We assume that the above Hamiltonian has two stable phases with average concentrations of the field $\phi(\mathbf{x})$ given by the constant values $\psi_1$ and $\psi_2$, the difference between the order parameter in the two different phases is denoted by by $\Delta \psi = \psi_2 - \psi_1 \rangle 0$. This means that we find the phase 1 as $z \to \infty$ and the phase 2 as $z \to -\infty$. The term $H_2$ is taken to be a simple quadratic coupling between the fields

$$H_2 = \int d\mathbf{x} \frac{\lambda}{2} (1 - \psi(\mathbf{x}) - \phi(\mathbf{x}))^2, \tag{4.3}$$

this is an approximative conservation law of total volume fraction of the phases. The field $\phi$ can be though of as the local volume fraction of the solvent in a colloidal system. However the presence of this solvent field does not change the effective equilibrium statistical mechanics of the colloid field $\psi$ as the partition function can be written as

$$Z = \int d[\phi] d[\psi] \exp(-\beta H_1[\psi] - \beta H_2[\psi, \phi]) = C Z_{eff}, \tag{4.4}$$

where $Z_{eff}$ is the effective partition function for the field $\psi$, after we have integrated out the degrees of freedom corresponding to the field $\phi$, and $C$ is a constant term resulting from this integration. The effective partition function is thus simply given by

$$Z_{eff} = \int d[\psi] \exp(-\beta H_1[\psi]), \tag{4.5}$$

and, as stated above, we see that the field $\phi$ thus has no effect on the equilibrium statistical mechanics of the field $\psi$.

We now consider the dynamics of the fields. We take local diffusive model B dynamics for the field $\psi$ and non-conserved model A dynamics for the field $\phi$

$$\frac{\partial \psi(\mathbf{x}, t)}{\partial t} + \mathbf{v} \cdot \nabla \psi(\mathbf{x}, t) = D\nabla^2 \frac{\delta H}{\delta \psi(\mathbf{x})} + \sqrt{2DT} \nabla \cdot \boldsymbol{\eta}_1(\mathbf{x}, t) \tag{4.6}$$

$$\frac{\partial \phi(\mathbf{x}, t)}{\partial t} = -\alpha \frac{\delta H}{\delta \phi(\mathbf{x})} + \sqrt{2\alpha T} \eta_2(\mathbf{x}, t). \tag{4.7}$$

The first equation corresponds to standard model B dynamics but with an advection term by a constant velocity field **v**. The second equation has no advection term and is simple model A dynamics. In principle we can also treat the case where the dynamics of the field $\phi$ is also diffusive and thus of model $B$ type, the analysis given here can be extended to this case but the analysis of the resulting equations is considerably more complicated. The use of model A dynamics for the solvent is justified by assuming that its dynamics is faster than that of the colloids and that the volume fraction can vary due to local conformational changes rather than diffusive transport.

The noise terms above are uncorrelated and Gaussian with zero mean, their correlation functions are given by

$$\langle \eta_{1i}(\mathbf{x},t)\eta_{1j}(\mathbf{x}',t)\rangle \;\; = \;\; \delta_{ij}\delta(t-t')\delta(\mathbf{x}-\mathbf{x}') \tag{4.8}$$

$$\langle \eta_2(\mathbf{x},t)\eta_2(\mathbf{x}',t)\rangle \;\; = \;\; \delta(t-t')\delta(\mathbf{x}-\mathbf{x}'), \tag{4.9}$$

and $T$ is the temperature in units where $k_B = 1$. These dynamical equations are thus explicitly given by

$$\frac{\partial\psi(\mathbf{x},t)}{\partial t} + \mathbf{v}\cdot\nabla\psi(\mathbf{x},t) = D\nabla^2[\frac{\delta H_1}{\delta\psi(\mathbf{x})} + \lambda(\phi(\mathbf{x},t)+\psi(\mathbf{x},t))] + \sqrt{2DT}\nabla\cdot\boldsymbol{\eta}_1(\mathbf{x},t) \tag{4.10}$$

and

$$\frac{\partial\phi(\mathbf{x},t)}{\partial t} = -\alpha\lambda[\phi(\mathbf{x},t)+\psi(\mathbf{x},t)] + \sqrt{2\alpha T}\eta_2(\mathbf{x},t). \tag{4.11}$$

Taking the temporal Fourier transform, defined with the convention

$$\tilde{F}(\mathbf{x},\omega) = \int_{-\infty}^{\infty} dt\,\exp(-i\omega t)F(\mathbf{x},t), \tag{4.12}$$

we can eliminate the field $\tilde{\phi}$ which is given by

$$\tilde{\phi}(\mathbf{x},\omega) = \frac{-\alpha\lambda\tilde{\psi}(\mathbf{x},\omega)+\sqrt{2\alpha T}\tilde{\eta}_2(\mathbf{x},\omega)}{i\omega+\alpha\lambda}, \tag{4.13}$$

this then gives the closed equation for $\tilde{\psi}$:

$$\left[1 - \frac{\lambda D\nabla^2}{i\omega+\alpha\lambda}\right]i\omega\tilde{\psi}(\mathbf{x},\omega) + \mathbf{v}\cdot\nabla\tilde{\psi}(\mathbf{x},\omega) = D\nabla^2\tilde{\mu}(\mathbf{x},\omega) + \tilde{\zeta}(\mathbf{x},\omega), \tag{4.14}$$

where

$$\mu(\mathbf{x}, t) = \frac{\delta H_1}{\delta \psi(\mathbf{x}, t)} \tag{4.15}$$

is the effective chemical potential associated with the field $\psi$ and the noise term is given by

$$\tilde{\zeta}(\mathbf{x}, \omega) = \frac{\sqrt{2\alpha T} D\lambda}{i\omega + \alpha\lambda} \nabla^2 \tilde{\eta}_2(\mathbf{x}, \omega) + \sqrt{2DT} \nabla \cdot \tilde{\boldsymbol{\eta}}_1(\mathbf{x}, \omega). \tag{4.16}$$

Inverting the temporal Fourier transform then gives the effective evolution equation

$$\frac{\partial \psi(\mathbf{x}, t)}{\partial t} - \lambda D \nabla^2 \int_{-\infty}^{t} dt' \exp(-\alpha\lambda(t - t')) \frac{\partial \psi(\mathbf{x}, t')}{\partial t} + \mathbf{v} \cdot \nabla \psi(\mathbf{x}, t) = D\nabla^2 \mu(\mathbf{x}, t') + \zeta(\mathbf{x}, t). \tag{4.17}$$

## 4.3 Effective interface dynamics

We now follow the method of [? ? ] to derive the dynamical equation for the interface between the two phases. It is assumed that the driving is in the $\mathbf{r} = (x, y)$ plane and that the system varies from phase 1 to phase 2 in the $z$ direction. The dynamical evolution for the field $\psi$ in Eq. (4.17) is first written as

$$\nabla^{-2} \left[ \frac{\partial \psi(\mathbf{x}, t)}{\partial t} + \mathbf{v} \cdot \nabla \psi(\mathbf{x}, t) \right] - \lambda D \int_{-\infty}^{t} dt' \exp(-\alpha\lambda(t-t')) \frac{\partial \psi(\mathbf{x}, t')}{\partial t'} = D\mu(\mathbf{x}, t') + \nabla^{-2}\zeta(\mathbf{x}, t). \tag{4.18}$$

We now assume that the field $\psi$ can be written in the form

$$\psi(\mathbf{x}, t) = f(z - h(\mathbf{r}, t)), \tag{4.19}$$

and $f(z) \to \psi_2$ as $z \to -\infty$ and $f(z) \to \psi_2$ as $z \to \infty$. We now note the following results

$$\frac{\partial f(z - h(\mathbf{r}, t))}{\partial t} = -f'(z - h(\mathbf{r}, t)) \frac{\partial h(\mathbf{r}, t)}{\partial t} \tag{4.20}$$

$$\nabla f(z - h(\mathbf{r}, t)) = [\mathbf{e}_z - \nabla h(\mathbf{r}, t)] f'(z - h(\mathbf{r}, t))] \tag{4.21}$$

$$\nabla^2 f(z - h(\mathbf{r}, t)) = f''(z - h(\mathbf{r}, t))[1 + [\nabla h(\mathbf{r}, t)]^2] - \nabla^2 h(\mathbf{r}, t) f'(z - h(\mathbf{r}, t)), \tag{4.22}$$

and thus we find

$$\mu(\mathbf{x}, t) = -\kappa \left( f''(z - h(\mathbf{r}, t))[1 + [\nabla h(\mathbf{r}, t)]^2] - \nabla^2 h(\mathbf{r}, t) f'(z - h(\mathbf{r}, t)) \right) + V'(f(z - h(\mathbf{r}, t)) - gz.$$
(4.23)

Multiplying both sides of the above by $f'(z - h(\mathbf{r}, t))$ yields

$$f'(z - h(\mathbf{r}, t))\mu(\mathbf{x}, t) =$$
$$-\kappa \left( f'(z - h(\mathbf{r}, t)) f''(z - h(\mathbf{r}, t))[1 + [\nabla h(\mathbf{r}, t)]^2] - \nabla^2 h(\mathbf{r}, t) f'(z - h(\mathbf{r}, t))^2 \right) + V'(f(z - h(\mathbf{r}, t)) f'(z - h(\mathbf{r}, t))$$
$$-gz f'(z - h(\mathbf{r}, t))$$

and then integrating over $z$ we obtain

$$
\begin{aligned}
\int_{-\infty}^{\infty} dz f'(z - h(\mathbf{r}, t))\mu(\mathbf{x}, t) &= \kappa \nabla^2 h(\mathbf{r}, t) \int_{-\infty}^{\infty} dz \ f'(z - h(\mathbf{r}, t))^2 - \int_{-\infty}^{\infty} dz gz f'(z - h(\mathbf{r}, t)) \\
&= \kappa \nabla^2 h(\mathbf{r}, t) \int_{-\infty}^{\infty} dz' \ f'(z')^2 - \int_{-\infty}^{\infty} dz' g(z' + h(\mathbf{r}, t)) f'(z') \\
&= \kappa \nabla^2 h(\mathbf{r}, t) \int_{-\infty}^{\infty} dz' \ f'(z')^2 - \Delta\psi g h(\mathbf{r}, t).
\end{aligned}
$$
(4.24)

In the above we have assumed that $\int_{-\infty}^{\infty} dz' z' f'(z') = 0$ by symmetry (this is also consistent with the approximation made later on in Eq. (4.28)). Furthermore one can show that [**?** **?** ]

$$\kappa \int_{-\infty}^{\infty} dz' \ f'(z')^2 = \sigma,$$
(4.25)

where $\sigma$ is the mean-field equilibrium Cahn-Hilliard estimate of the surface tension, obtained by assuming that $f(z) = \psi_{MF}(z)$ is the equilibrium mean field profile of the field $\psi$. We thus find

$$\int_{-\infty}^{\infty} dz f'(z - h(\mathbf{r}, t))\mu(\mathbf{x}, t) = \sigma[\nabla^2 h(\mathbf{r}, t) - m^2 h(\mathbf{r}, t)]$$
(4.26)

where $m^2 = \Delta\psi g/\sigma$. We now carry out the same operation on the left hand side of Eq. (4.18). First we have

$$
\begin{aligned}
\nabla^{-2}\frac{\partial\psi(\mathbf{x},t)}{\partial t} \quad &+ \quad \mathbf{v}\cdot\nabla\psi(\mathbf{x},t) + \lambda D \int_{-\infty}^{t} dt' \exp(-\alpha\lambda(t-t'))\frac{\partial\psi(\mathbf{x},t')}{\partial t'} = \\
&- \quad \nabla^{-2}f'(z-h(\mathbf{r},t))[\frac{\partial h(\mathbf{r},t)}{\partial t} + \mathbf{v}\cdot\nabla h(\mathbf{r},t)] + \lambda D \int_{-\infty}^{t} dt' \exp(-\alpha\lambda(t-t'))f'(z-h(\mathbf{r},t')) \\
&\approx \quad -\nabla^{-2}f'(z)[\frac{\partial h(\mathbf{r},t)}{\partial t} + \mathbf{v}\cdot\nabla h(\mathbf{r},t)] + \lambda D \int_{-\infty}^{t} dt' \exp(-\alpha\lambda(t-t'))f'(z)\frac{\partial h(\mathbf{r},t')}{\partial t'},
\end{aligned}
$$

where in the last line above we have neglected terms quadratic in $h$. Note that the neglecting of these additional terms is not strictly justified, they could potentially induce non-perturbative effects which render the surface fluctuations non-Gaussian. However we see here that the first order computation we carry out tends to reduce fluctuations with respect to equilibrium or non-driven interfaces and so if the equilibrium theory can be described by an equation which is linear in height fluctuations, it seems physically reasonable to assume that the the approximation also holds for the driven interface. Again, we multiply the above by $f'(z)$ and integrate over $z$. In the first term we make use of the approximation

$$
f'(z) = \Delta\psi\delta(z) \tag{4.28}
$$

and in the second we use the relation in Eq. (4.25). Putting this all together we obtain

$$
\Delta\psi^2 \int d\mathbf{r}G(0,\mathbf{r}-\mathbf{r}')[\frac{\partial h(\mathbf{r},t)}{\partial t}+\mathbf{v}\cdot\nabla h(\mathbf{r},t)]+\frac{\sigma\lambda D}{\kappa}\int_{-\infty}^{t} dt' \exp(-\alpha\lambda(t-t'))\frac{\partial h(\mathbf{r},t')}{\partial t'} = \sigma[\nabla^2 h(\mathbf{r},t)-m^2 h(\mathbf{r},t)] \tag{4.29}
$$

where $G = -\nabla^{-2}$, or more explicitly

$$
\nabla^2 G(z-z',\mathbf{r}-\mathbf{r}') = -\delta(z-z')\delta(\mathbf{r}-\mathbf{r}'). \tag{4.30}
$$

The noise term $\xi$ is given by

$$
\xi(\mathbf{r},t) = \int_{-\infty}^{\infty} dz f'(z-h(\mathbf{r},t))\nabla^{-2}\zeta(\mathbf{x},t). \tag{4.31}
$$

Now, as the equations of motion have been derived to first order in $h$ and we wish to recover the correct equilibrium statistics for the non-driven system, we ignore the $h$ dependence in

the noise and make the approximation

$$\xi(\mathbf{r}, t) \approx \int_{-\infty}^{\infty} dz f'(z) \nabla^{-2} \zeta(\mathbf{x}, t). \tag{4.32}$$

The correlation function of this noise is most easily evaluated in terms of its Fourier transform with respect to space and time defined by

$$\hat{F}(\mathbf{q}, \omega) = \int dt d\mathbf{r} \exp(-i\omega t - i\mathbf{q} \cdot \mathbf{r}) F(\mathbf{r}, t). \tag{4.33}$$

Using the relations Eqs. (4.25) and (4.28) one can show that

$$\langle \hat{\xi}(\mathbf{q}, \omega) \hat{\xi}(\mathbf{q}', \omega') \rangle = 2T(2\pi)^d \delta(\omega + \omega') \delta(\mathbf{q} + \mathbf{q}') \left[ \frac{\sigma}{\kappa} \frac{\alpha D^2 \lambda^2}{\omega^2 + \alpha^2 \lambda^2} + \frac{D \Delta \psi^2}{2q} \right]. \tag{4.34}$$

In full Fourier space the equation of motion for the field $\psi$ then reads

$$\left[ i(\omega + \mathbf{q} \cdot \mathbf{v}) \frac{\Delta \psi^2}{2q} + \frac{D\sigma\lambda}{\kappa} \frac{i\omega}{\alpha\lambda + i\omega} \right] \hat{h}(\mathbf{q}, \omega) = -D\sigma(q^2 + m^2)\hat{h}(\mathbf{q}, \omega) + \hat{\xi}(\mathbf{q}, \omega) \tag{4.35}$$

From this, the full Fourier transform of the correlation function of the interface height is given by

$$\hat{C}(\mathbf{q}, \omega) = 2TD \frac{\left[ \frac{\Delta \psi^2}{2q}(\omega^2 + \alpha^2 \lambda^2) + \frac{\sigma \alpha D \lambda^2}{\kappa} \right]}{\left| i[\frac{\alpha\lambda\Delta\psi^2}{2q}(\omega + \mathbf{q} \cdot \mathbf{v}) + \frac{\lambda\sigma D}{\kappa}\omega + D\sigma(q^2 + m^2)\omega] + [\alpha\lambda D\sigma(q^2 + m^2) - \frac{\Delta\psi^2}{2q}\omega(\omega + \mathbf{q} \cdot \mathbf{v})] \right|^2}. \tag{4.36}$$

Using the above we can extract the equal time height-height correlation function in the steady states. Its spatial Fourier transform can shown to be given by

$$
\begin{aligned}
\tilde{C}_s(\mathbf{q}) &= \frac{1}{2\pi} \int d\omega \hat{C}(\mathbf{q}, \omega) \\
&= T \frac{(2D\sigma q(\kappa[q^2 + m^2] + \lambda) + \alpha\kappa\lambda\Delta\psi^2)^2 + \kappa^2 \Delta\psi^4 (\mathbf{q} \cdot \mathbf{v})^2}{\sigma[q^2 + m^2] (2D q\sigma(\kappa[q^2 + m^2] + \lambda) + \alpha\kappa\lambda\Delta\psi^2)^2 + \kappa (\kappa\sigma[q^2 + m^2] + \lambda\sigma) \Delta\psi^4 (\mathbf{q} \cdot \mathbf{v})^2}
\end{aligned} \tag{4.37}
$$

An outline of the derivation of this result is given in the Appendix to the paper. In the absence of driving, *i.e.* when $\mathbf{v} = \mathbf{0}$ we recover the equilibrium correlation function

$$\tilde{C}_s(\mathbf{q}) = \tilde{C}_{eq}(\mathbf{q}) = \frac{T}{\sigma[q^2 + m^2]}, \tag{4.38}$$

here we see that $1/m = \xi_{eq}$ is the so called capillary length, which is the equilibrium correlation length of the height fluctuations. We also notice that the correlation function for wave vectors perpendicular to the driving direction is simply the equilibrium one.

If we write $C_s(\mathbf{q}) = T/H_s(\mathbf{q})$ we can interpret $H_s(\mathbf{q})$ as an effective quadratic Hamiltonian for the height fluctuations, it is thus given by

$$H_s(\mathbf{q}) = \sigma[q^2 + m^2] + \frac{\kappa\lambda\sigma\Delta\psi^4(\mathbf{q}\cdot\mathbf{v})^2}{(2D\sigma q(\kappa[q^2 + m^2] + \lambda) + \alpha\kappa\lambda\Delta\psi^2)^2 + \kappa^2\Delta\psi^4(\mathbf{q}\cdot\mathbf{v})^2} \tag{4.39}$$

For small $q$ we find

$$H_s(\mathbf{q}) = \sigma m^2 + \sigma q^2(1 + \frac{v^2\cos^2(\theta)}{\alpha^2\lambda\kappa}), \tag{4.40}$$

where $\theta$ is the angle between the wave vector $\mathbf{q}$ and the direction of the driving. This thus gives a direction dependent surface tension

$$\sigma_s(\theta) = \sigma(1 + \frac{v^2\cos^2(\theta)}{v_0^2}), \tag{4.41}$$

where we have introduced the intrinsic velocity $v_0 = \sqrt{\alpha^2\lambda\kappa}$ which depends on the microscopic *dynamical* quantity $\alpha$ associated with the model A dynamics of the field $\phi$, as well as the microscopic static quantities $\kappa$ (which generates the surface tension) and $\lambda$ the coupling between the field $\psi$ and $\phi$. This appearance of dynamical and static quantities that are otherwise hidden in equal time correlation functions in equilibrium is already implicit in the works of Onsager [**?** ] where it is used to compute the conductivity of Brownian electrolytes and the explicit expressions were derived using stochastic density functional theory in [**?** ]. We also note that the universal thermal Casimir effect between model Brownian electrolyte systems driven by an electric field exhibits similar features, developing a dependency on both additional static and dynamical variables with respect to the equilibrium case [**?** ]

However for this small $q$ expansion we see that the microscopic quantities $D$, the diffusion constant of the field $\phi$, and the order parameter jump $\Delta\psi$ do not appear.

From the above, we see that in the direction of the driving the surface tension increases and the fluctuations of the surface are thus suppressed. We may also write

$$H_s(\mathbf{q}) = \sigma_s(\theta)[q^2 + m_e^2(\theta)], \tag{4.42}$$

with

$$m_s^2(\theta) = \frac{m^2}{1 + \frac{v^2 \cos^2(\theta)}{v_0^2}}, \tag{4.43}$$

this corresponds to a correlation length

$$\xi_s = \xi_{eq}\sqrt{1 + \frac{v^2 \cos^2(\theta)}{v_0^2}}, \tag{4.44}$$

and we see that it is increased in the direction of the driving.

As we have just remarked that the above results appear to be independent of the order parameter jump $\Delta\psi$ and the diffusion constant $D$, however the next order correction to $H_s$ for small $q$ is given by

$$H_s(\mathbf{q}) = \sigma_s(\theta)[q^2 + m_e^2(\theta)] - \frac{4Dq\sigma^2(\lambda + \kappa m^2)(\mathbf{q} \cdot \mathbf{v})^2}{\alpha^3 \kappa^2 \lambda^2 \Delta\psi^2}, \tag{4.45}$$

and so the small $\mathbf{q}$ expansion breaks down at $\Delta\psi = 0$, indeed one can see that the system has exactly the equilibrium correlation function when $\Delta\psi = 0$.

In the limit of large $q$ we see that the effective Hamiltonian is given, to leading order, by the original equilibrium Hamiltonian and so the out of equilibrium driving has no effect on the most energetic modes of the system.

The results here predict that for unconfined surfaces the long range height fluctuations are described by an isotropic form of capillary wave theory with an anisotropic surface tension which is largest in the direction of driving. Numerical simulations of driven lattice gases in two dimensions [?] show a more drastic change upon driving and find $C_s(q) \sim 1/q^{.66}$ and thus a strong deviation from capillary wave theory.

## 4.4 A model of active interfaces

We can apply the results derived in the previous section to analyse a simple model for surfaces formed between two phases of active colloids. Activity is modelled by assuming that the colloidal field $\psi$ has a temperature different to that of the solvent field $\phi$. This models the effect that activity leads to enhanced colloidal diffusivity over and above the Brownian motion of particles due to thermal fluctuations [?].

In the absence of any driving the dynamical equations for the field $\psi$ and $\phi$ become

$$\frac{\partial \psi(\mathbf{x},t)}{\partial t} = D\nabla^2 \frac{\delta H}{\delta \psi(\mathbf{x})} + \sqrt{2DT_1}\nabla \cdot \boldsymbol{\eta}_1(\mathbf{x},t) \tag{4.46}$$

$$\frac{\partial \phi(\mathbf{x},t)}{\partial t} = -\alpha \frac{\delta H}{\delta \phi(\mathbf{x})} + \sqrt{2\alpha T_2}\eta_2(\mathbf{x},t). \tag{4.47}$$

Following the same arguments as above we find that

$$\hat{C}(\mathbf{q},\omega) = 2D\frac{\left[T_1\frac{\Delta\psi^2}{2q}(\omega^2 + \alpha^2\lambda^2) + T_2\frac{\sigma\alpha D\lambda^2}{\kappa}\right]}{\left|i\omega[\frac{\alpha\lambda\Delta\psi^2}{2q} + \frac{\lambda\sigma D}{\kappa} + D\sigma(q^2+m^2)] + [\alpha\lambda D\sigma(q^2+m^2) - \frac{\Delta\psi^2}{2q}\omega^2]\right|^2}. \tag{4.48}$$

The equal time steady state height fluctuations thus have correlation function

$$\tilde{C}_s(q) = \frac{T_1}{\sigma(q^2+m^2)}\left[1 - (1 - \frac{T_2}{T_1})\frac{\lambda\sigma}{\kappa}\frac{1}{\frac{\alpha\lambda\Delta\psi^2}{2Dq} + \frac{\lambda\sigma}{\kappa} + \sigma(q^2+m^2)}\right]. \tag{4.49}$$

We see, again, that the inclusion of a non-equilibrium driving changes the statistics of height fluctuations and leads to a steady state that depends on both dynamical variables $D$ and $\alpha$ as well as static ones $\Delta\psi$, $\lambda$ and $\kappa$ that remain hidden in the equilibrium case. This phenomenon is again seen in the behavior of the universal thermal Casimir force between Brownian conductors held at different temperatures [**?** ].

If we assume strong activity we can take the limit $T_1 \gg T_2$, in this case we find

$$\tilde{C}_s(q) = \frac{T_1}{\sigma(q^2+m^2)}\frac{\frac{\alpha\lambda\Delta\psi^2}{2Dq} + \sigma(q^2+m^2)}{\frac{\alpha\lambda\Delta\psi^2}{2Dq} + \frac{\lambda\sigma}{\kappa} + \sigma(q^2+m^2)}. \tag{4.50}$$

Interpreted in terms of an effective Hamiltonian for an equilibrium system at the temperature $T_1$ the above gives

$$H_s(q) = \sigma(q^2+m^2)\left[1 + \frac{\lambda\sigma}{\kappa}\frac{q}{\frac{\alpha\lambda\Delta\psi^2}{2D} + q\sigma(q^2+m^2)}\right]. \tag{4.51}$$

psi In the case of an unconfined interface (where there is no gravitational effect on the

surface fluctuations) *i.e.* $m = 0$ we see that for small $q$

$$H_s(q) \approx \sigma q^2 + \frac{2D\sigma^2}{\kappa\alpha\Delta\psi^2}q^3. \qquad (4.52)$$

We see that the effective surface tension is not modified but a reduction of fluctuations due to the presence of the term in $q^3$ arises. As in the case of a driven system, we see that the large $q$ behavior of the effective Hamiltonian is given by the equilibrium case where $T = T_1 = T_2$.

In the case where the interface is confined, we see that for small $q$ one obtains

$$H_s(q) \approx \sigma m^2 \left[ 1 + \frac{2D\sigma}{\kappa\alpha\Delta\psi^2}q \right], \qquad (4.53)$$

and thus at the largest length scales of the problem there is a qualitative departure from capillary wave behavior induced by activity, and the correlation length of height fluctuations at the largest length scales is given by

$$\xi_a = \frac{2D\sigma}{\kappa\alpha\Delta\psi^2}. \qquad (4.54)$$

The above result should be compared with that obtained in [**?** ] for systems with anisotropic thermal white noise, which breaks detailed balance and mimics random driving of the system parallel to the interface; for free interfaces it was found that $C_s(q) \sim 1/q$.

## 4.5 Conclusions

We have presented a model to analyse the effect of uniform driving on the dynamics of the interface in a two phase system. In order to generate a non-equilibrium state a second *hidden* order parameter was introduced. This models the behaviour of a local or solvent degree of freedom which is not influenced by the driving field. In this way, we obtain out of equilibrium interface fluctuations which are described by Gaussian statistics as found in the experimental study of [**?** ]. The agreement with this experimental study also extends to qualitative agreement with the increase of the effective surface tension in the direction of driving and also an increase in the correlation length of the height fluctuations with respect to a non-driven equilibrium interface. However, we note that numerical simulations of a sheared Ising interface [**?** **?** ] also reveal a reduction of interface fluctuations but the

lateral correlation length is found to be reduced.

The basic idea underlying this study would be interesting to apply to a number of possible variants of this model, for instance both the dynamics of the main field $\phi$ and the solvent field $\phi$ could be varied. To make a direct link with driven colloidal interfaces one should study model H type dynamics for the main field $\phi$ and other variants for the dynamics of the solvent field $\phi$ could also be considered.

As mentioned above, in lattice based models driving induces non-equilibrium states even in the simple Ising lattice gas. A model analogous to that studied here can be formulated in a lattice based systems using the Hamiltonian

$$H = -J \sum_{(ij)} S_i S_j (1 + \sigma_{(ij)}), \tag{4.55}$$

where $S_i = \pm 1$ are Ising spins at the lattice sites $i$, and $\sigma_{(ij)} = \pm 1$ are Ising like dynamical solvent variables associated with the lattice links $(ij)$. The static partition function is given by

$$Z = \mathrm{Tr}_{\sigma_{ij}, S_i} \exp \left[ \beta J \sum_{(ij)} S_i S_j (1 + \sigma_{(ij)}) \right], \tag{4.56}$$

and the trace over the solvent variables can be trivially carried out to give

$$Z = \mathrm{Tr}_{S_i} \left( \exp \left[ \beta J \sum_{(ij)} S_i S_j \right] \prod_{(ij)} 2 \cosh(\beta J S_i S_j) \right) = [2 \cosh(\beta J)]^L \mathrm{Tr}_{S_i} \exp(\beta J \sum_{(ij)} S_i S_j),$$
$$\tag{4.57}$$

where $L$ is the number of links on the lattice of the model. We thus see that the underlying effective static model is precisely the zero field Ising model.

This model can then be driven in a number of ways, for instance using conserved Kawasaki dynamics for the Ising spins to model diffusive dynamics in the presence of a uniform driving field parallel to the surface between the two phases at a temperature below the ferromagnetic ordering temperature $T_c$. The dynamics of the Ising spins on the lattice links can be given by non-conservative single spin flip, for instance Glauber, dynamics to keep the analogy with the continuum model discussed in the paper but diffusive dynamics or indeed a mixture of diffusive and non-conserved dynamics could be implemented. It would be interesting to see to what extent this modification of the driven lattice gas model affects the non-equilibrium driven states that arise.

It is also clear that this lattice model can be used to simulate the effect of activity where the Ising spins $S_1$ corresponding to the colloid field undergo Kawasaki dynamics at the temperature $T_1$ where as the link variables $\sigma_{(ij)}$ undergo single spin flip non-conserved dynamics at the temperature $T_2$.

# Chapter 5

# Beyond Solid-On-Solid : the Particles-Over-Particles model

In Sec 1.3.2 we introduced the Solid-On-Solid model with Hamiltonian

$$H_{SOS} = \sum_i |h_i - h_{i+1}| + \frac{V(h_i) + V(h_{i+1})}{2} \qquad (5.1)$$

We discuss in this chapter a variant the model which is formed distinct particle types, and explain the numerical algorithm it obeys. For a single particle type, numerical simulations show that it is a better approximation to the Ising model than the SOS model for temperatures lower than $T_C$. This model allows for model C dynamics where particle types belong to different thermodynamic ensembles and have different kinetic of diffusive coefficients. In the multiple particles systems, we show that driving one of the particles types leads to an increase in surface fluctuations. We theoretically explain these results in terms of stochastic functional theory.

## 5.1 The Single-type Particles-Over-Particles model

The SOS Hamiltonian is directly derived from the Ising model thanks to the overhangs' absence approximation. Even though, while doing numerical simulations in both systems, it is striking to see that simulations do not behave identically. In the Ising model, if there are $n_{+,i}$ positive spins and $n_{-,i}$ negative spins at column $i$, in Monte Carlo simulations for each spin can be randomly chosen with a uniform probability for a spin-flip attempt.

On the contrary, in the SOS model as we described in Chapter 2, we randomly choose a column $i$ with a uniform probability. We see that even though the Hamiltonian is the same, the dynamic is different.

If the height profiles represent particle numbers, fixing the total number of particles to be $N$ and taking them to be identical, the partition function is given by

$$Z_{POP}(N) = \frac{1}{N!} \sum_{h_1, h_2 \cdots h_{L'}} \delta_{\sum_{i=1}^{L'} h_i, N} \frac{N!}{\prod_{i=1}^{L'} h_i!} \exp\left(-\beta J \sum_{i=1}^{L'} |h_{i+1} - h_i| - \beta \sum_{i=1}^{L'} V(h_i)\right)$$

$$(5.2)$$

Here the combinatorial term $\frac{N!}{\prod_{i=1}^{L} h_i!}$ represents the number of ways that the $h_i$ particles on each site can be chosen from the $N$ particles available. In the same fashion as the Solid-On-Molid, we call this model the **Particles-Over-Particles model**, since we stack particles in columns of height $h_i$ .The constraint on the particle number makes the computation of the partition function at fixed $N$ complicated both analytically and numerically. However, if we change to the grand canonical ensemble using the formula

$$\Xi = \sum_N \exp(\beta\mu N) Z_N \qquad (5.3)$$

where $\Xi$ is the grand partition function and $\mu$ the chemical potential, we find

$$\Xi_{POP} = \sum_{h_1, h_2 \cdots h_{L'}} \frac{1}{\prod_{i=1}^{L'} h_i!} \exp\left(-\beta J \sum_{i=1}^{L'} |h_{i+1} - h_i| - \beta \sum_{i=1}^{L'} [V(h_i) - \mu h_i]\right) \qquad (5.4)$$

The model differs from the usual solid on solid model in that a number of particle configurations give rise to the same height configurations. The grand partition function can then be written as

$$\Xi = \sum_{h_1, h_2 \cdots h_{L'}} \exp\left(-\beta H_{eff}(h_1, h_2 \cdots h_{L'})\right) \qquad (5.5)$$

where

$$H_{eff} = J \sum_{i=1}^{L'} |h_{i+1} - h_i| + \sum_{i=1}^{L'} [V(h_i) - \mu h_i + \frac{1}{\beta} \ln(h_i!)] \qquad (5.6)$$

The transfer matrix is

$$T_{POP}(h, h') = T_{SOS}(h, h') \exp\left(-\frac{\ln(h) + \ln(h')}{2}\right) \qquad (5.7)$$
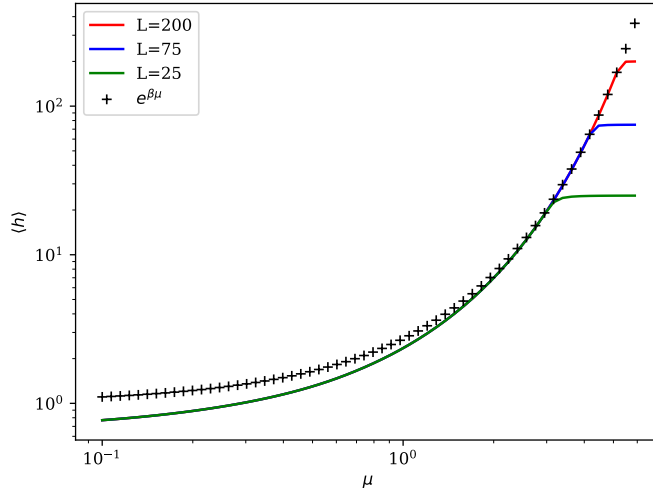
Figure 5.1: Mean height of the POP model with respect to chemical potential $\mu$ through transfer matrix with different maximal heights in the thermodynamic limit $L' \to \infty$, compared to the Striling's approximation Eq (5.10),at $\beta = 1$. add MC sim
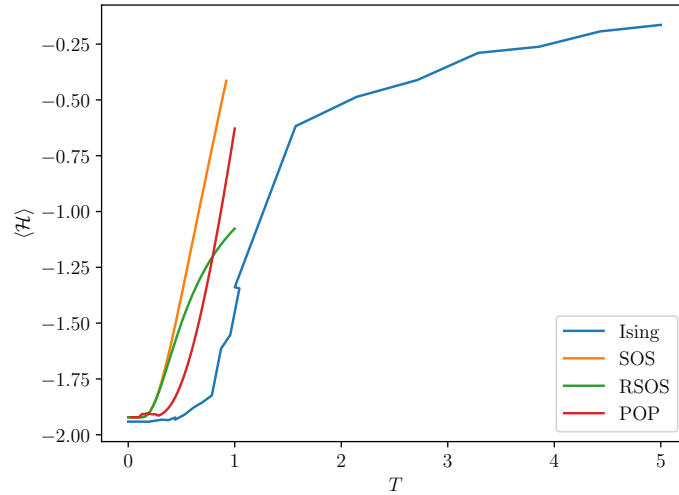


Figure 5.2: Comparison of the internal mean total energy of the Ising, SOS, RSOS and POP models with respect to temperature in absence of external field and $\mu = 0$, from Monte Carlo simulations at $L' = 126$ and $L = 30$ with Glauber dynamics. We used Eq 1.121 to compare energies between the interface models and the Ising one. redo sims for Ising, need MCIA, takes too long otherwise

The Monte Carlo implementation is as follows. Each particle is labeled with the site $i$ in which it is, and $h_i$ is the number of particles numbered at that site. In the Glauber dynamics, particles can be exchanged with a reservoir. With a probability $1/2$ one attempts to add a particle and with probability $1/2$ one attempts to takeaway a particle. In the first case, a site $i$ is chosen with a uniform distribution, and we attempt to create a new particle labeled at site $i$ with probability $min(1, \exp(-\beta \Delta E))$. In the latter, a particle is selected uniformly between all existing particles, and an attempt to remove it is done [1]. Kawasaki dynamics is implemented by randomly choosing a particle $n$ with probability $\frac{1}{N}$ at each Monte Carlo step, then trying to move the particle to the left or right using Metropolis acceptance rate.

In Fig 5.2, we plot the internal energy of the Ising, SOS, RSOS and POP models with respect to temperature in absence of external fields and $\mu = 0$ wtih non-conserved dynamics. discuss the graph once plots are better

Contrary to the SOS model where there needs to be a confining external field in order to localize the interface [90, 91], the entropic term gives a stable position for the interface. In absence of external field, the effective potential is given by

$$V_{eff}(h) = -\mu h + \frac{1}{\beta} \ln(h!) \tag{5.8}$$

If the chemical potential is large enough, the number of particles $N$ is large enough, so we can use Striling's formula and approximate a continuous derivative with the finite-difference in $h$, so we have

$$V_{eff}(h)' = -\mu + \frac{1}{\beta} \ln(h) \tag{5.9}$$

which gives the mean height

$$\langle h \rangle = \exp(\beta \mu) \tag{5.10}$$

In Fig 5.1, we show the mean height (5.10) compared to the transfer matrix diagonalisation with different matrix size and the Monte Carlo simulations at$\beta = 1$. We see that when

---

[1]In C++, we can use a $std :: vector$ in which we add or remove particles. After each success attempt, we rebuild the distribution $std :: uniform\_int\_distribution(0, N-1)$, where N is the number of particles. This operation is lightweight and should not cause any slowing down. For the next section's algorithm with multiple particle types, we use $std :: discrete\_distribution\langle\rangle$.

$\langle h \rangle \gg 1$, the Stirling's formula becomes valid and Eq (5.10) becomes accurate. Since $\langle h \rangle$ cannot exceed the maximum size of the system, saturation occurs at large $\mu$.

## 5.2 $M$-particles POP system

We consider a model of a surface delimiting a bulk phase of $L'$ sites which contains $M$ different particle types $p_1...p_M$, $N_m$ is the total number of particles of type $m$ and $n_{m,i}$ denotes the number of particles of type $m$ at site $i$. The interface height is $h_i = \sum_m n_{m,i}$. Taking into account the entropic contribution, the effective Hamiltonian for the model is

$$H[M] = J\sum_i |h_i - h_{i+1}| + \sum_i V(h_i) - \sum_m \mu_m \sum_i n_{m,i} + \frac{1}{\beta}\sum_m \sum_i \ln(n_{m,i}) \qquad (5.11)$$

We assume that the particles in each column are demixed, i.e. the permitted particle configurations are taken to be stacked vertically such that the stack of $p_{m+1}$ particles lies on top of the $p_m$ particles, as seen in Fig 5.3 for $M = 2$. The first term in the Hamiltonian corresponds to the surface tension with a gas phase above the stacks of particles. As disccused with the SOS model, we can have a restricted or gaussian version of Eq 5.11.

The grand partition function is given by

$$\Xi = \sum_{\mathbf{n_1...n_M}} \exp(-\beta H[M]) \qquad (5.12)$$

The motivation for a $M$ particle theory is that when one develops a continuous, off latice theory, based on Brownian dynamics, any single particle theory is insensitive to constant driving due to Galilean invariance, the presence of two or more different particle types breaks this invariance and yields non-equilibrum effects.

If $M = 2$, the the statics of the above can be reduced to the study of a single particle model by making the change of variable $n_{2,i} = h_i - n_{1,i}$. Using the binomial relation $(a+b)^{n_1} = \sum_{h'=0}^{h} \frac{h!}{h'!(h-h')!} a^{h'} b^{h'-h}$, the sum over the variables $n_{1,i}$ can be trivially carried out and we find

$$\Xi = \sum_{\mathbf{h}} \exp\left(-\beta J\sum_i |h_i - h_{i+1}| - \sum_i \ln(h_i!) + \beta\mu_e \sum_i h_i\right)$$

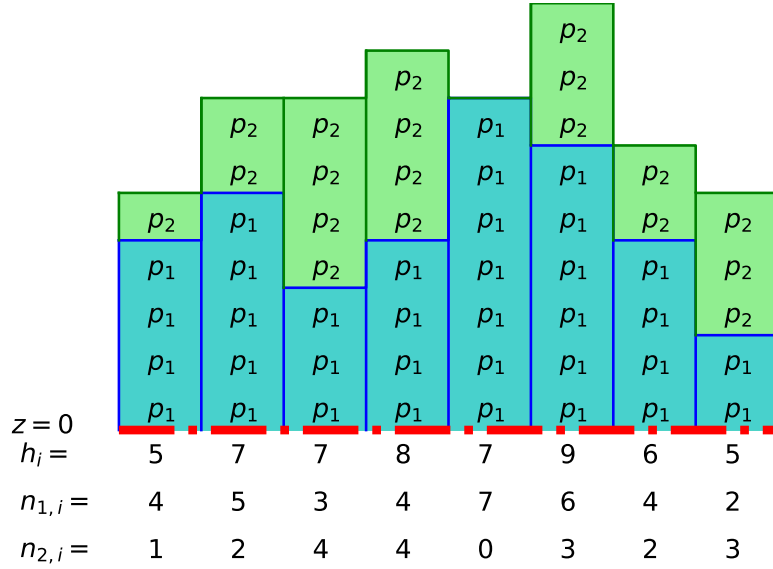$$= \sum_{\mathbf{h}} \exp\left(-\beta H_{eff}(h_1, h_2...h_{L'})\right) \qquad (5.13)$$

Figure 5.3: Possible POP configuration with two types of particles $p_1$ and $p_2$. The red line shows the origin $z = 0$. In the $i$-th column the interface is at height $h_i$, with $n_{1,i}$ particles of type $p_1$ at site $i$, and same for particles $p_2$. Over the interface, there are no particles.

where $\mu_e = \frac{1}{\beta} \ln(\exp(\beta\mu_1) + \exp(\beta\mu_2))$ is the effective chemical potential for the variables $h_i$. If we add a third type of particle, we see clearly see that the same reduction can be carried out. Thus, by recursivity, we can show that for any number of particle type $M$, we have the same effective Hamiltonian as the single particle system (5.6), with an effective chemical potential

$$\mu_e = \frac{1}{\beta} \ln \left( \sum_m \exp(\beta\mu_m) \right) \tag{5.14}$$

An interesting thing to remark is that even if the chemical potential of a particle type $\mu_m = 0$, its contribution to the effective chemical potential is nonzero. This reduced theory can be numerically solved in equilibrium by transfer matrix methods.

Now let the subset $\bar{M}$ of particle types from the $M$ particle types be in the canonical ensemble, while all the other ones are in the grand-canonical one. which kind of physical

The total partition function is then

$$\Xi = \sum_h \exp\left(-\beta H_{eff}(h_1, h_2...h_{L'})\right) \prod_{m \in \bar{M}} \delta_{\sum_{i=1}^{L'} h_i, N_m} \tag{5.15}$$

Mixing Glauber and Kawasaki dynamics for different particle types is implemented using the following algorithm. Each non-conserved particle type posseess a kinetic coefficient $\alpha_m$, while each conserved particle type has a diffusive coefficient $D_m$. We set $p_m = \alpha_m$ is the particle is non-conserved, and $p_m = D_m$ otherwise, and we normalize it in order to have $\sum_m p_m = 1$. At each Monte Carlo step, a particle of type $m$ is chosen with probability $p_m$, and then we proceed with Glauber or Kawasaki dynamics for a single-type particle system, as described in the previous section. To test the algorithm with a view to studying the driven system, we have implemented it in for two particles types both in the grand-canonical ensemble for the case of no driving and have compared the results with the equilibrium transfer matrix which we carried out numerically. In the case where the dynamics is conserved we compared them to the non-conserved case.

In order to compare the equilibrium calculation to the numerical simulations, we fix the average number of particles $\langle n_{m,i} \rangle$ at each by

$$\begin{aligned}
\langle n_m \rangle &= \frac{1}{\beta L'} \frac{\partial}{\partial \mu_m} \ln(\Xi) \\
&= \frac{1}{\beta L'} \frac{\partial \mu_e}{\partial \mu_m} \frac{\partial}{\partial \mu_e} \ln(\Xi) \\
&= \frac{\exp(\beta \mu_m)}{\sum_m \exp(\beta \mu_m)} \langle h \rangle
\end{aligned} \tag{5.16}$$

where $\langle h \rangle = \langle \sum_m n_m \rangle$.

## 5.3 Continuum Theory

In order to understand the statics of the model we write a continuum version of the theory with $M$ field $n_m(x)$ and we take the a Gaussian form for the surface energy

$$H = \int dx \frac{\sigma}{2} [\frac{d}{dx}(\sum_m n_m)]^2 + V(n_1(x), ..., n_M(x)) \tag{5.17}$$

where $\sigma$ is the surface tension and

$$V(n_1(x), ...n_M(x)) = \sum_m -\mu_m n_m(x) + T n_m(x)[\ln(n_m(x)) - 1] \tag{5.18}$$

We have used Stirlings formula and thus assumed that the typical value of $n_m(x)$ aree large. We now expand $V(n_1(x), ...n_M(x))$ by writing $n_m(x) = \bar{n}_m + \phi_m(x)$ where $(\bar{n}_1, ..\bar{n}_M)$ is the minimum of $V(n_1, ..n_M)$. Here we find

$$\bar{n}_m = \exp(\beta \mu_m) \tag{5.19}$$

This gives an effective Hamiltonian for the fluctuations of the fiels $\phi_m$

$$H_f = \frac{\sigma}{2} \int dx [\frac{d}{dx}(\sum_m \phi_m)^2 + \sum_m r_m \phi_m^2(x) \tag{5.20}$$

where

$$r_m = \frac{T}{\sigma \bar{n}_m} \tag{5.21}$$

A straight forward calculation then shows that the Fourier transform of the connected height-height fluctuation correlation function is

$$\tilde{C}_{hh}(k) = \frac{T}{\sigma} \frac{1}{k^2 + r_e} \tag{5.22}$$

where $r_e = \prod_m r_m / \sum_m r_m$. We thus find

$$\langle h^2 \rangle = \frac{T}{2\sigma m_e} = \frac{1}{2} \sqrt{\frac{T\bar{h}}{\sigma}}, \tag{5.23}$$

where $\bar{h} = \sum_m \bar{n}_m$.

## 5.4 Dynamics of the continuum model for two particles

### 5.4.1 Conserved diffusive dynamics

We now study a system of two particle types $A$ and $B$, where one is a a solvent and the other one a particle in suspension, for example. Assuming Brownian dynamics for the particles, the stochastic density functional equations for the continuum fields $n_A$ and $n_B$

are given by

$$\frac{\partial n_A(x)}{\partial t} = \frac{\partial}{\partial x}\beta D_A n_A(x)\frac{\partial}{\partial x}\frac{\delta H}{\delta n_A(x)} + \frac{\partial}{\partial x}\sqrt{2D_A n_A(x)}\eta_A(x,t) \qquad (5.24)$$

and

$$\frac{\partial n_B(x)}{\partial t} = \frac{\partial}{\partial x}\beta D_B n_B(x)\frac{\partial}{\partial x}\frac{\delta H}{\delta n_B(x)} + \frac{\partial}{\partial x}\sqrt{2D_B n_B(x)}\eta_B(x,t) \qquad (5.25)$$

where $D_A$ and $D_B$ are the diffusion constants of the particles. The noise terms are independent , zero mean, spatiotemporal Gaussian white noise with

$$\langle\eta_A(x,t)\eta_A(x',t')\rangle = \langle\eta_B(x,t)\eta_B(x',t')\rangle = \delta(x-x')\delta(t-t'). \qquad (5.26)$$

As we are interested in what happens when one of the species is driven, we add a term

$$H_D = -\int dx\, x f n_A(x) \qquad (5.27)$$

to the Hamiltonian, this corresponds to a force which pushes the particles of type $A$ to the right. We also assume periodic boundary conditions, and thus a current will exist in the resulting steady state. This introduces term in the equation for $n_A(x)$ which becomes

$$\frac{\partial n_A(x)}{\partial t} + \frac{\partial}{\partial x}D_A\beta f n_A(x) = \frac{\partial}{\partial x}\beta D_A n_A(x)\frac{\partial}{\partial x}\frac{\delta H}{\delta n_A(x)} + \frac{\partial}{\partial x}\sqrt{2D_A n_A(x)}\eta_A(x,t). \qquad (5.28)$$

It is important to note that in the absence of the particles of type $B$, the resulting equation for the field $n_A(x,t)$ can be rendered independent of the force $f$ via the Galilean transformation

$$n(x,t) = n(x-vt,t) \qquad (5.29)$$

where $v = D_A\beta f$ is the induced drift on the particles of type $A$. Note that the Galilean invariance can also be broken if the force $f$ acts on both particle types but the diffusion coefficients $D_A$ and $D_B$ are different.

We now expand the deterministic part of the two equations to first order in the density fluctuations about its mean value and the noise terms to zeroth order. This approximation respects detailed balance for the effective quadratic Hamiltonian and has been used with accuracy in a wide variety of contexts. The resulting dynamics of of a model B and Fourier

transforming in space gives

$$\frac{\partial \tilde{\Phi}(k,t)}{\partial t} = -\beta \tilde{A}(k)\Phi(k,t) + \tilde{\eta}(k,t), \tag{5.30}$$

where

$$\Phi(k,t) = \begin{pmatrix} \tilde{\phi}_A(k,t) \\ \tilde{\phi}_B(k,t) \end{pmatrix} \tag{5.31}$$

The noise correlation function is given by

$$\langle \eta^T(k,t)\eta(k',t')\rangle = 4\pi \tilde{R}(k)\delta(t-t')\delta(k+k') \tag{5.32}$$

where

$$\tilde{R}(k) = 2 \begin{pmatrix} D_A \bar{n}_A k^2 & 0 \\ 0 & D_B \bar{n}_B k^2 \end{pmatrix}, \tag{5.33}$$

and

$$\tilde{A}(k) = \sigma \begin{pmatrix} D_A \bar{n}_A k^2 (k^2 + m_A^2) - i\frac{D_A k f}{\sigma} & D_A \bar{n}_A k^4 \\ D_B \bar{n}_B k^4 & D_B \bar{n}_B k^2 (k^2 + m_B^2). \end{pmatrix} \tag{5.34}$$

The Fourier transform steady state correlation function matrix defined by

$$\langle \tilde{\Phi}^T(k)\tilde{\Phi}(k')\rangle = 2\pi\delta(k+k')\tilde{C}(k) \tag{5.35}$$

is then given by the solution to the Lyapounov equation

$$\tilde{A}(k)\tilde{C}(k) + \tilde{C}(k)\tilde{A}^T(-k) = 2T\tilde{R}(k). \tag{5.36}$$

Solving this we find that

$$\tilde{C}_{hh}(k) = \frac{T}{\sigma} \frac{k^2(m_A^2 + m_B^2)(D_A \bar{n}_A[k^2 + m_A^2] + D_B \bar{n}_B[k^2 + m_B^2])^2 + \frac{f^2}{\sigma^2}D_A^2(2k^2 + m_A^2 + m_B^2)}{k^2(D_A \bar{n}_A[k^2 + m_A^2] + D_B \bar{n}_B[k^2 + m_B^2])^2(m_A^2 m_B^2 + k^2(m_A^2 + m_B^2)) + \frac{f^2}{\sigma^2}D_A^2(k^2 + m_A^2)(k^2 + m_B^2)} \tag{5.37}$$

In the equilibrium or non-driven system where $f = 0$ the above formula yields the static result Eq. (5.22). Of particular interest is the strong driving limit where we find that as $f \to \infty$ the result

$$\tilde{C}_{hh}(k) = \frac{T}{\sigma} \left[ \frac{1}{k^2 + m_A^2} + \frac{1}{k^2 + m_B^2} \right] \tag{5.38}$$

The effect of strong driving is to decouple the fluctuations of $n_A$ and $n_B$ and we see that the total height fluctuation is that of the sum two independent interfaces. The height variance is then given by

$$\langle h^2 \rangle_s = \frac{T}{2\sigma m_d} \tag{5.39}$$

where

$$m_d = \frac{m_A m_B}{m_A + m_B} \tag{5.40}$$

From this we find that

$$\frac{\langle h^2 \rangle_s}{\langle h^2 \rangle_{eq}} = \frac{m_A + m_B}{\sqrt{m_A^2 + m_B^2}}. \tag{5.41}$$

We also see that, as $m_A$ and $m_B$ are positive, the fluctuations in limit of infinite driving are always larger than in the equilibrium state.

Imagine now that the $B$ particles constitute the bottom layer and that $D_B \ll D_A$ this mimics the solid on solid dynamics where only the top layer of the particles participate in the dynamics. This gives

$$\tilde{C}_{hh}(k) = \frac{T}{\sigma} \frac{k^2(m_A^2 + m_B^2)(\overline{n}_A[k^2 + m_A^2])^2 + \frac{f^2}{\sigma^2}(2k^2 + m_A^2 + m_B^2)}{k^2(\overline{n}_A[k^2 + m_A^2])^2(m_A^2 m_B^2 + k^2(m_A^2 + m_B^2)) + \frac{f^2}{\sigma^2}(k^2 + m_A^2)(k^2 + m_B^2)}. \tag{5.42}$$

Assuming the $A$ layer is thinner that the $B$ layer so $m_B \ll m_A$ gives

$$\tilde{C}_{hh}(k) = \frac{T}{\sigma} \frac{k^2 m_A^2(\overline{n}_A[k^2 + m_A^2])^2 + \frac{f^2}{\sigma^2}(2k^2 + m_A^2)}{k^2(\overline{n}_A[k^2 + m_A^2])^2(m_A^2 m_B^2 + k^2 m_A^2) + \frac{f^2}{\sigma^2}(k^2 + m_A^2)(k^2 + m_B^2)}. \tag{5.43}$$

which simplifies to give

$$\tilde{C}_{hh}(k) = \frac{T}{\sigma} \frac{k^2 m_A^2(\overline{n}_A[k^2 + m_A^2])^2 + \frac{f^2}{\sigma^2}(2k^2 + m_A^2)}{(k^2 + m_A^2)(k^2 + m_B^2)[(n_A^2 m_A^2 k^2(k^2 + m_A^2) + \frac{f^2}{\sigma^2}]} \tag{5.44}$$

$$\tilde{C}_{hh}(k) = \frac{T}{\sigma} \frac{1}{k^2 + m_B^2} + \frac{T}{\sigma} \frac{\frac{f^2}{\sigma^2} k^2}{(k^2 + m_A^2)(k^2 + m_B^2)[(n_A^2 m_A^2 k^2(k^2 + m_A^2) + \frac{f^2}{\sigma^2}]} \tag{5.45}$$

$$= \frac{T}{\sigma} \left[ \frac{1}{(k^2 + m_B^2)} + \frac{f^2}{\sigma^2 \overline{n}_A^2 m_A^2} \frac{k^2}{(k^2 + m_A^2)(k^2 + m_B^2)(k^4 + m_A^2 k^2 + \frac{f^2}{\sigma^2 n_A^2 m_A^2})} \right] \tag{5.46}$$

The height fluctuations are then given by

$$\langle h^2 \rangle = \frac{T}{2\sigma m_B} + \frac{T}{2\sigma} \frac{f^2}{\sigma^2 \overline{n}_A^2 m_A^2} \frac{m_A + m_B + m_+ + m_-}{(m_A + m_B)(m_+ + m_B)(m_- + m_B)(m_A + m_+)(m_A + m_+)(m_+ + m_-)},$$
(5.47)

where

$$m_\pm = \sqrt{\frac{m_A^2 \pm \sqrt{m_A^4 - \frac{4f^2}{\sigma^2 n_A^2 m_A^2}}}{2}}$$
(5.48)

## 5.4.2  Non conserved dynamics

We now consider the case where the particles of type $B$ are in contact with a reservoir of the same particles in a vapour phase. To model this we modify the dynamics of the B phase by introducing a component of non-conserved dynamics for these particles

$$\frac{\partial n_B(x)}{\partial t} = \frac{\partial}{\partial x} \beta D_B n_B(x) \frac{\partial}{\partial x} \frac{\delta H}{\delta n_B(x)} + \frac{\partial}{\partial x} \sqrt{2D_B n_B(x)} \eta_B(x,t) - K_B \beta \frac{\delta H}{\delta n_B(x)} + \sqrt{2K_B} \eta'_B(x,t),$$
(5.49)

here if $\eta'_B(x,t)$ is a new spatio-temporal white noise independent of the others, the undriven system obeys detailed balance. Now the average value of the $n_B$ is determined by taking the average in the steady state. As the system is invariant under translation, the average of the first diffusive term on the right-hand-side is zero and so we find

$$\langle \frac{\delta H}{\delta n_B(x)} \rangle = 0,$$
(5.50)

where the averaging is over the system in the steady state. Again invariance by translation in space can be applied to write

$$\langle \frac{\partial V(n_A, n_B)}{\partial n_A} \rangle = 0$$
(5.51)

Here we have $V(n_A, n_B) = U(n_A) + U(n_B)$ where $U(x) = Tx(\ln(x) - 1) - \mu x$ and so expanding about $\overline{n}_A$ we find to second order that

$$\langle U'(\overline{n}_A) + U''(\overline{n}_A)\phi_A + \frac{1}{2}U'''(\overline{n}_A)\phi_A^2 \rangle = 0,$$
(5.52)

the equation to first order gives

$$U'(\overline{n}_A) = 0 \tag{5.53}$$

which gives $\overline{n}_A = n_m$ where $n_m$ is the value for which $U$ attains its minimum. However if we keep the next order term we find

$$U'(\overline{n}_A) + \frac{1}{2}U'''(\overline{n}_A)\langle\phi_A^2\rangle = 0. \tag{5.54}$$

If the renormalization of the average value of $\overline{n}_A$ is assumed to be small we can write

$$\overline{n}_A = n_m + \delta, \tag{5.55}$$

which gives

$$\delta = -\frac{1}{2}\frac{U'''(n_m)}{U''(n_m)}\langle\phi_A^2\rangle. \tag{5.56}$$

For the (entropic) potential in question here we have

$$\delta = \frac{1}{2n_m}\langle\phi_A^2\rangle, \tag{5.57}$$

we thus see that the average height of the interface is increased due to fluctuations. The non-equilibrium fluctuations are stronger an thus the height increases under driving.

# Appendix A

# Evaluating Fourier integrals

Here we outline how the Fourier integration leading to Eq. (4.37) is carried out. Defining

$$I(f(\omega)) = \int \frac{d\omega}{2\pi} \frac{f(\omega)}{|i(A\omega + B) + (C - D\omega - E\omega^2)|} \tag{A.1}$$

we see that the integral we need to evaluate can be written in the form

$$I = aI(\omega^2) + bI(1). \tag{A.2}$$

The calculation leading to Eq. (4.35) can be carried out in the presence of a forcing term on the height profile in order to compute the response function for the surface which has a denominator of the form

$$\text{Den} = i(A\omega + B) + (C - D\omega - E\omega^2), \tag{A.3}$$

and due to causality the above only has poles in the upper complex plane (due to the convention of Fourier transforms used here). Consequently we find that

$$\int \frac{d\omega}{2\pi} \frac{1}{i(A\omega + B) + (C - D\omega - E\omega^2)} = 0, \tag{A.4}$$

as one may close the integration contour in the lower half of the complex plane. Taking the real and imaginary part of Eq. (A.4) leads to

$$CI(1) - DI(\omega) - EI(\omega^2) = 0 \tag{A.5}$$

$$AI(\omega) + BI(1) = 0. \tag{A.6}$$

Using this we can express $I(\omega^2)$ as a function of $I(1)$, and explicitly we have

$$I(\omega^2) = \frac{I(1)}{E}[C + \frac{DB}{A}]. \tag{A.7}$$

To evaluate $I(1)$ we now use

$$I(1) = -\mathrm{Im} \int \frac{d\omega}{2\pi} \frac{1}{A\omega + B} \frac{1}{i(A\omega + B) + (C - D\omega - E\omega^2)}. \tag{A.8}$$

The integrand above has no poles in the lower half of the complex plane but has a *half pole* at $\omega = -B/A$ on the real axis, thus using standard complex analysis we find

$$I(1) = \frac{1}{2(CA + BD - \frac{EB^2}{A})}. \tag{A.9}$$

Then after some laborious, but straightforward algebra, the results Eq. (4.37) is obtained.

# Bibliography

[1] David S Dean, Paul Gersberg, and Peter C W Holdsworth. The effect of driving on model C interfaces. *Journal of Statistical Mechanics: Theory and Experiment*, 2020(3):033206, March 2020.

[2] Mésocentre de Calcul Intensif Aquitain. https://redmine.mcia.fr/projects/mcia.

[3] P. C. Hohenberg and B. I. Halperin. Theory of dynamic critical phenomena. *Reviews of Modern Physics*, 49(3):435–479, July 1977.

[4] A. J. Bray. Theory of phase-ordering kinetics. *Advances in Physics*, 43(3):357–459, June 1994.

[5] Lars Onsager. Crystal Statistics. I. A Two-Dimensional Model with an Order-Disorder Transition. *Physical Review*, 65(3-4):117–149, February 1944.

[6] L. Landau and E. Lifchitz. *Physique théorique - T9 Physique Statistique.* Éditions Mir Moscou. 1990.

[7] J. A. Tuszyński, R. Paul, and R. Chatterjee. Exact solutions to the time-dependent Landau-Ginzburg model of phase transitions. *Physical Review B*, 29(1):380–386, January 1984.

[8] John W Cahn and John E Hilliard. Free Energy of a Nonuniform System. I. Interfacial Free Energy. *The Journal of Chemical Physics*, 28(2):11, February 1958.

[9] Y. Hennequin, D. G. A. L. Aarts, J. H. van der Wiel, G. Wegdam, J. Eggers, H. N. W. Lekkerkerker, and Daniel Bonn. Drop Formation by Thermal Fluctuations at an Ultralow Surface Tension. *Physical Review Letters*, 97(24), December 2006.

[10] Javier Atencia and David J. Beebe. Controlled microfluidic interfaces. *Nature*, 437(7059):648–655, September 2005.

[11] H. W. Diehl, D. M. Kroll, and H. Wagner. The interface in a Ginsburg-Landau-Wilson model: Derivation of the drumhead model in the low-temperature limit. *Zeitschrift f?r Physik B Condensed Matter and Quanta*, 36(4):329–333, December 1980.

[12] Alan J. Bray, Andrea Cavagna, and Rui D. M. Travasso. Interface fluctuations under shear. *Physical Review E*, 64(1):012102, June 2001.

[13] Alan J. Bray, Andrea Cavagna, and Rui D. M. Travasso. Interface fluctuations, Burgers equations, and coarsening under shear. *Physical Review E*, 65(1), December 2001.

[14] S. F. Edwards and D. R. Wilkinson. The Surface Statistics of a Granular Aggregate. *Proceedings of the Royal Society of London. Series A, Mathematical and Physical Sciences*, 381(1780):17–31, 1982.

[15] Timothy Halpin-Healy and Yi-Cheng Zhang. Kinetic roughening phenomena, stochastic growth, directed polymers and all that. Aspects of multidisciplinary statistical mechanics. *Physics Reports*, 254(4-6):215–414, March 1995.

[16] Raja Paul, Sanjay Puri, and Heiko Rieger. Domain growth in Ising systems with quenched disorder. *Physical Review E*, 71(6), June 2005.

[17] David A. Huse. Corrections to late-stage behavior in spinodal decomposition: Lifshitz-Slyozov scaling and Monte Carlo simulations. *Physical Review B*, 34(11):7845–7850, December 1986.

[18] Martin Niss. History of the Lenz-Ising Model 1920–1950: From Ferromagnetic to Cooperative Phenomena. *Archive for History of Exact Sciences*, 59(3):267–318, March 2005.

[19] Martin Niss. History of the Lenz–Ising Model 1950–1965: from irrelevance to relevance. *Archive for History of Exact Sciences*, 63(3):243, May 2009.

[20] Rajan Gupta, Jerry DeLapp, George G. Batrouni, Geoffrey C. Fox, Clive F. Baillie, and John Apostolakis. Phase Transition in the 2 D XY Model. *Physical Review Letters*, 61(17):1996–1999, October 1988.

[21] Michel Le Bellac, Fabrice Mortessagne, and G George Batrouni. *Equilibrium and Non-Equilibrium Statistical Thermodynamics*. Cambridge University Press, 2004.

[22] Michael Aizenman. Proof of the Triviality of $\phi$ d 4 Field Theory and Some Mean-Field Features of Ising Models for d > 4. *Physical Review Letters*, 47(1):1–4, July 1981.

[23] L.J. de Jongh and A.R. Miedema. Experiments on simple magnetic model systems. *Advances in Physics*, 23(1):1–260, January 1974.

[24] W.P. Wold. The Ising Model and Real Magnetic Materials. *Brazilian Journal of Physics*, 30(4):794–810, December 2000.

[25] Hironobu Ikeda and Kinshiro Hirakawa. NEUTRON SCATI'ERING STUDY OF TWO-DIMENSIONAL ISING NATURE OF K2CoF4. *Solid Sate Communications*, 14:529–532, November 1973.

[26] Jiirg Frohlich. On the triviality of $\lambda\varphi4$ theories and the approach to the critical point in D>4 dimensions. *Nuclear Physics B*, 200:281–296, August 1981.

[27] Nigel Goldenfeld. *Lectures on Phase Transitions and the Renormalization Group*. CRC Press, 1 edition, March 2018.

[28] A L Talapov and H W J Blöte. The magnetization of the 3D Ising model. *Journal of Physics A: Mathematical and General*, 29(17):5727–5733, September 1996.

[29] Tobias Preis, Peter Virnau, Wolfgang Paul, and Johannes J. Schneider. GPU accelerated Monte Carlo simulation of the 2D and 3D Ising model. *Journal of Computational Physics*, 228(12):4468–4477, July 2009.

[30] J. Stecki, A. Maciol/ek, and K. Olaussen. Magnetization profiles of the planar fluctuating interface in a $d =2$ Ising strip. *Physical Review B*, 49(2):1092–1103, January 1994.

[31] Howard L. Richards, M. A. Novotny, and Per Arne Rikvold. Numerical transfer-matrix study of surface-tension anisotropy in Ising models on square and cubic lattices. *Physical Review B*, 48(19):14584–14598, November 1993.

[32] D. B. Abraham and P. Reed. Interface profile of the Ising ferromagnet in two dimensions. *Communications in Mathematical Physics*, 49(1):35–46, February 1976.

[33] D. B. Abraham and A. Martin-Löf. The transfer matrix for a pure phase in the two-dimensional Ising model. *Communications in Mathematical Physics*, 32(3):245–268, September 1973.

[34] Robert H. Swendsen. Roughening transition in the solid-on-solid model. *Physical Review B*, 15(2):689–692, January 1977.

[35] J. M. J. van Leeuwen and H. J. Hilhorst. Pinning of a rough interface by an external potential. *Physica A: Statistical Mechanics and its Applications*, 107(2):319–329, June 1981.

[36] G. H. Gilmer and P. Bennema. Simulation of Crystal Growth with Surface Diffusion. *Journal of Applied Physics*, 43(4):1347–1360, April 1972.

[37] M Elwenspoek and J P van der Eerden. Kinetic roughening and step free energy in the solid-on-solid model and on naphthalene crystals. *Journal of Physics A: Mathematical and General*, 20(3):669–678, February 1987.

[38] M. R. Wilby, D. D. Vvedensky, and A. Zangwill. Scaling in a solid-on-solid model of epitaxial growth. *Physical Review B*, 46(19):12896–12898, November 1992.

[39] G Gompper and D. M Kroll. Steric Interactions in Multimembrane Systems: A Monte Carlo Study. *Europhysics Letters (EPL)*, 9(1):59–64, May 1989.

[40] Michael E Fisher. Walks, walls, wetting, and melting. *Journal of Statistical Physics*, 34(5/6):63, October 1983.

[41] V. Privman and N. M. Švrakić. Transfer-Matrix Spectrum for Systems with Interfaces. *Physical Review Letters*, 62(6):633–636, February 1989.

[42] Yup Kim, D. K. Park, and Jin Min Kim. Conserved growth in a restricted solid-on-solid model. *Journal of Physics A: Mathematical and General*, 27(15):L533, 1994.

[43] I. Vaysburd. Critical RSOS models in external fields. *Nuclear Physics B*, 446(3):387–404, July 1995.

[44] H. J. F. Knops. Exact Relation between the Solid-on-Solid Model and the $\mathrm{XY}$ Model. *Physical Review Letters*, 39(12):766–769, September 1977.

[45] Grégory Schehr and Satya N. Majumdar. Universal asymptotic statistics of maximal relative height in one-dimensional solid-on-solid models. *Physical Review E*, 73(5):056103, May 2006.

[46] Robert H. Swendsen. Monte Carlo studies of the interface roughening transition. *Physical Review B*, 15(11):5421–5431, June 1977.

[47] Aleksander L. Owczarek and Thomas Prellberg. Exact solution of the discrete (1+1)-dimensional SOS model with field and surface interactions. *Journal of Statistical Physics*, 70(5-6):1175–1194, March 1993.

[48] Satya N. Majumdar and Alain Comtet. Airy Distribution Function: From the Area Under a Brownian Excursion to the Maximal Height of Fluctuating Interfaces. *Journal of Statistical Physics*, 119(3-4):777–826, May 2005.

[49] Martin Siegert and Michael Plischke. Scaling behavior of driven solid-on-solid models with diffusion. *Journal de Physique I*, 3(6):1371–1376, June 1993.

[50] Paul A Pearce and Katherine A Seaton. Exact solution of cyclic solid-on-solid lattice models. *Annals of Physics*, 193(2):326–366, August 1989.

[51] Didi Derks, Dirk G. A. L. Aarts, Daniel Bonn, Henk N. W. Lekkerkerker, and Arnout Imhof. Suppression of Thermally Excited Capillary Waves by Shear Flow. *Physical Review Letters*, 97(3), July 2006.

[52] A. Girot, J. Petit, R. Saiseau, T. Guérin, H. Chraibi, U. Delabre, and J. P. Delville. Conical Interfaces between Two Immiscible Fluids Induced by an Optical Laser Beam. *Physical Review Letters*, 122(17), May 2019.

[53] Didi Derks, Hans Wisman, Alfons van Blaaderen, and Arnout Imhof. Confocal microscopy of colloidal dispersions in shear flow using a counter-rotating cone–plate shear cell. *Journal of Physics: Condensed Matter*, 16(38):S3917–S3927, September 2004.

[54] Ludovic Berthier and Jean-Louis Barrat. Nonequilibrium dynamics and fluctuation-dissipation relation in a sheared fluid. *The Journal of Chemical Physics*, 116(14):6228–6242, April 2002.

[55] Ludovic Berthier and Jean-Louis Barrat. Shearing a Glassy Material: Numerical Tests of Nonequilibrium Mode-Coupling Approaches and Experimental Proposals. *Physical Review Letters*, 89(9), August 2002.

[56] Marine Thiébaud and Thomas Bickel. Nonequilibrium fluctuations of an interface under shear. *Physical Review E*, 81(3), March 2010.

[57] Thomas HR Smith. *Driven interfaces in the Ising model.* PhD thesis, University of Bristol, 2010.

[58] Thomas H. R. Smith, Oleg Vasilyev, Douglas B. Abraham, Anna Maciołek, and Matthias Schmidt. Interfaces in Driven Ising Models: Shear Enhances Confinement. *Physical Review Letters*, 101(6):067203, August 2008.

[59] Thomas H R Smith, Oleg Vasilyev, Douglas B Abraham, Anna Maciołek, and Matthias Schmidt. Interfaces in confined Ising models: Kawasaki, Glauber and sheared dynamics. *Journal of Physics: Condensed Matter*, 20(49):494237, December 2008.

[60] M. E. J. Newman and G. T. Barkema. *Monte Carlo Methods in Statistical Physics*. Oxford University Press, Oxford, New York, February 1999.

[61] V. Privman and N. M. Švrakić. Asymptotic degeneracy of the transfer matrix spectrum for systems with interfaces: Relation to surface stiffness and step free energy. *Journal of Statistical Physics*, 54(3-4):735–754, February 1989.

[62] Nicholas Metropolis and S. Ulam. The Monte Carlo Method. *Journal of the American Statistical Association*, 44(247):335–341, September 1949.

[63] Paul Gersberg. Github with all my programs, 2020. https://github.com/Bulbille/Curta.

[64] S. Wansleben and D. P. Landau. Monte Carlo investigation of critical dynamics in the three-dimensional Ising model. *Physical Review B*, 43(7):6006–6014, March 1991.

[65] Roy J. Glauber. Time-Dependent Statistics of the Ising Model. *Journal of Mathematical Physics*, 4(2):294–307, February 1963.

[66] Kyozi Kawasaki. Diffusion Constants near the Critical Point for Time-Dependent Ising Models. I. *Physical Review*, 145(1):224–230, May 1966.

[67] O. Vasilyev, A. Gambassi, A. Maciołek, and S. Dietrich. Universal scaling functions of critical Casimir forces obtained by Monte Carlo simulations. *Physical Review E*, 79(4), April 2009.

[68] David Lopes Cardozo, Hugo Jacquin, and Peter C. W. Holdsworth. Critical Casimir forces in a magnetic system: An experimental protocol. *Physical Review B*, 90(18), November 2014.

[69] Martin Ankerl. Fast random bool in C++. https://martin.ankerl.com/2018/12/08/fast-random-bool/.

[70] H. B. G. Casimir. On the attraction between two perfectly conducting plates. *Royal Netherlands Academy of Arts and Sciences,*, 51(7):793–498, 1948.

[71] Richard Feynman. Feynman Lectures on Physics_ Mainly Electromagnetism and Matter., 1963.

[72] Cosima Stubenrauch and Regine von Klitzing. Disjoining pressure in thin liquid foam and emulsion films—new concepts and perspectives. *Journal of Physics: Condensed Matter*, 15(27):R1197–R1232, July 2003.

[73] B. Carazza and G. P. Guidetti. The Casimir Electron Model. *Archive for History of Exact Sciences*, 35(3):273–279, 1986.

[74] Timothy H. Boyer. Quantum Electromagnetic Zero-Point Energy of a Conducting Spherical Shell and the Casimir Model for a Charged Particle. *Physical Review*, 174(5):1764–1776, October 1968.

[75] Kimball A. Milton, Lester L. DeRaad, and Julian Schwinger. Casimir self-stress on a perfectly conducting spherical shell. *Annals of Physics*, 115(2):388–403, October 1978.

[76] M. E. Bowers and C. R. Hagen. Casimir energy of a spherical shell. *Physical Review D*, 59(2), December 1998.

[77] Kimball A. Milton, Lester L. DeRaad, and Julian Schwinger. Casimir self-stress on a perfectly conducting spherical shell. *Annals of Physics*, 115(2):388–403, October 1978.

[78] Julian Schwinger, Lester L DeRaad, and Kimball A. Milton. Casimir Effect in Dielectrics. *Annals of Physics*, pages 1–23, 1978.

[79] J. Schwinger. Casimir energy for dielectrics. *Proceedings of the National Academy of Sciences*, 89(9):4091–4093, May 1992.

[80] S.M. Rytov, Yu A. Kravtsov, and V.I. Tatarskii. *Principles of Statistical Radiophysics Vol 3*. Elements of Random Fields. Springer, Berlin, 1989.

[81] I M Lifshits and A M Kosevich. On the theory of magnetic susceptibility of metals at low temperatures. *Zh. Eksp. Teor. Fiz.*, 53(6):730–742, 1955.

[82] N.G. Van Kampen, B.R.A. Nijboer, and K. Schram. On the macroscopic theory of Van der Waals forces. *Physics Letters A*, 26(7):307–308, February 1968.

[83] B W Ninham and V A Parsegian. van der Waals Forces. 10:18, 1970.

[84] Takeo Matsubara. A New Approach to Quantum-Statistical Mechanics. *Progress of Theoretical Physics*, 14(4):351–378, October 1955.

[85] Andrea Gambassi. The Casimir effect: From quantum to critical fluctuations. *Journal of Physics: Conference Series*, 161:012037, April 2009.

[86] D. J. Amit and Victor Martin Mayor. *Field theory, the renormalization group, and critical phenomena: graphs to computers*. World Scientific, Singapore ; New Jersey, 3rd ed edition, 2005.

[87] A. Gambassi, A. Maciołek, C. Hertlein, U. Nellen, L. Helden, C. Bechinger, and S. Dietrich. Critical Casimir effect in classical binary liquid mixtures. *Physical Review E*, 80(6), December 2009.

[88] H. Arthur Weldon. Scalar Field Propagators in the Microcanonical Ensemble. *Annals of Physics*, 193:166–179, 1989.

[89] Claude Cohen-Tannoudji, Bernard Diu, and Franck Laloë. *Mécanique quantique*, volume 1. EDP-Sciences, 2018.

[90] T. W. Burkhardt. Localisation-delocalisation transition in a solid-on-solid model with a pinning potential. *Journal of Physics A: Mathematical and General*, 14(3):L63, 1981.

[91] S. T. Chui and John D. Weeks. Pinning and roughening of one-dimensional models of interfaces and steps. *Physical Review B*, 23(5):2438–2441, March 1981.